



Review article

Insights into properties, synthesis and emerging applications of polypyrrole-based composites, and future prospective: A review

Yuvika Sood^a, Kartika Singh^a, Harish Mudila^a, P.E. Lokhande^b, Lakhveer Singh^c, Deepak Kumar^a, Anil Kumar^{a,*}, Nabisab Mujawar Mubarak^{d,e,***}, Mohammad Hadi Dehghani^{f,g,**}

^a Department of Chemistry, School of Chemical Engineering and Physical Sciences, Lovely Professional University, Phagwara, Punjab, 144411, India

^b Departamento de Ingeniería Mecánica, Facultad de Ingeniería, Universidad Tecnológica Metropolitana, Av. José Pedro Alessandri 1242, Santiago, 7810003, Chile

^c Department of Chemistry, Sardar Patel University, Mandi, Himachal Pradesh, 175001, India

^d Petroleum and Chemical Engineering, Faculty of Engineering, Universiti Teknologi Brunei, Bandar Seri Begawan BE1410, Brunei Darussalam

^e Department of Biosciences, Saveetha School of Engineering, Saveetha Institute of Medical and Technical Sciences, Chennai, India

^f Department of Environmental Health Engineering, School of Public Health, Tehran University of Medical Sciences, Tehran, Iran

^g Center for Solid Waste Research, Institute for Environmental Research, Tehran University of Medical Sciences, Tehran, Iran

ARTICLE INFO

Keywords:

Polypyrrole
Conducting polymer
Composite materials
Sensor
Supercapacitors
Biocidal effects

ABSTRACT

Recent advancements in polymer science and engineering underscore the importance of creating sophisticated soft materials characterized by well-defined structures and adaptable properties to meet the demands of emerging applications. The primary objective of polymeric composite technology is to enhance the functional utility of materials for high-end purposes. Both the inherent qualities of the materials and the intricacies of the synthesis process play pivotal roles in advancing their properties and expanding their potential applications. Polypyrrole (PPy)-based composites, owing to their distinctive properties, hold great appeal for a variety of applications. Despite the limitations of PPy in its pure form, these constraints can be effectively overcome through hybridization with other materials. This comprehensive review thoroughly explores the existing literature on PPy and PPy-based composites, providing in-depth insights into their synthesis, properties, and applications. Special attention is given to the advantages of intrinsically conducting polymers (ICPs) and PPy in comparison to other ICPs. The impact of doping anions, additives, and oxidants on the properties of PPy is also thoroughly examined. By delving into these aspects, this overview aims to inspire researchers to delve into the realm of PPy-based composites, encouraging them to explore new avenues for flexible technology applications.

1. Introduction

Intrinsic conducting polymers (ICPs) attract the interest of the scientific community because of their exciting properties, such as optical, magnetic, electrical, and thermal [1,2]. Intrinsic conducting polymers also referred as “synthetic metals” having a

* Corresponding author.

** Corresponding author.

*** Corresponding author.

E-mail addresses: rsanil.nit@gmail.com (A. Kumar), mubarak.yaseen@gmail.com (N.M. Mubarak), hdehghani@tums.ac.ir (M.H. Dehghani).

Π -conjugated system in the polymeric chains. Various conducting polymers available on the market are polyaniline(PANI), polyfuran (Pfu), poly (phenylene sulfide) (PSS), polystyrene sulfonate (PEDOT: PSS), poly(*p*-phenylene) (PPP), polythiophene (PTh), and polypyrrole (PPy). However, these polymers differ from insulating polymers due to different kind of structures. The year 2000 marked a turning point for conductive polymer research. Alan MacDiarmid, Alan Heeger, and Hideki Shirakawa were awarded the Nobel Prize in Chemistry for their groundbreaking work in developing polyacetylene, a conductive plastic. Their discovery hinged on manipulating the unique properties of conjugated systems, where alternating single and double bonds between carbon atoms create delocalized electrons that can be influenced to conduct electricity. These conducting polymers find their competence applications in multi-disciplinary areas such as thermoelectric, electromagnetic shielding, chemical, electronics, electrochemical, electrical, electro-luminescence, sensors, electro-rheological, membrane, electromechanical, batteries, and capacitors [3–5]. These conducting polymers have different electrical conductivity in pure and composite forms. For instance, Kumar et al. synthesized polyaniline with other methods and proposed electrical conductivity of 3.3×10^{-2} S/cm for PANI [5], 1.8×10^{-1} S/cm for PANI/f-MWCNT [6], 3.59 S/cm for PANI with SDS and 5.90 for PANI with DBSA [7]. Tiwari et al. studied the electrical properties of a polymer with an AgSiO₂ hybrid composite whose electrical conductivity value is 4.26×10^2 S/cm [8]. Dong et al. studied the role of processing solvent on the electrical conductivity of PEDOT: PSS by AFM, which increases conductivity by improving the coherence of charge transportation on PEDOT domains, leading to better distribution of PEDOT in PSS [9,10].

Among ICPs, polypyrrole composed of a 5-membered ring with a nitrogen (N) heteroatom is most favorable because of its particular interest, such as better stability in the oxidized state, low-cost monomer, ease of synthesis, interesting redox properties, processibility in aqueous and non-aqueous media compared to other conjugated polymers [11]. ‘Pyrrole black,’ was first prepared through chemical methods in 1915 by oxidizing the pyrrole monomer with the oxidant H₂O₂ (hydrogen peroxide) [12–16]. It was not until many years later that, in 1968 Dall’Olio et al. followed the electrochemical polymerization method for polymerizing pyrrole monomer with sulfuric acid on a platinum electrode. Subsequently, many researchers have widely used an electrochemical process for depositing polypyrrole on various substrates [17].

Moreover, most intrinsic conducting polymers and polypyrrole have disadvantages like limited solubility in most solvents, infusibility, weak electrical conductivity compared to metals, weak mechanical properties, especially mechanical strength, and shorter life cycles [18–23]. Among all these drawbacks, the mechanical strength and shorter cycle life of ICPs are produced by a gradual worsening of the electrical conductivity that starts during doping and de-doping [24]. The solubility of particular ICPs can be enhanced by using a proper dopant or modifying the preliminary monomer. Various polymerization methods are available for the synthesis of PPy and its nanocomposites such as electrochemical polymerization (ECP), template polymerization, enzymatic polymerization, photopolymerization, plasma polymerization, chemical oxidative polymerization, and some other special methods. Exploiting the favorable properties of ICP makes them a suitable candidate for an appropriate composite system [25].

The current review article mainly focus on how to prepare pure PPy and organic/inorganic hybrid nanocomposites (various metal oxides or sulfides-based PPy composites, CNT or graphene) and discusses various techniques adopted for their preparation and various methods explained are chemical oxidative polymerization, electrochemical polymerization (ECP), template polymerization, enzymatic polymerization, photopolymerization, plasma polymerization and interfacial polymerization. PPy-based hybrid nanocomposites can be prepared in a variety of ways; the most popular methods are chemical and electrochemical polymerization. Because the chemical oxidative polymerization process is easily handled and allows for large-scale material synthesis, it is seen to be more practical for industrial use. The electrochemical synthesis method is a straightforward process that yields CPs in the form of free-standing, self-supporting films with a high degree of accuracy and purity. We have also focused on the use of PPy nanocomposites in various applications. Finally, we conclude the article with a discussion on future perspectives of polypyrrole based nanocomposites.

2. Synthesis of polypyrrole

An overview of all the proposed research methodologies for the synthesis of PPy composites is presented in this section.

2.1. Chemical oxidative polymerization of pyrrole

Chemical oxidative polymerization is a facile and easy method for synthesizing polypyrrole [19,26–28]. This method has been adopted to improve the properties, such as thermal stability, processability, and conductivity of PPy, for future advanced applications [29–31]. In this direction, various researchers have used different oxidants like FeCl₃, APS, and H₂O₂ - the pyrrole monomer. This reaction generally proceeds at a very fast rate. As reported by Yussuf et al. [32], better electrical conductivity has been achieved through the use of oxidant and surfactant ferric chloride (FeCl₃) ammonium persulfate (N₂H₈S₂O₈) and sodium dodecyl sulfate (C₁₂H₂₅NaO₄S), respectively. The result shows that FeCl₃ achieved better performance than N₂H₈S₂O₈ due to its lower resistivity of about 60 Ω at room temperature, indicating higher conductivity of the PPy samples with FeCl₃ as an oxidant. Wen et al. used the chemical oxidative polymerization method to synthesize PPy nanoparticles using FeCl₃ as a filler in electrically conductive adhesives to reduce electrical resistivity. This method is favorable, as there is no requirement for complex instruments [33]. Du et al. synthesized PPy using the chemical oxidative polymerization method and developed various morphologies like particles, nanotubes, and nanowires (NWs). The findings indicate that the morphologies of polypyrrole (PPy) can be effectively manipulated, exerting a significant impact on their thermoelectric properties. Notably, PPy nanowires demonstrate superior electrical conductivity and Seebeck coefficient when compared to various PPy structures, including particles, nanotubes, and nanowires. Consequently, PPy nanowires were selected for the fabrication of PPy nanowire/graphene thermoelectric composites in which both the electrical conductivity and Seebeck coefficient exhibited an increase with the rise in graphene content from 0 to 20 wt%, as well as with the elevated measured

temperature ranging from 300 K to 380 K. The highest power factor of $1.01 \mu\text{Wm}^{-1} \text{K}^{-2}$ at $\sim 380 \text{ K}$ was obtained for the PPy nanowire/graphene composites with 20 wt % PPy nanowire, which is about 3.3 times higher than that of the pure PPy nanowire [34].

The synthesis of two types of polypyrrole (PPy) was conducted through a chemical oxidative approach, utilizing distinct oxidizing agents—ammonium peroxydisulfate (APS) and ferric chloride (FeCl_3) by Sood et al. Subsequent analyses involved the examination of electrical resistivity and morphology using a two-probe technique and scanning electron microscopy (SEM), respectively. X-ray diffractometry was employed to discern the crystalline or amorphous nature of the synthesized polymers. Thermogravimetric analysis was performed to assess the thermal stability of the polymers in a nitrogen atmosphere. The findings revealed that PPy prepared with APS and FeCl_3 oxidants exhibited distinct resistivity characteristics, with FeCl_3 demonstrating higher conductivity at $2.22 \times 10^{-4} \text{ S/cm}$ compared to APS, which exhibited a conductivity value of $0.16 \times 10^{-4} \text{ S/cm}$. Further investigation indicated that using 1 M and 2 M concentrations of monomer and FeCl_3 oxidant, respectively, resulted in superior thermal stability compared to APS [35].

2.2. Electrochemical polymerization of pyrrole

Electrochemical polymerization is another important method for synthesizing conducting polypyrrole [36]. This method is environmentally friendly, facile, and has a low cost of fabrication under mild conditions [37]. Fig. 1 shows a general scheme for electrochemical polymerization [38]. Monomer units are adsorbed onto the surface of the working electrode resulting in one-electron oxidation to form a pyrrole cation radical. These cations then couple with themselves, with other cations or with neutral monomers from solution. In each case, this leads to the formation of a dimer dication, which undergoes a double deprotonation to give a neutral molecule. These more stable dimer radicals have a lower oxidation potential compared with the monomer units and chain growth then occurs by preferential coupling between the dimers and monomers. Anion (A^-) is required to maintain electro neutrality [38,39]. This route can easily control the process rate and lead to crosslinking between the polymeric chains during electro-deposition. The production of electroactive/conductive films is accomplished using this technique [40–42]. Adjusting electrolysis conditions such as electrode potential, solvent, current density, and electrolyte, the properties of the film are controlled [43–46]. This method is simple to produce CPs as free-standing films and colloids due to their purity and high precision rate of accuracy. Istakova et al. followed an electrochemical route for the synthesis of polypyrrole. The combination of all the benefits of electrochemical methods, including the wide range of precise oxidation potential variation, direct control of process speed and product yield, the ability to alter the nature of the doping anion/cation, and the absence of chemical oxidative reagents in the reaction mixture has been explained. The authors found that the yield of polypyrrole particles in the solution phase was approximately 6–9%, which was increased to 10–12 % with the addition of a 1 mM bromide redox mediator, that is, TBABr (tetrabutylammonium bromide). Again, the yield increased to 60–80 % when the perforated platinum disk was used as the working electrode instead of the carbon electrode with holes of 0.3 mm diameter [47].

Nautiyal et al. used this method to deposit PPy on a carbon steel substrate as an anticorrosive and antimicrobial material. They considered it the most efficient method due to its lower processability problem [48,49]. The authors used different dopants such as sulfuric acid (SA), sodium dodecyl sulfate (SDS), *p*-toluene sulfonic acid (*p*-TSA), and sodium dodecylbenzene sulfonate (SDBS). They explained the effect of different dopants on the passivation of carbon steel, which was explored by linear potentiodynamics and compared with morphology. The results showed that both *p*-TSA and SDBS contain extra benzene ring stacking together to form a lamellar sheet-like barrier to chloride ions, thus making suitable dopants for PPy coating in suppressing the corrosion at a significant level. Maiti et al. also electrochemically polymerized pyrrole and studied the effects of various factors such as polymerization time, monomer concentration, dopant concentration, and applied voltage on yield and conversion. The authors observed that with increasing monomer concentration, the yield also increased; on the other hand, the conversion decreased [50]. However, with the polymerization time, both conversion and yield increased. They also found that, at higher dopant concentrations, yield and conversion also increased because of the increased system current and higher charge taking place in the bath. The authors found that as the voltage

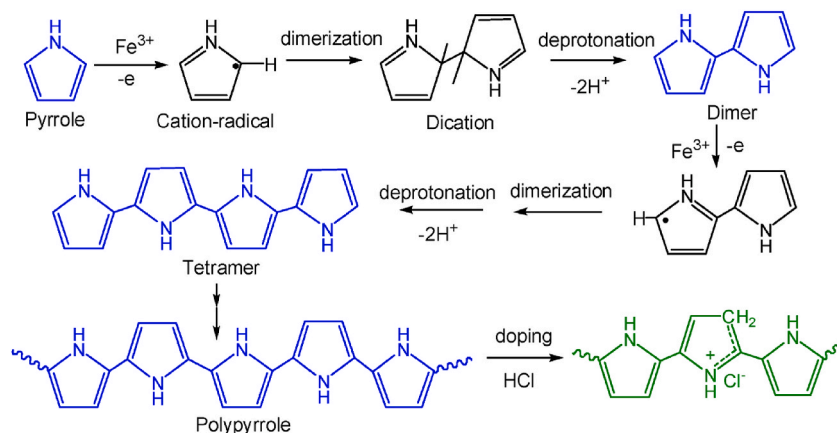


Fig. 1. Mechanism of Electropolymerization of pyrrole [38].

applied, both yield and conversion increased gradually to 2.5 V; however, there was a sharp increase beyond this voltage. It happened because of the considerable rise in ionization, which led to an increase in the number of charge carriers and, therefore, facilitated the polymerization process.

Kim et al. synthesized PPy films by an electrochemical method. They deposited them on an ITO electrode to enhance its performance, where PPy was responsible for improved conductivity and polydopamine (PDA) for better adhesion of the coating to the surface of the electrode surface [51]. Resultant PDA/PPy films exhibit significantly increased adhesion strengths up to $3.7 + 0.8$ MPa, and modified electrodes had electrochemical impedances two or three orders of magnitude lower than that of an unmodified electrode.

Polypyrrole nanowires synthesized by Ramirez et al. using mesoporous silica as a template generate a homogenous film over a thin layer of PPy so that PPy-nw grows within the nanochannels of the mesoporous silica and adheres firmly to the surface. SEM reveals the brush-type conformation of PPy-nw (30 nm in diameter). Using electrochemical techniques: a cheap, simple, highly repeatable method is used in situ to prepare electrodes modified with nanostructured polymers [52].

2.3. Photo-polymerization of pyrrole

Photopolymerization is also suitable for synthesizing Polypyrrole [53–60]. This method is attractive due to its easy processability, comparatively lower temperature, environment-friendly, and better thermal stability [61]. Rinaldi et al. performed solid-phase photopolymerization of pyrrole in the polyvinyl chloride (PVC) matrix. They initiated it with chlorine radical, the synthesis's polypyrrole reaction process. It is well-known that the chemical and electrochemical route for producing conducting polymers provides powders or intractable solids with low processability and weak mechanical properties. Therefore, the advantage of the photopolymerization method is that it allows better mechanical properties and polymer processability when different additives and flexibilities have been incorporated into the photopolymerizable formulations [62]. Kasisomayajula et al. explores the facile preparation of conductive polypyrrole coatings with optimized binding and conductive properties for various electronic applications, such as printing circuit boards and conductive inks, using a simultaneous photopolymerization method. This method involves the concurrent, independent polymerization processes of pyrrole and acrylate monomers to produce a conductive coating. AgNO_3 serves as the oxidizing agent for the photopolymerization of pyrrole, while Irgacure 907 is used as the photoinitiator for the acrylate monomer, 1,6-hexanediol diacrylate. Real-time Fourier Transform Infrared (RT-FTIR) spectroscopy characterization revealed that selecting appropriate initial concentrations of monomers and photoinitiators is crucial for achieving optimized conductive and binding properties in the final coating. Additionally, microscopic techniques such as TEM and SEM showed that the size, morphology, and dispersion of polypyrrole are influenced by the initial concentrations. Finally, conductivity measurements obtained via the four-point probe method and conductive AFM were correlated with the spectroscopic and microscopic characterization to determine the optimal conditions for preparing conductive polypyrrole/acrylate coatings using this method [55]. Asmussen et al. [57] reported the hybrid composite system through photopolymerization with both ultraviolet and visible light having wavelengths of 365 and 470 nm, respectively.

2.4. Plasma polymerization of pyrrole

Plasma polymerization is a crucial method to obtain a thin polymer film in the nanometer range [63–65]. It is an advantageous process, as it is solvent-free and can occur at room temperature [66]. Yague et al. performed plasma polymerization in a reactor under pulsed plasma conditions for 1–5 min. The plasma polymerization conditions described promote the formation of thin solid PPy films with slight roughness value and controlled thickness, which was further used in sensor applications [67]. Atmospheric Pressure Plasma Polymerization (APP) provides less extreme conditions for synthesizing plasma polymer films, which can have various properties and attach well to most substrates. To assess the active layer's suitability for electrochemical toxic gas sensors, resistance variations of the pPPy nanoparticles on interdigitated gas sensor electrodes through iodine doping were investigated. Consequently, the proposed APPJ device demonstrated the capability to produce high-density and ultra-fast single-crystalline pPPy thin films, presenting a promising solution for diverse gas sensor applications [68]. Park et al. used this technique to synthesize single-crystalline high-density pyrrole (pPPy) nanoparticles on different substrates such as gas sensor electrodes, which were further doped several times with 1g of solid iodine to increase the conductivity that has application in the gas sensor [69].

The volume change caused by doping/undoing of the polymer can lead to the separation of layers, which is the main reason for the device's failure in actuators. To overcome this problem and enhance the binding interaction with metal electrodes, plasma polymerization has been used to synthesize thin polymer films of uniform thickness. This process can be easily controlled by varying the polymerization conditions and having various biological applications [70].

2.5. Enzymatic polymerization of pyrrole

There was a need to synthesize PPy using a greener technique with fewer side products. Therefore, enzyme polymerization came into existence [71–73]. This method does not require harsh conditions, high temperatures, or harmful solvents. Thus, it can be considered an alternative polymerization method [74]. Enzyme catalysis helps synthesize a more defect-free polymer as the polymerization occurs in a more controlled manner at low temperatures. Since the oxidation potential (E_p) of pyrrole is higher ($E_p = 1.2\text{V}$) (Ag/AgCl), an enzyme that can directly oxidize the pyrrole monomer without making the reaction complicated was required. Therefore, Bouldin et al. used soybean peroxidase having an oxidation potential of 1.2V (Ag/AgCl) to oxidize the pyrrole monomer in which Poly(sodium 4-styrene sulfonate) (PSS) served as both a charge-balancing dopant and a dispersant for PPy to monitor alterations in the polymer's absorption spectra over time. The polymerization method, however, is adaptable to various dopants, including

smaller molecules like 10-camphor sulfonic acid. Spectroscopic analysis confirmed the conductivity of PPy, revealing that it could be synthesized with higher yields and faster rates at lower temperatures. Precise temperature regulation, coupled with the judicious selection of dopants, ensured the production of PPy with enhanced electrical conductivity, surpassing 3 S/cm [75].

KJ and their co-worker used enzyme polymerization to polymerize pyrrole using the *Trametes versicolor* Laccase (TvL) enzyme and dioxygen (O₂) in an aqueous solution at 3.5 pH [76]. The formation of PPy in its conductive bipolaron state has high absorption at wavelengths of 450 nm and 1000 nm. According to Bustamante et al., the enzymatic method for synthesizing PPy is eco-friendly. Therefore, they synthesized PPy using this method, in which soybean peroxidase was used as a catalyst along with natural redox mediators such as acetosyringone, syringaldehyde, and vanillin, which enhanced the yield and electrical conductivity of the conducting polymer without modification of their electronic structure [77].

2.6. Template polymerization of pyrrole

Template synthesis is an easy and efficient method to synthesize conducting polymer nanostructures. It consists of soft template and hard template methods [78]. A hollow polymer nanostructure is better used in energy storage devices. Therefore, Ahn et al. synthesized hollow spherical PPy nanoparticles using the surfactant template technique in an aqueous solution where surfactant molecules were required as vesicles to be used as the template. The results showed that the diameter of the hollow nanoparticles also increased because of the increase in pyrrole/SBD (Sodium Dodecyl Benzenesulfonate) molar ratio. Also, controlling the concentration of the surfactant easily regulated the diameter of the hollow nanoparticles. Following this adjustment, an exploration of size-dependent electrochemical properties, such as redox characteristics and charge/discharge behavior, was conducted. Capitalizing on the structural benefits, the specific capacitance of PPy hollow nanoparticles reached a maximum of 326 F/g, nearly double that of solid PPy nanospheres [79].

Bui et al. formed micro/mesoporous PPy (mp-PPy) using a Cu₃(BTC)₂ template by polymerizing the FeCl₃ vapor phase. Material characterizations confirmed the formation of Cl-doped PPy. Additionally, the resulting product exhibited intriguing microstructure features characterized by an octahedron-like shape and high porosity. These characteristics are likely attributed to the Cu₃(btc)₂ template. The porous PPy exhibited a BET surface area of 455 m²/g, with pore sizes distributed in the range of 1–10 nm. In initial cyclic voltammetry measurements, the micro/mesoporous PPy-modified electrode demonstrated a superior quasi-reversible electrochemical response for ferricyanide compared to a bare glass carbon electrode [80]. Therefore, Wang et al. reported a simple method for the synthesis of 1D and 3D PPy nanostructures using an MnO₂ template where MnO₂ started polymerization and also acted as the support for the growth of the PPy nanostructure. Solid MnO₂ was converted to soluble Mn²⁺ and, therefore, was eliminated after the polymerization; hence, this method is environmentally friendly. These PPy nanotubes have applications in supercapacitors as they can be used as electrode material [81].

Uemura et al. considered template synthesis a good technique for forming porous polymers. Showcased was a template synthesis of PPy within 3D coordination channels, resulting in a polymer material with specific porosity. This study has not only revealed distinctive pore functions inherent to PPy but has also positioned porous organic polymers at the forefront of extensive research, particularly for storage and separation applications. Their approach holds promise, offering advantages in tailoring porous structures through adjustments in the host matrix or preparation conditions. Furthermore, it provides opportunities for the development of novel porous properties, leveraging the attractive functions of polymers [82].

2.7. Interfacial polymerization of pyrrole

Interfacial polymerization is a slow and controllable method for the synthesis of pyrrole as compared to the conventional polymerization method. It is a supporting method for the massive production of nanospheres, ultrathin layers, and nanofibers of conducting polymers [83]. Therefore, several researchers have approached interfacial polymerization because of certain limitations of conventional synthesis methods of conducting polymers [84]. Katarzyna et al. proposed a novel method for synthesizing working polymer

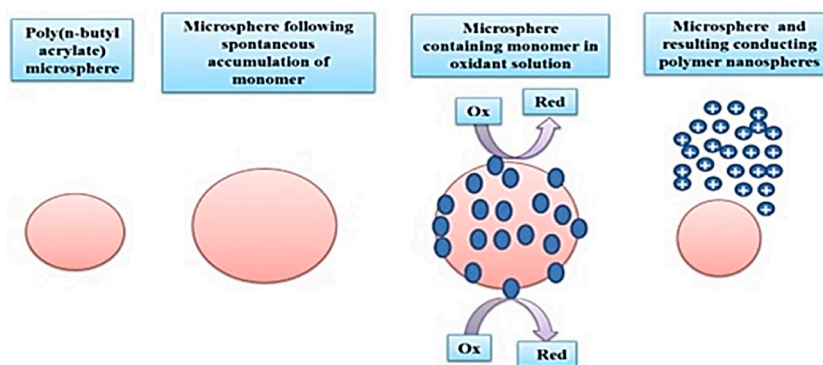


Fig. 2. Schematic representation of the conducting polymer nanosphere formation.

nanoparticles with a narrow size distribution and high electrochemical activity without using any template or surfactant, as shown in Fig. 2.

The authors have claimed that prepared nanostructures have great potential to be used in various fields ranging from additives, conductive coatings, and increasing electronic conductivity to electrochemical sensor applications [85,86]. Yang et al. used interfacial polymerization to prepare the PPy film using Span80 surfactant. The results indicated that with an increase in the surfactant concentration, the specific capacitance increased, and it was found to be 368.18F/g at 3.32 g/L of Span80 concentration [87]. Hazarika et al. considered that nanofibers and nanotubes of PPy are better suited to be used in supercapacitors and sensors than bulk material. They used oil-water interfacial polymerization to form 1-D PPy nanofibers using HCl and *p*-toluene sulfonic (*p*-TSA) as dopants. The method was cost-effective and yielded good results. The authors also obtained very interesting results that show that the average diameter of PPy nanofibers doped with *p*-TSA was smaller than that of nanofibers doped with HCl. An absorption study for these nanofibers showed a higher conjugation length of PPy nanofibers doped with *p*-TSA [88]. Shen et al. synthesized a porous PPy film via interfacial polymerization using ionic liquid 1-butyl-3-methylimidazolium tetrachloroferrate [Bmim(FeCl₄)] as an oxidant. When the oxidant concentration was increased to 0.075 M, π - π interactions between pyrrole cations and iminazole ring Bmim(FeCl₄) affected the packing of PPy chains. They caused the formation of the porous structure of PPy. Also, the electrochemical performance of the PPy porous structure displayed the best specific capacitance of 170F/g at a current density of 2 A/g in 1 M H₂SO₄ solution and has potential applications as supercapacitor materials [89].

3. Properties of polypyrrole

Polypyrrole is known for its various excellent properties. There is a direct link between the synthesis, properties, and application of the materials. The change in the structure of materials (shape and size) through the synthesis process greatly impacts the material's properties. In this section, the authors have given a detailed discussion of the significant properties of polypyrrole, like electrical, mechanical, thermal, optical, and magnetic properties, which the synthesis process has tuned.

3.1. Electrical properties

Conducting polymers possess the delocalization of π electrons, which is why they exhibit good electrical properties and can be used in various electronic devices [90]. Electrical properties are also affected by doping and the route adopted for the preparation of the polymer [91]. Among numerous conducting polymers, polypyrrole possesses good electrical conductivity, and this property can be further improved by using an appropriate oxidant during polymerization. Yussuf et al. used two different oxidants to polymerize the pyrrole monomer, which were FeCl₃ and ammonium persulfate (N₂H₈S₂O₈). They reported that the sample containing FeCl₃ had higher conductivity due to the formation of fibrillar structural morphology, which had a better ability to transfer electrons than the sample containing ammonium persulfate, which had a spherical structure. The authors also studied the effect of FeCl₃ and monomer pyrrole concentration on polypyrrole resistivity of polypyrrole [32]. The researchers studied the electrical resistance of PPy that was produced through modified chemical oxidation polymerization using FeCl₃·6H₂O as an oxidant in aqueous medium [92–95]. In addition, they prepared their compounds with metallic fillers. The authors found a good correlation between the morphology of the PPy and the electrical properties. In the pure form of PPy, the authors observed the pores and the weak linkage (in polymeric chains) in their structural morphology. Due to this, no proper path was framed for the movement of the charge carrier, which reduced the conductivity of PPy [96]. The parameters important for the electrical conductivity of PPy are reaction temperature, ratio of oxidant to pyrrole, reaction time, and processing method. Among all these parameters, the processing technique is the basis that deeply affects the electrical conductivity as it is directly linked to the structural morphology. Majumdar et al. evaluated the effect of different dopants (HCl, CSA, PTSA) on PPy film coated on FP substrate conductivity. The results showed that the conductivities of the PPy film increased

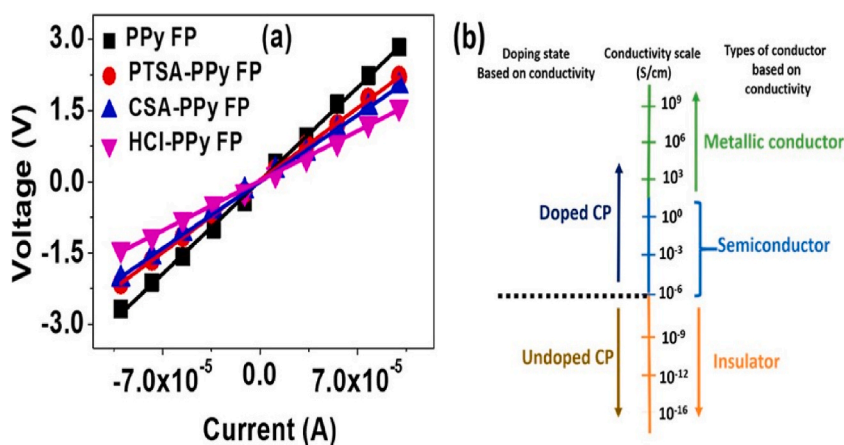


Fig. 3. (a) *I*-*V* plots of PPy-FP, PTSA-PPy-FP, CSA-PPy-FP, and HCl-PPy-FP. (b) Possible conductivity range of insulator to metallic conductor [97].

from 1.78×10^{-5} S/cm (undoped) to 3.34×10^{-5} , 2.49×10^{-5} , 2.30×10^{-5} S/cm with the use of HCl, CSA and PTSA dopants, respectively, shown in Fig. 3 [97].

3.2. Mechanical properties

Mechanical properties, for example-toughness, stiffness, and strength, depend upon the molecular weight of the polymer [98–104]. If the molecular weight of the polymer is high, then the viscosity, transition temperature, and mechanical properties will also be increased and vice-versa. In other words, it can also be defined as the capacity for a material to take the mechanical load upon itself without breaking or deforming. PPy has average mechanical properties that can be enhanced by adding or incorporating fillers [105, 106].

The mechanical properties of the PPy paper have been improved by Zhang et al. by following the in situ polymerization method. The authors used a dopant and dispersant, i.e., Sulfonated alkaline lignin (SAL), horseradish peroxidase polymerized sulfonated alkaline lignin (HSAL), and poly(sodium styrene sulfonate) (PSS) for the preparation of PPy paper. The primary purpose of using dopant and dispersant was to provide a significant interfacial interaction between cellulose fibers and PPy due to abundant carboxyl, phenolic hydroxyl, and sulfonic groups of HSAL. It resulted in an improvement in molecular weight that facilitated the enhancement of mechanical properties. The authors confirmed that out of (HSAL-PPy)n/paper and (PSS-PPy)n/paper, (HSAL-PPy)n/paper displayed superior mechanical properties because of cellulose compatibility, anti-oxidant capability, excellent dispersibility along with the hydrophobicity of HSAL. Even (HSAL-PPy)n/paper showed stronger tensile strength as compared to the (SAL-PPy)n/paper, which was attributed to the high MW (molecular weight) of HSAL that allowed the smooth polymerization of pyrrole monomer over the surface of cellulose fibers [107].

3.3. Optical properties

The optical properties of a material are associated with the modification that occurs when light interacts with a particular material. It includes absorption, reflection, refraction, etc [108]. Zhao et al. synthesized PPy and its five derivatives using interfacial polymerization using APS as an oxidant. They studied their NLO (Nonlinear Optical Measurements) properties for different applications using the Z-scan technique measurements at 532 nm. At a consistent mass concentration of 0.15 mg mL^{-1} , all PPy derivatives displayed evident reverse saturable absorption behavior, while PPy exhibited a saturable absorption response.

Additionally, notable distinctions in their nonlinear optical performances were observed, underscoring the impact of the aromatic segments of conjugated polymers on their optical nonlinearity [109]. Thombare et al. synthesized PPy films using *p*-Toluenesulfonic acid (*p*-TSA), oxalic acid, and H_2SO_4 and reported their optical conductivity. The best optical conductivity was exhibited by *p*-TSA [110,111]. The chemical oxidative polymerization of pyrrole monomer for the synthesis of polypyrrole was done by Gurbuz et al. Firstly, they prepared an ionic liquid of tributylamine and oleic acid salt to polymerize pyrrole. After that, the optical properties of prepared PPy were measured through an ultraviolet–visible spectrometer in the wavelength range of 270–800 nm. The penetration of a particular wavelength of light into the material is associated with the absorption coefficient (α), which further helps to calculate the optical band gap (E_g). Results showed that the E_g of the prepared sample decreased from 4.36 to 4.27 eV, which corresponds to the blue and green light for the infrared (IR) detector and optoelectronic devices [112].

4. Preparation of polypyrrole composites

Composite is something that is prepared by adding suitable fillers to the matrix. These are synthesized to enhance the properties of the individual matrix. There are three types of composites, i.e., MMC (metal matrix composites), CMC (ceramic matrix composites), and PMC (polymer matrix composites). Among all these matrix systems, PMCs are widely accepted by the scientific community due to their lightweight, easy processability, cost-effectiveness, no corrosion, and accessible transportation [113]. Therefore, several methods are available in the literature mentioned here in detail to prepare these composites, such as in situ, enzymatic, interfacial, electrochemical, emulsion methods, etc.

4.1. In situ chemical oxidative polymerization

In situ, chemical oxidative polymerization is widely accepted for preparing PPy-based composites [30,114]. Many researchers have moved towards this method due to its significant use in the application part. The product formed through this route is very effective and of good quality because the monomer polymerization occurs during the reaction. Nanocomposites comprising nanoclay, graphene, and polypyrrole (PPy) were successfully synthesized through both in-situ and ex-situ chemical oxidative polymerization methods by Oraon et al. The electrochemical performance of these nanocomposites was assessed through cyclic voltammetry, potentiostatic-charging–discharging, and electrochemical impedance spectroscopy. Comparing the two synthesis approaches, the in-situ nanocomposite exhibited a higher specific capacitance (347 F/g) than the ex-situ nanocomposite, particularly at a scan rate of 10 mV/s in a 1 M KCl electrolyte. The study also investigated the impact of sequentially adding nanoclay on the specific capacitance. Overall, these findings underscore the promising potential and appealing applications of the synthesized nanocomposite for energy storage purposes [115]. Wen et al. reported the doping of conjugated poly(pyrrolidone) (PPy) nanoparticles into the matrix of electrically conductive adhesives (ECAs) and developed low-electrical resistivity interconnecting materials. The developed materials' electrical conductivity improved by adding a small quantity of PPy NPs to silver-flakes-filled ECAs and traditional epoxy resin. The authors measured the

electrical resistivity for 70 wt% silver-filled ECAs and found that the resistivity decreased from $1.6 \times 10^{-3} \Omega \text{ cm}$ to $9.4 \times 10^{-5} \Omega \text{ cm}$ at 2.5 wt% of PPy [33]. According to J. Marimuthu et al., the metal oxide/PPy core-shell structure displayed better properties than the individual component. They prepared PPy/CuO nanocomposites following the in situ chemical oxidative polymerization method using FeCl_3 as an oxidizing agent for fuel cell application. The product obtained was fine black color nanoparticles [116]. Bacterial nanocellulose (BNC) is in high demand for polymeric hybrid nanocomposites because of its easy synthesis and low cost. Therefore, Daliana Muller et al. formed BNC/PPy.CuCl₂ nanocomposite by one step in situ oxidative polymerization using CuCl_2 dehydrate as an oxidant and conducting material in the nanocomposite having 0.04 and 0.08 molL^{-1} of pyrrole concentration. The authors found that as the pyrrole concentration increased from 0.04 to 0.08 molL^{-1} for a 2:1 M ratio, there was an increase in PPy incorporation into the BNC matrix [117]. The synthesis of a composite comprising polypyrrole (PPy) quantum dots and graphene oxide (GO), denoted as PPy/GO, is achieved through an in situ polymerization process by Hamid et al. [118]. The PPy/GO composite exhibits remarkable optical properties, particularly in UV, Vis, and near-IR regions, boasting a small bandgap of 1.66 eV. These attributes position the composite as a promising candidate for a photoelectrode for H_2 gas evolution in sewage water (third treated stage, pH 7.2). The H_2 evolution rate is quantified through electrochemical measurements of current density. The impact of on/off chopped light on the photoelectrode's responsivity is explored, revealing an increase in J_{ph} values from -4 to $-12 \mu\text{A cm}^{-2}$, respectively. Additionally, the J_{ph} value changes from -4.32 to $-4.89 \mu\text{A cm}^{-2}$, correlating with a decrease in monochromatic wavelengths from 730 to 440 nm, respectively. This electrochemical testing underscores the PPy/GO thin film photoelectrode's efficacy in H_2 gas production from wastewater.

Xie et al. produced a lightweight, environmentally friendly, and wearable PPy/cotton composite by in situ polymerization using a 1: 4, 1:1, 1:2, 2:1, 3:1, and 4:1 pyrrole/ $\text{FeCl}_3 \cdot 6\text{H}_2\text{O}$ ratio having excellent electrical, mechanical and electrothermal properties. SEM images of raw cotton and PPy/cotton composite synthesized using different ratios of Py/ $\text{FeCl}_3 \cdot 6\text{H}_2\text{O}$ are shown in Fig. 4 [119]. The morphology obtained from the prepared composites displayed that the amount of PPy on the cotton fabric had increased with increasing Py and FeCl_3 ratios. It is exciting to see that when the ratio of Py and FeCl_3 is 2:1, the amount and weight gain rate of PPy over the cotton fabric are more significant than the other composites. The authors also showed decreased resistivity with increased Py/ $\text{FeCl}_3 \cdot 6\text{H}_2\text{O}$ concentration. It had the lowest value of 0.37 cm at 2:1, which didn't change further due to increased PPy formation [119].

Maity et al. followed the same in situ polymerization route for synthesizing polypyrrole-based knitted, conductive, and nonwoven composite fabrics using FeCl_3 as an oxidant [120]. The procedure for composite fabrication is depicted in Fig. 5 for better understanding. The surface resistivity of prepared composites was in the range of 1–2 k Ω . The authors further investigated the response of these compounds to humidity, pH, and mechanical strain. The study explores the impact of humidity and mechanical strain on various fabrics. Consistent trends are observed across all fabric types in terms of resistivity concerning pH. The composite fabric resistance rises with higher alkalinity in pH. However, when subjected to bending strain, cotton fabrics show a significant decrease in resistance, polyester fabrics experience a sharp increase, and wool fabrics initially decrease and then increase in resistance. In terms of humidity sensitivity, sigmoid curves are evident for all fabric types.

A highly flexible and high-performance negative electrode, constituting a PPy/ $\text{TiO}_2/\text{Ti}_3\text{C}_2\text{TX}$ nanocomposite film, was fabricated by Azizi and his co-worker through the electrochemical deposition of PPy/ TiO_2 onto carbon cloths (CC) as a substrate [121]. Moreover, an asymmetric supercapacitor was constructed by combining PPy/ $\text{TiO}_2/\text{Ti}_3\text{C}_2\text{TX}$ as the negative electrode with acid-treated carbon cloth (TCC) as the positive electrode, thereby expanding the potential window of the system. The assembled device demonstrated noteworthy specific capacitance of 191.4 mF cm^{-2} at 1.0 mA cm^{-2} , excellent energy density of 1.2 mWh cm^{-3} at a power density of 23.1 mW cm^{-3} , as well as outstanding power density of 41.5 mW cm^{-3} at 0.12 mWh cm^{-3} . The capacitance retention remained at 87 %

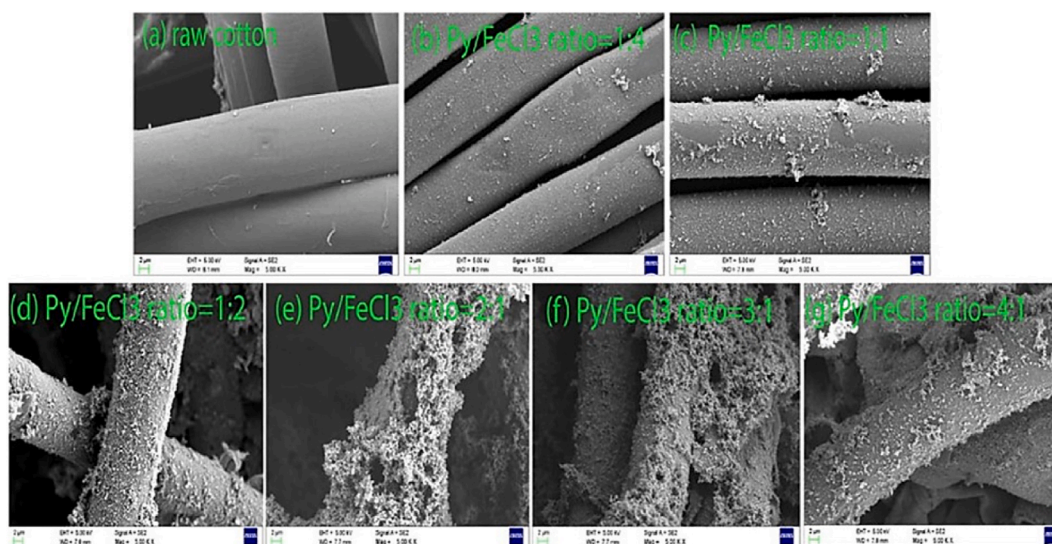


Fig. 4. SEM images of the surface of (a) raw cotton and (b–g) PPy/cotton composites with different Py/ FeCl_3 ratios [119].

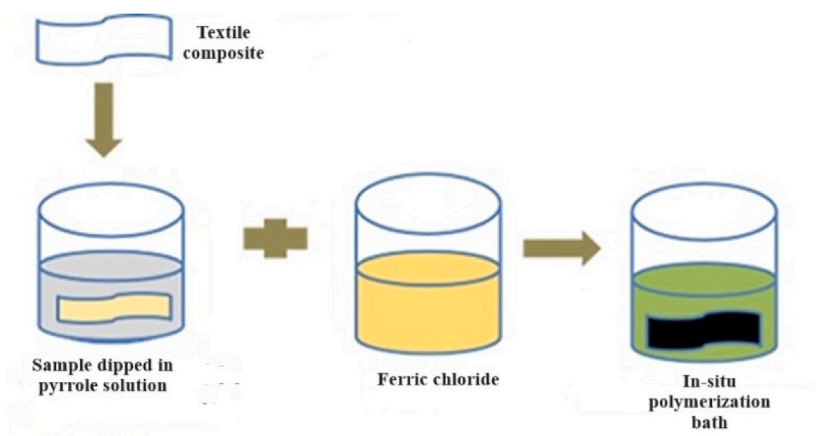


Fig. 5. In situ chemical polymerization of pyrrole onto textile fabrics.

after 13,000 cycles, underscoring the significant potential of the PPy/TiO₂/Ti₃C₂TX nanocomposite film as an electrode material for the fabrication of asymmetric supercapacitors. Various compositions of PPy embedded with tantalum disulphide (TaS₂) were synthesized using the chemical polymerization technique by Kumar et al. [122]. The AC conductivity of these composites was investigated at room temperature across a frequency range of 50 Hz to 5 MHz. The AC conductivity exhibited an increasing trend with the rising weight percentage of TaS₂, attributed to the hopping of polarons. Specifically, the PPy/TaS₂-50 wt% composite demonstrated a conductivity of $4.6 \times 10^{-3} \text{ Scm}^{-1}$ at 100 Hz, outperforming other compositions. The dielectric response of these composites was interpreted through Maxwell–Wagner polarization, while the tangent loss curves were analyzed using the Rezlescu model. These versatile composites hold potential for applications in the design of low and mid-frequency devices.

Utilizing an in situ chemical polymerization method, composites of polypyrrole/tungsten disulphide (PPy/WS₂) were synthesized with varying compositions, specifically 10, 20, 30, and 40 wt% of WS₂ in PPy by Kumar et al. The structural and morphological characteristics of these composites were thoroughly examined. AC response studies of the composites were conducted at room temperature across a frequency range of 50 Hz–1 MHz. In comparison to pristine PPy, the composites demonstrated heightened conductivity, as evidenced by the complex plane impedance plots. This enhancement suggests a conduction mechanism attributed to the

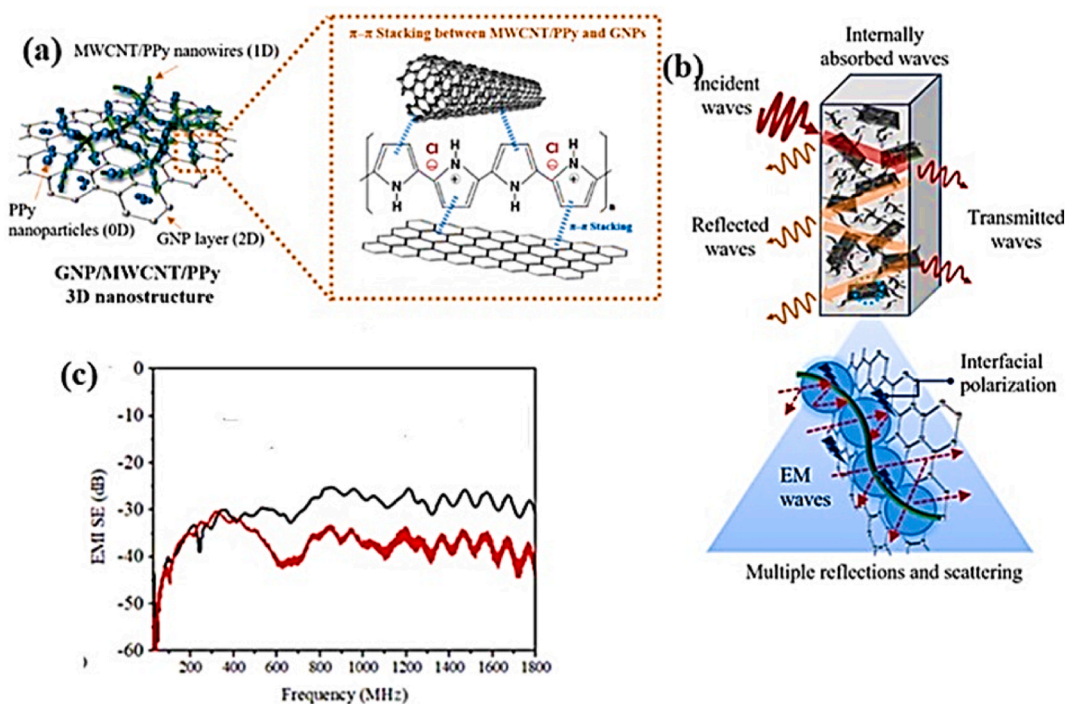


Fig. 6. (a) Schematic illustration of 3-D nanostructure of GNP/MWCNT/PPy and interactions between GNPs, MWCNTs and PPy (b) Shielding mechanism of GNP/MWCNT/PPy/PU nanohybrid (c) Results of GNP/MWCNT/PPy/PU with different PPy contents [126].

hopping of charge carriers. The analysis of loss tangent curves for the composites was elucidated using the Rezlescu model [123]. Sutar et al. synthesized Zinc-cobalt oxide nanoparticles were produced through a hydrothermal method, and subsequently, polypyrrole and zinc cobalt oxide (PPy/ZCO) composites were synthesized using an in-situ chemical polymerization approach [124]. The electrical properties of the PPy/ZCO composites were investigated with varying concentrations of ZCO in the frequency range of 10^2 – 10^6 Hz. The alternating current (ac) conductivity plotted against frequency displayed a direct current (dc) plateau between 10^2 – 10^6 Hz, indicating an isolated network within the composites. At higher frequencies, there was an increase in ac conductivity following the universal dynamic response (UDR). The UDR suggested that conduction in the PPy/ZCO composites occurred through hopping along the polymer chains due to the presence of filler nanoparticles. The Nyquist plot, illustrating the real and imaginary parts of impedance, revealed that conduction involved contributions from both grains and grain boundaries. Gahlout et al. prepared polypyrrole-MWCNTs/polyurethane composites in which polyurethane (TPU) is used as matrix and polypyrrole/MWCNT as filler inheriting conducting, dielectric and magnetic attributes of polypyrrole/MWCNT filler using in-situ polymerization of pyrrole monomer by chemical oxidative method. The study examined how the content of polypyrrole (PPy) and multiwalled carbon nanotubes (MWCNTs) impacts the electrical and microwave shielding effectiveness of thermoplastic polyurethane (TPU) composites, aiming to assess their potential as efficient electromagnetic interference (EMI) shields [125]. Lin and his co-worker reported synthesis of graphene nanoplatelet (GNP)/multiwalled carbon nanotube (MWCNT)/PPy hybrid filler using in-situ chemical oxidative polymerization method. Hybrid fillers were integrated into polyurethane (PU) to produce nano-hybrids consisting of GNP/MWCNT/PPy/PU. The remarkable electrical conductivity of these nano-hybrids was achieved through a synergistic enhancement facilitated by the exceptional conductivity of the hybrid fillers. Through optimization experiments, we identified the ideal formulation for crafting three-dimensional (3D) nanostructures of GNP/MWCNT/PPy. Employing this formulation, we successfully generated two-dimensional GNP/PPy nanolayers extensively coated with one-dimensional MWCNT/PPy nanowires, which interconnect to create a 3D GNP/MWCNT/PPy nanostructure as shown in Fig. 6 [126]. When integrated into a polyurethane (PU) matrix to create a nano-hybrid, these 3D nanostructures establish a continuous network of conductive paths comprised of GNP–PPy–CNT–PPy–GNP and further used for EMI shielding [126].

Conducting polymer hydrogels composed of polypyrrole (PPy) and chitosan (CS) are prepared by polymerizing pyrrole using methyl orange (MO) as the dopant and $\text{Fe}_2(\text{SO}_4)_3$ as the oxidant in an aqueous CS solution by Chen et al. These PPy/CS composite hydrogels not only exhibit good electrical conductivity but also demonstrate excellent swelling/deswelling behavior, attributed to the integration of one-dimensional conducting PPy blocks within the hydrogel network. The study investigates the effects of the oxidant amount and ionic strength on the physical properties of PPy/CS composite hydrogels. The findings indicate that PPy/CS composite hydrogels have enhanced water absorbency in saline solutions compared to conventional polyelectrolyte hydrogels [127].

4.2. Electrochemical polymerization

The electrochemical method is a simple technique that can be easily monitored or controlled and leads to the formation of very thin films within the range of a few micrometers [128]. This method is also less time-consuming and leads to more homogeneous product formation than the chemical method [129]. Jafari et al. synthesized PPy/nanoclay film by electrochemical polymerization. Results exhibited dense morphology of pure PPy when compared to PPy/nanoclay film. Moreover, the PPy/nanoclay nanocomposites exhibited a porous configuration in contrast to PPy alone, a feature ascribed to the incorporation of PPy into the clay galleries. The authors claimed that this notably porous structure would substantially amplify the surface area available on the coated fiber, thereby

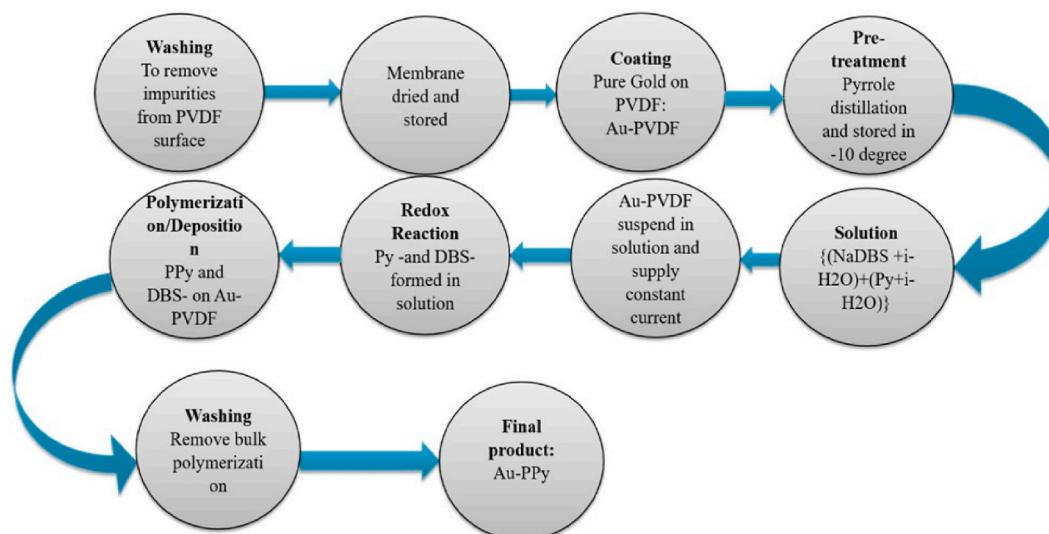


Fig. 7. Step-by-step synthesis of PPy actuator.

augmenting the extraction efficiency in solid-phase microextraction (SPME). This assertion was validated by the successful detection of diazinon and fenthion pesticides through gas chromatography corona discharge ion mobility spectrometer (GC-CD-IMS) analysis [130]. Castro et al. synthesized a novel PPy/Cashew gum composite electrochemically via potentiostatic and potentiodynamic techniques. The composite was found to have better conductive properties, ease of synthesis, flexibility, etc [131,132]. Gupta et al. electrochemically deposited Ag nanoparticles on PPy. According to them, there was no need to add any additive in the electrochemical deposition of silver metal. There was no generation of any byproduct, and it also led to the uniform distribution of Ag nanoparticles. This could be further exploited for the fabrication of novel and inexpensive hydrogen peroxide sensors [133].

Panda et al. formed an actuator based on gold PPy by electrochemical polymerization using sodium dodecylbenzene sulphonate (SDBS), as shown in Fig. 7 [134]. Mudila et al. synthesized Graphene oxide/Polypyrrole nanocomposites using ferric chloride as an oxidant for electrocapacitive performance. The result showed that PNC with 20 % w/w of GO offers the highest C_s of 1073.64 compared to 92.33 for pure PPy at a scan rate of 0.001 V/s. PNCs showed a low electrocapacitive decrease during the first 500 cycles at a scan rate of 0.1 V/s, indicating their appreciable electrochemical performance for fabricating supercapacitor electrodes [135].

A single-step electrochemical synthesis method was employed to create a novel composite on carbon fabric consisting of graphitic oxide, polypyrrole, and 2-acrylamido-2-methyl-1-propanesulfonic acid by Yazar et al. [136]. This composite was designed to serve as a highly efficient positive electrode for supercapacitor applications. The 2-acrylamido-2-methyl-1-propanesulfonate monomers acted as dopants within the 3D polypyrrole network, forming a synergistic coupling with graphitic oxide. These monomers, with their free acrylic groups, interacted to generate a polymer-hydrogel layer on the external surface, facilitating the transport of aqueous electrolyte ions inside the electrode. By carefully adjusting the dopant concentration to 0.01 M, the most effective electrode material was synthesized. In a full-cell configuration utilizing the composite electrode and a graphite counter electrode, the system operated at 2.2 V in a 3 M NaCl solution, achieving values comparable to the highest performance reported for aqueous supercapacitors. This cell demonstrated an impressive capacitance of 698.8 F/g at 5 mV/s and maintained its initial value even after undergoing 10,000 continuous cyclic voltammetry (CV) cycles at 1000 mV/s. Furthermore, it exhibited a high-energy density of 446.1 W h kg⁻¹ at a power density of 366.7 W kg⁻¹, with a retained energy density of 65.2 W h kg⁻¹ at 18.3 kW kg⁻¹. Remarkably, the asymmetric capacitor, with a 1 × 1 cm² area, successfully illuminated a red light-emitting diode. A one-step electrosynthesis technique to fabricate polypyrrole (PPy)/graphene oxide (GO) composites on a graphite felt (GF) electrode was done by Lv et al. This involved electropolymerization of pyrrole using GO as the anionic dopant. The resulting PPy/GO composites exhibited uniform coating on the GF surface, presenting enhanced surface area, electronic conductivity, biocompatibility, and stability when compared to electrodes modified solely with PPy or graphene. In a dual-chamber microbial fuel cell (MFC), the GF anode modified with PPy/GO demonstrated a maximum power density of 1326 mWm⁻² (obtained from linear sweep voltammetry at a scan rate of 0.5 mVs⁻¹). This value was significantly higher than that of the unmodified GF anode (166 mWm⁻²), electrochemically reduced GO-modified GF anode (318 mWm⁻²), chemically reduced GO-modified GF anode (924 mWm⁻²), and PPy-modified GF anode (1100 mWm⁻²). These findings highlight the effectiveness of PPy/GO composites, synthesized through a straightforward electropolymerization approach, as valuable materials for enhancing electricity generation and ensuring long-term stability in microbial fuel cells (MFCs) [137].

4.3. Enzymatic polymerization

Polymerization, in which enzymes are used as unique biocatalysts, can be considered the third phase of polymer synthesis. Interestingly, classical catalysts like Lewis acids, Brønsted acids, Lewis bases, and radical-generating compounds were used in the first phase of polymeric synthesis, which started in the 1920s. However, in the second phase of polymeric synthesis (starting in the 1950s), metathesis catalysts based on transition metals, Ziegler-Natta catalysts, and rare earth metal-based catalysts were used for polymerization [138]. This synthesis method uses a suitable catalyst enzyme and does not require any harsh reaction conditions. It is a more controlled one-step process [139]. German et al. used glucose oxidase (GOx) to synthesize the PPy composite. PPy/GOx composite was formed using 0.05 molL⁻¹ glucose, 0.75 mgmL⁻¹ Gox, and 0.50 molL⁻¹ pyrrole at room temperature in darkness. The PPy/GOx composite nanoparticles were free of surfactants and have applications in the biomedical field. Using this technique, they also synthesized a PPy nanocomposite with glucose and gold nanoparticles, as shown in Fig. 8.

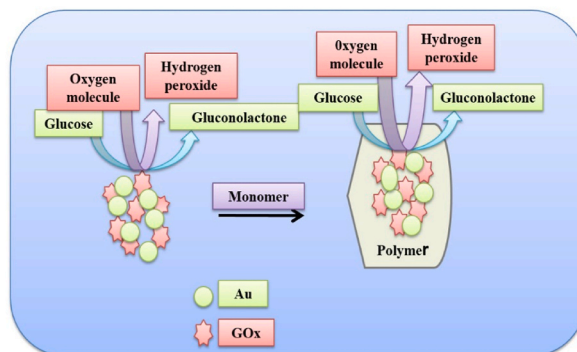


Fig. 8. The formation of polymer/AuNPs-GOx-based nanocomposites by enzymatic polymerization.

AuNP (0.6 mmol L^{-1}) was the most appropriate concentration for forming the PPy nanocomposite. Synthesized PPy nanocomposites are known to have applications in biosensors [140]. Park et al. followed an in situ enzymatic polymerization route for the preparation of multiwalled carbon nanotubes (MWCNTs) coated polypyrrole (PPy) composites catalyzed by a laccase (benzenediol: oxygen oxidoreductase) from *Trametes versicolor* which confirms the formation of MWCNTs/PPy composites in which the use of laccase, the composites become duller and less transparent than that of pristine MWCNTs [141].

4.4. Template polymerization

According to Du et al., graphene is a suitable filler for polymer nanocomposites [142], and PPy/Graphene composites can have applications in supercapacitors lithium. They synthesized PPy-NW/graphene TE (thermoelectric) composites by soft template polymerization method using cetyltrimethylammonium bromide (CTAB) as the template, as shown in Fig. 9. Kim et al. used the template polymerization method to synthesize PPy and PANI-coated MWCNTs using HCl as an oxidizing agent and APS as an initiator for their application in EMI shielding [143].

4.5. Interfacial polymerization

Interfacial polymerization is an easy and simple route to carry out a controllable and slow-rate reaction. It is typically executed in a biphasic system (organic/aqueous). For the synthesis of polypyrrole-based conductive composites, pyrrole monomer is dissolved in an organic solvent with oxidant addition [143–145]. Many researchers adopted this method for polymerization purposes, Georgakilas et al. synthesized two types of PPy/CNT composites, PPy/MWNT-f-ODA and PPy/p-MWNT via one-step interfacial polymerization using $\text{Fe}(\text{NO}_3)_3 \cdot 9\text{H}_2\text{O}$ as an oxidant. In this method, the rate of reaction is low, which allows the trapping of nanostructures in a controlled manner, which further leads to a better dispersion of nanostructures like carbon nanotubes in the matrix of polymer, which is an advantage of this method. This method also allows the synthesis of highly soluble PPy using polystyrene sulfonate that acts as a counterbalancing anion [84]. The liquid-liquid interfacial polymerization route was followed by Bora et al. for the production of a PPy/Graphene (GR) composite. The authors found that the obtained composites had high electrical conductivity, thermal stability, and good electrochemical properties [146]. The electrical conductivity of pure conjugated PPy and its composites with graphene was 0.210 S/cm and 50.4 S/cm , respectively. The increment in electrical conductivity of PPy/Graphene (GR) composites compared to the pure PPy was due to the high surface area and aspect ratio of the GR sheets filler functioning as a conducting bridge between matrix particles. Tian et al. successfully crafted the core-shell structure PPy@PANI by utilizing as-prepared PPy microspheres as nucleation sites for aniline monomer polymerization for EMI shielding, illustrated in Fig. 10 [147]. Result states that microwave absorption of PPy@PANI composites can be simple modulated not only by the thickness of the absorbers, but also the shell thickness to satisfy the applications in different frequency bands.

5. Properties of polypyrrole composite

5.1. Electrical properties

Materials are generally classified into semiconductors, conductors, and non-conductors based on their electrical properties [101, 148–155]. Various researchers have prepared compounds with fascinating electrical properties for electromagnetic interference shielding, sensors, and biomedical applications [156]. Utilizing an electrostatic self-assembly approach, Jian et al. synthesized carbon quantum dots (CQDs) reinforcing polypyrrole nanowires (PPy-NW). The resulting CQDs/PPy-NW composite exhibited exceptional electrochemical properties attributed to its distinctive dotted line structure, offering a large specific area, increased active sites, and impressive electronic conductivity. Consequently, the composite electrode showcased a specific capacitance of 306 F/g at a current density of 0.5 A g^{-1} , maintaining 66.8 % capacitance even with an 80-fold increase in current density (from 0.5 to 40 A g^{-1}).

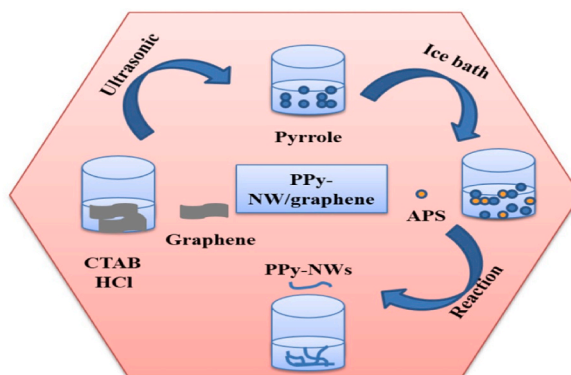


Fig. 9. Schematic representation of the formation of PPy-NW/graphene composite.

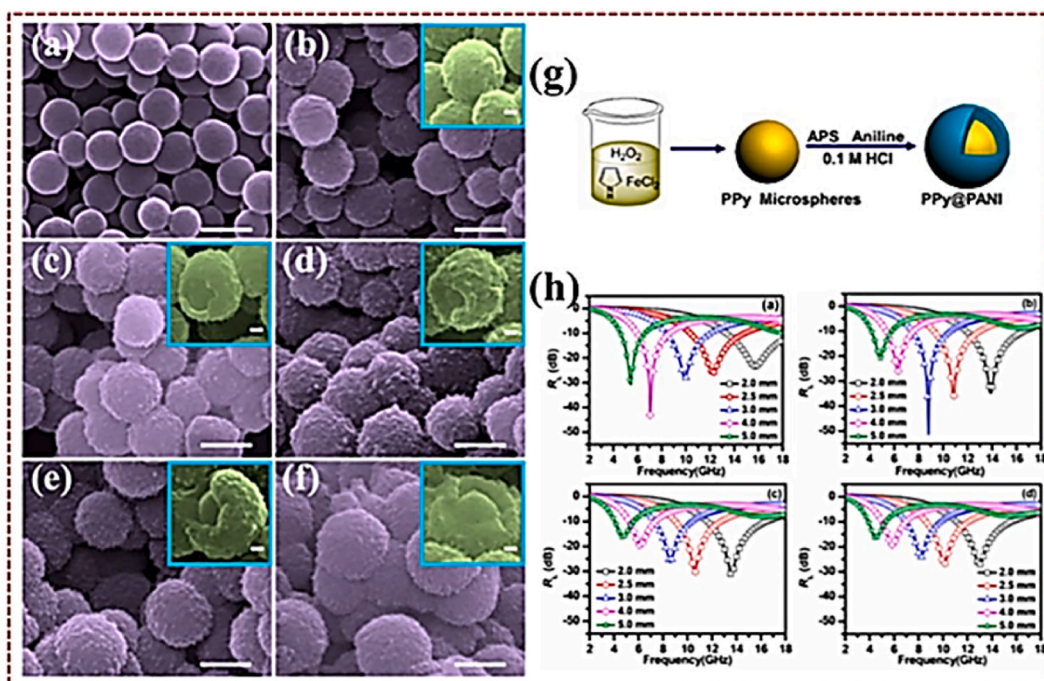


Fig. 10. (a) SEM images of PPy microspheres and core shell PPy@PANI composites with different PANI content: PPy@PANI-0.4 (b), PPy@PANI-0.8 (c), PPy@PANI-1.2 (d), PPy@PANI-1.6 (e), and PPy@PANI-2.0 (f). Schematic illustration of preparing core shell PPy@PANI composites (g), RL curves of PPy@PANI at some different matching thicknesses (h) [147].

Furthermore, the symmetric supercapacitor crafted from this composite demonstrated a substantial areal capacitance of 248.5 mF cm^{-2} at 0.2 mA cm^{-2} and exhibited commendable rate capability. Even at a high current density of 5 mA cm^{-2} , the supercapacitor exhibited robust cycling stability with an 85.2 % capacitance retention after 5000 cycles. The remarkable electrochemical properties underscore the considerable potential of CQDs/PPy-NW in advancing high-performance supercapacitor electrode materials [157].

Muller et al. found that with an increase in PPy concentration, electrical conductivity also increased from 1.64×10^{-4} to $1.54 \times 10^{-3} \text{ S/cm}$ for the 2:1 M ratio 2:1 which further got enhanced with an increase in molar ratio as shown in Table 1 which can be due to the rise in the concentration of copper chloride [117]. Xie et al. studied the effect of the PPy/ $FeCl_3$ ratio on the resistivity of the PPy/cotton compound, as shown in Table 2, and found that 2:1 is the optimum ratio. The resistance was reduced to 0.37 cm when the molar ratio was 2:1, which didn't reduce further due to the adhesion of PPy to cotton fabrics [119].

Both experimentally and theoretically, Wilczewska et al. explored the impact of graphene quantum dots (GQDs) on the physico-chemical properties of polypyrrole nanoparticles (PPyNPs) [158]. The synthesis of the non-covalent PPyNPs/GQDs material followed a well-established procedure involving chemical pyrrole polymerization in the presence of a potent oxidant (ammonium persulfate, APS) and a surfactant (decyltrimethylammonium bromide, DeTAB). The resulting hybrids manifested as spherical polymeric particles enveloped with GQDs, with their diameter contingent on polymerization time and the quantity of GQDs introduced during synthesis. Notably, the morphology and porosity of the materials were influenced by the polymerization conditions, with composites featuring a higher GQD content exhibiting a greater BET-specific surface area. The incorporation of GQDs into the polymeric network induced significant alterations in the energy level distribution at the interface between PPy and GQDs. The electronic interaction between both components facilitated GQDs' participation in charge transfer processes involving PPy, making oxidation of the mixed PPyNPs/GQDs system more facile than that of the polymer alone. Moreover, charge transfer processes involving PPyNPs/GQDs composites exhibited higher speeds than those of electroactive films formed solely from PPyNPs. Additionally, a substantial increase in double-layer capacitance current was observed for composite materials.

Folorunso et al. introduce an efficient approach for quantifying the diameter and length of graphene nanofillers, utilizing the Weibull distribution to model experimentally measured graphene parameters. The derived length and diameter of the graphene

Table 1
Electrical conductivity of BNC/PPy. $CuCl_2$ nanocomposites [117].

[Py] $CuCl_2 \cdot 2(H_2O)$:Py	Conductivity (S/cm)
[0.04] 2:1	$1.64 \times 10^{-4} \pm 1.93 \times 10^{-5}$
[0.08] 2:1	$1.54 \times 10^{-3} \pm 9.10 \times 10^{-3}$
[0.04] 4:1	$1.85 \times 10^{-2} \pm 5.94 \times 10^{-2}$
[0.08] 4:1	$8.13 \times 10^{-1} \pm 4.32 \times 10^{-3}$

Table 2
Resistivity and weight gain rate changes of PPy/cotton composites with the different Py/FeCl₃ ratios [119].

Py/FeCl ₃ ratio	Resistivity (Ω cm)	Weight gain rate (%)
4:1	3.02	4.3
1:1	1.52	6.67
1:2	0.61	14.86
2:1	0.37	26.5
3:1	0.78	26.1

nanofillers were then employed to predict the electrical conductivity of the graphene-loaded polypyrrole. A well-distributed filler facilitates the reliable dispersion of the filler in the matrix. An analytical model was developed to investigate the conductivity of the polypyrrole-graphene (PPy-Gr) composite, taking into account the interfacial effects of the composite constituents. The electrical conductivity of the composite was determined using the simple-sum method. The percolation threshold and electrical conductivity dependencies of the composites were assessed by simultaneously varying the potential barrier, filler electrical conductivity, interfacial thickness, and matrix conductivity [159]. Varshney et al. synthesized nanoarchitected polypyrrole composites incorporating monodisperse Fe₃O₄ nanoparticles (8–12 nm) through an in situ oxidative polymerization process using a ferrofluid base [160]. The composite exhibited a maximum shielding effectiveness value (SE_{Amax}) of 20.4 dB (approximately 99 % attenuation), attributed to microwave absorption, particularly in the frequency span of 12.4–18 GHz. The attenuation level varied with the loading of ferrofluid. The electrical conductivity of the PFF composite reached the order of 10⁻² S cm⁻¹ and displayed a superparamagnetic nature with a saturation magnetization (M_s) of 5.5 emu/g. These lightweight PFF composites, characterized by high attenuations, enable precise control over atomic structure and hold promise for practical EMI shielding applications in commercial electronic appliances.

5.2. Optical properties

The optical properties of polymer-based composites provide important information about the physical properties of materials, which depend upon the nature of their defects, impurities, and vibrational and electronic states [161–169]. A number of scientists have developed various composites based on PPy with variable optical properties. Bora et al. studied the optical properties of PPy/Graphene composites. They reported the optical band gap of PPy and PPy/Graphene composites, as given in Table 3, using the following equation [170].

$$E_g^{\text{opt}} (\text{eV}) = 1240 / \lambda_{\text{edge}} (\text{nm}) \quad (1)$$

E_g^{opt} is the optical band gap, and λ_{edge} is the absorption edge [146]. Inamdar et al. synthesized PPy/NiO-doped nanocomposites by in situ polymerization and studied their optical properties using diffuse reflectance spectra (DRS). The energy band gap (E_g) was found to be 1.84 eV and was determined using Kubelka-Munk (K-M) theory [170]. Tarmizi et al. synthesized the PPy/zeolite composite using the chemical oxidation method to improve the physical properties of PPy [171–174]. The optical bandgap values were 2.26, 2.23, 2.19, and 2.21 eV, having 5 %, 10 %, 15 %, and 20 % zeolite, respectively. The results indicated that adding FeCl₃ dopant and zeolite increased the conductivity and reduced the bandgap of PPy. Therefore, it is inferred that some ionic groups of zeolites can be used as a dopant during polymerization [175]. Abdi et al. synthesized a polypyrrole-chitosan (PPy-CHI) composite film. They studied its optical properties to determine the optical transition characteristics and the energy band gap using different concentrations of pyrrole. They found that the composite with 0.3 mol/L pyrrole possessed the highest conductivity and lowest optical band gap [176].

The investigation employed Density Functional Theory (DFT) to analyze the optical, electronic, and charge transfer attributes of polypyrrole-Titanium dioxide (TiO₂) composites by Ullah et al.—this exploration aimed at designing an efficient photocatalyst. Through the interaction of Titanium dioxide (Ti₁₆O₃₂) with various pyrrole (Py) oligomers, the study sought to identify the optimal composition of the nPy-TiO₂ composite, possessing a favorable band structure for enhanced photocatalytic performance. The findings indicated that Py-Ti₁₆O₃₂ composites exhibited a narrower band gap and superior absorption of visible light compared to their components. The optimized nPy-Ti₁₆O₃₂ systems showcased simulated results of band structure, molecular orbitals, and UV–vis spectra, supporting the presence of robust interactions between Py and TiO₂ within the composite. The observed red-shifting in λ_{max} , narrowed band gap, and substantial intermolecular interaction energy (–41 to –72 kcal/mol) in nPy-Ti₁₆O₃₂ composites affirmed the existence of potent covalent-type interactions [177].

Gulmen et al. synthesized Chitosan/Polypyrrole/Sepiolite Nanocomposites (Cs/PPy/Sep.NC) with the oxidant to pyrrole mole ratio

Table 3
The optical band gap of PPy and their composites [146].

Sample	λ_{edge} (nm)	$E_{\text{opt g}}$ (eV)
PPy	550	2.23
GRPPy1	590	2.10
GRPPy2	650	1.90
GRPPy3	680	1.82

0.67:1 showed conductivity of 3.7×10^{-4} S/cm for 0.016 g chitosan, and 3.0×10^{-4} S/cm for 0.5 g chitosan. The oxidant to pyrrole molar ratio 0.8 is proposed to be the optimum stoichiometry for the better conductivity while the ratio for the highest yield was obtained for molar ratio of 1.0. The obtained results showed that ESEM micrograph for the surface of Chitosan/Polypyrrole/Clay Nanocomposite has average size of 28.63 nm. The yield of the product (polymer) and electrical conductivity of the product are investigated as physical characteristics. The electrical conductivities of Cs/PPy/Sep. NC were determined by four point probe technique [178].

5.3. Magnetic properties

Belief about the material that can be affected in numerous ways utilizing magnetic field is very old thinking [179]. The information we know is relatively reliable in technological applications where magnetic fields create huge forces [180–190]. Varshney et al. reported that adding Fe_3O_4 nanoparticles improves the carbon fiber magnetic properties of the polypyrrole composite. In this work, ferrofluid (FF) shows a saturation magnetization (M_s) value of 9.1 emu/g without any hysteresis loop, showing its superparamagnetic behavior, which was found to be 1.5 emu/g when a 1:1 vol ratio of aqueous ferrofluid with Fe_3O_4 nanoparticles was added to the PPy composite having carbon fibers, indicating the ferromagnetic behavior of the PS2 composite sheets [191]. Basavaraja et al. synthesized PPy nanocomposites having Fe nanoparticles attached to 2-acrylamido-2-methyl-1-propanesulfonic acid (AMP). They studied their magnetic properties at room temperature. There was an increase in magnetic saturation (M_s) moment from PPy–Fe–AMP-20, PPy–Fe–AMP-40, and PPy–Fe–AMP-50 composites which were 3.8, 4.2, and 5.75 emu/g. Thus, it can be inferred that keeping the Fe concentration constant and increasing the AMP concentration increased the ferromagnetic behaviour [192]. Xiao et al. synthesized PPy composites by four methods, adding magnetic additives, and found that the magnetic additives were responsible for the electromagnetic properties of the PPy composites. They reported that $\gamma\text{-Fe}_2\text{O}_3$ -PPy composite showed excellent magnetic properties [193]. Batool et al. studied the magnetic properties of PPy/hematite compounds in which PPy possessed weak anti-ferromagnetic/paramagnetic behaviour. Still, after adding Fe_2O_3 , it changed into ferromagnetic due to the alignment of magnetic domains. There was an increase in ferromagnetic behaviour upon an increase in the Fe_2O_3 concentration from 10 % to 30 %, as inferred from the M_s values, which increased from 22 to 36 emu/g [194]. Bashir et al. synthesized the nanocomposite PPy- Fe_2O_3 using the in situ chemical oxidative polymerization method and studied its magnetic properties. They reported that saturation magnetization was increased from 0.466 to 3.65emu/g with an increase in Fe_2O_3 concentration from 10 to 50 % by weight, and coercivity was also found to be increased from 152 to 163 Oe [195].

Composites of Fe_3O_4 /polypyrrole (PPy) were synthesized by Yang and co-workers through the polymerization of the conductive monomer pyrrole onto the surface of Fe_3O_4 [196]. Additionally, a subsequent step involved the synthesis of Fe_3O_4 /PPy/carbon nanotube (CNT) composites by blending CNTs with the Fe_3O_4 /Py composites. Microwave absorbers based on epoxy resin were then crafted at varying thicknesses (1, 2, and 3 mm), incorporating 20 % by weight of the prepared composites. Complex permittivity ($\epsilon' - j\epsilon''$) and permeability ($\mu' - j\mu''$) were measured in the frequency range of 2–18 GHz. Remarkably, the composites demonstrated a substantial enhancement in microwave absorption (reflection loss ≤ -10 dB) within the X-band (8–12.5 GHz), achieved by aligning the magnetic properties of Fe_3O_4 with the dielectric properties of PPy and CNTs at a filler concentration of 20 % in 3-mm thickness absorbers. Furthermore, the introduction of CNTs into H- Fe_3O_4 /PPy composites resulted in a further improvement, lowering the minimum reflection loss from -15.8 to -25.9 dB. These findings suggest a promising path for constructing microwave absorbers tailored to achieve desired reflection losses at specific frequencies, emphasizing the effective synergies between the complex permittivity and permeability of the nanocomposites.

6. Applications

6.1. Electrically conductive adhesives

ECAs are an alternative to traditional lead-free solders as they possess various advantages, such as high flexibility for wearable gadgets and lower operating temperatures for delicate integrated circuits [197–199]. It is a glue that is used for electronics. It consists of a conductive component that can be silver, nickel, copper, or graphite and an adhesive component such as varnish, synthetic resin, or silicone [200,201]. PPy NPs doped ECAs are known to possess low electrical resistivity and more electrical conductivity. Wen et al. reported that 2.5 wt% PPy NPs, when used as a dopant, reduced the electrical resistivity of 70 wt% Ag-filled ECAs cured at 160°C for 60 min from 1.6×10^{-3} Ωcm to 9.4×10^{-5} Ωcm by occupying the gaps between silver flakes, which provided a more conductive pathway and therefore reduced electrical resistance. PPy NPs were also useful in reducing cost, as they reduced the amount of silver used in ECAs, enhancing electrical conductivity and allowing the formation of flexible paper and polyimide-based circuits that allowed the lighting of the LEDs in which they were used and gave good conductivity even when folded due to its good flexibility [33]. The electrical conductivity was calculated using the formula [202]:

$$f = R (A / l) \quad (2)$$

$$\sigma = 1 / f \quad (3)$$

where, R, A, l, and s are resistivity (V cm), resistance (V), area of the pallet (cm^2), length of the pallet (cm), and conductivity (S/cm), respectively.

Mir et al. prepared PPy/Epoxy composites. They reported that the PPy addition in the epoxy matrix was appropriate for its application as isotropically conductive adhesives (ICAs), and the best results were shown when 15 wt % PPy was incorporated [203]. Cao et al. fabricated ECAs with excellent electrical and mechanical properties. In this PPy nanotube, the structure of the conductive network of conventional ECAs is changed, and its conductivity is increased. When adding 3 wt % PPy nanotubes, the resistivity ($5.8 \times 10^{-5} \Omega \cdot \text{cm}$) of the ECA containing 55 wt% silver decreased to 1/1000 of the comparative ECAs without PPy nanotubes. The result showed that the electrical resistivity of the new PPy nanotube containing ECAs remained stable after being rolled at a bending radius of 6 mm for over 5000 cycles or pressed below 1200 kPa [204].

6.2. Corrosion resistance

Polypyrrole has anticorrosive properties and, therefore, can be used against chloride ion attacks, as reported by Nautiyal et al., where they used PPy coating on carbon steel using a suitable dopant [48]. They used short-chain dopants such as para toluene sulfonic acid (*p*-TSA), camphor sulfonic acid (CSA), sulfuric acid (SA), and long-chain dopants such as SDS and SDBS to study anticorrosive behaviour by using different concentrations (0.1–1 M for short-chain dopants and 5mM–30mM for long-chain dopants). In the case of short-chain dopants, the effect of dopant concentration was studied by performing a linear potentiodynamic scan. The results showed that the lower the passivation potential, the better the coating and the better the anticorrosive property. Large-sized anions were considered to be more suitable since they cannot be exchanged easily with corrosive ions, such as chloride ions, and for short-chain dopants to protect long-chain, they should form a strong, uniform, and adherent passive layer before electrodeposition of the polymer. In the case of SDBS, as the concentration was from 5 mM to 25 mM, E_{corr} was increased. Still, increasing further to 30 mM was reduced as the formation of the PPy coating was prevented due to increased adsorption of surfactant molecules on the surface. Ohtsuka et al. described two ways of corrosion protection: the physical barrier effect and the anodic protection mechanism. In physical barriers, the polymer film prevents the entry of anions by acting as a protective barrier, while in an anodic protection mechanism, the conducting polymer acts as an oxidizing agent to shift the potential of steel to the passive state [205].

Among the different conjugated conductive polymers, PPy is the best polymer for corrosion protection because of its various physical-chemical properties and better conductivity than the other polymers. Jaouhari et al. electrodeposited zinc phosphate (ZP), Polypyrrole (PPy), and zinc phosphate/PPy coatings on stainless steel (SS) to study their corrosion protection behavior. Electrochemical analysis proved that electrochemically synthesized ZP/PPy coatings showed better protection against corrosion because of the deposition of PPy at uncoated sites of stainless steel, the structural defects of ZP coating were rectified, and the entry of corrosion-causing ions was prevented. The corrosion rate was also reduced due to the increase in the ZP/PPy coating thickness up to 0.26 μm

Table 4
Studies that have used PPy as a corrosion-resistant coating

Substrate	Coating	Coating technique	Corrosion solution	Corrosion behavior	Ref.
MS	PPy	Cyclic voltammetry	0.1 mol/dm ³ H ₂ SO ₄	PPy film provides anticorrosion performance for MS, and corrosion velocity is reduced by at least a factor of 20.	[208]
SS	PPy/CMC	Potentiostatic and galvanostatic methods	3 % NaCl	1-PPy/CMC is a better material for anticorrosion applications than PPy. The 2-potentiostatic method is better than the galvanostatic method.	[209]
Low C steel	PPy + PANI	Aqueous electro polymerization	3.5 NaCl	Better corrosion-resistant properties are obtained when the adhesion strength of the coatings increases.	[210]
MS	PPy/TiO ₂	Salt spray corrosion tests (ASTM B 117)	3.5 % NaCl	The PPy/TiO ₂ composite shows a better corrosion performance than PPy.	[211]
MS	ZP/PPy	Galvanostatic technique	3 % NaCl	The ZP/PPy coatings are anticorrosion due to the formation of PPy in the areas not coated by ZP.	[206]
304 SS	PPy/GO	Galvanostatic technique	0.1 M H ₂ SO ₄	The adhesion strength of the coating is improved due to the presence of GO in the PPy matrix, leading to a stronger long-term anticorrosion performance for 304SS	[212]
MS	PPy + M (M = Al, Zn, Ti, Ce, and Sn)	potentiostatic method	0.5 M H ₂ SO ₄	Al ₂ O ₃ /PPy corrosion protection shows no significant changes after 96 h immersion in a 0.5 M H ₂ SO ₄ solution. Thus, the PPy/Al ₂ O ₃ nanocomposite is a good coating for the anticorrosion performance of MS.	[213]
AA2024	PPy/CeO	Galvanostatic polarization	0.6 M NaCl	The PPy coatings with CeO ₂ nano-particles can be a suitable coating for the anticorrosion performance of AA2024 alloys	[214]
Al-2024	PPy/ZnO	Cyclic voltammetry, galvanostatic, and potentiostatic methods	3.5 % NaCl	The optimum coating provides appropriate corrosion protection up to 14 days after soaking.	[215]
Al	PPy/Al ₂ O ₃	–	H ₂ SO ₄	A protective film is electrochemically deposited in the regime of galvanostatic oxidation of a conducting PPy on the reinforcing highly porous Al ₂ O ₃ layer formed in advance on an Al film.	[216]
AZ91D	PPy/Ag	Potentiostatic technique (salicylate solution)	Ringer solution	Excellent antibacterial activity and corrosion protection are obtained for the Ag-modified composite coating	[217]
AZ31	PPy/PEG	Cyclic voltammetry	0.05 M NaCl	The charge transfer resistance of un-doped PPy and PPy coatings was about two and five times lower than that of doped PPy coating, respectively.	[218]

[206]. S et al. electrochemically deposited PPy/G (Graphene) composite coating on stainless steel bipolar plates. The results showed that the PPy/G composite showed good corrosion resistance and retained graphene's good conductivity. The mixed layer was better than the single PPy coating [207]. According to Liu et al., carbon steel has applications in industries and for domestic purposes because of its good properties. Still, as an active metal, it is prone to corrosion. Therefore, they synthesized PPy coating on the carbon steel surface for protection. The results showed that the Tafel plot significantly reduced the corrosion. It shows that the uncoated carbon steel has E_{corr} of -0.247V , which is lower than the coated carbon steel having an E_{corr} value of -0.035V , which means PPy-WP₁₂ enhanced corrosion resistance, as confirmed by Nyquist plot of electrochemical impedance spectra [37]. Table 4 summarizes the studies that have used PPy as a corrosion-resistant coating.

The electrochemical protection of metals and alloys through the electropolymerization of PPy on their surfaces is a viable approach. However, achieving optimal protection requires careful consideration of factors such as the appropriate electrolyte, current, voltage, pH, and time. It is crucial to recognize that using identical parameters for two distinct metals does not ensure effective coating and corrosion resistance. Additionally, certain metals like carbon steel may be easily coated, whereas more active metals, such as Mg and its alloys, demand specific parameters and conditions for successful coating.

6.3. Biocidal effect

Polypyrrole has antimicrobial properties and can be used against bacterial attack using a suitable dopant [219–225]. Nautiyal et al. studied the biocidal activity of polypyrrole coating on carbon steel using dopants such as *p*-TSA and SDBS. It was found that carbon steel without any dopant caused 86.32 % bacterial kill after a contact time of 10 min. Carbon steel (CS) with a PPy coating and *p*-TSA dopant showed 98.79 % bacterial kill after 10 min. Carbon steel (CS) having PPy coating and SDBS dopant showed 100 % bacterial kill after 10 min contact time. Therefore, a long-chain dopant like SDBS is more suitable for the antimicrobial properties, as shown in Table 5 [48].

Ramirez et al. studied the antibacterial properties of polypyrrole-treated fabrics by ultrasound deposition to treat polyester fabric with nanoparticles to obtain an optimal antibacterial coating that eradicates the bacteria, as shown in Fig. 11 [226]. The result showed that the treated fabric with approximately 4 g/m^2 of PPy had logarithmic bacteria reductions of 6.0 against *Staphylococcus aureus* and 7.5 against *Escherichia coli*. The combination of PPy synthesis in water nanoparticle dispersions and a continuous coating of fabrics supported by ultrasound overcomes some issues of upscaling the traditional in situ chemical deposition used to produce PPy-coated textiles.

6.4. Supercapacitors

Electrochemical capacitors are in great demand these days due to the increased use of portable electrical devices that require better energy storage and release [227]. Supercapacitors, also considered electrochemical capacitors or ultracapacitors, have gained the interest of many researchers due to their high power density, long cycle lifetime, excellent reliability, large number of charging-discharging cycles, and robust thermal operating range, giving more importance over conventional energy storage devices. It can also be used in various energy generation and storage applications, either unaided or accompanied by fuel cells or batteries. Carbon nanotubes (CNTs), graphene, metal oxides, and metal sulfides with excellent electrical conductivity and high surface area have been utilized for supercapacitor fabrications [228,229]. Lota et al. synthesized carbon/polypropylpyrrolidone composites for their application in electrochemical capacitors. The results showed an increase in the propagation of charge upon incorporating carbon material, and the capacitance was actually due to PPy since it did not rise above 10Fg^{-1} . The PPyC2-3 composite with 14 % carbon nanotube content showed the highest capacitance values [230]. The basic structure of the supercapacitor consists of two electrodes having an electrolyte and a porous substrate [231]. As a result of the excess usage of energy in domestic and industrial areas, the demand for energy storage devices has increased. Khati et al. synthesized hemoglobin (Hb)/PPy composites (HPPyCs) by CTAB-assisted polymerization of Py using different concentrations of Hb (1–3%). It was considered suitable for supercapacitor use due to its ease of utilization, low cost, high stability rate, and known structure [232].

Zhao et al. used the MCC/PPy-Co-PANI composite in the supercapacitor electrodes, displaying great electroactivity with a rectangular cyclic voltammogram. According to them, it was suitable for use in electronic devices [233]. Nanoclay-based hierarchical interconnected mesoporous CNT/PPy-based nanocomposites were synthesized by Oraon et al. for high-performance supercapacitors. The nanoclay emerged as a predominant dopant, playing a crucial role in facilitating electron transfer through hopping mechanisms. Electrochemical measurements, specifically through cyclic voltammetry (CV) analysis, unveiled that the in situ composite with

Table 5
Biocidal activity of polypyrrole coating on carbon steel obtained from different dopants [48].

Samples	Contact Time	Bacteria reduction(log)	Bacteria kill (%)
CS	10min	0.86	86.32
CS-PPy- <i>p</i> -TSA	1min	0.57	73.24
	5min	0.96	89.12
	10min	1.92	98.79
	1min	3.23	99.94
CS-PPy-SDBS	5min	3.53	99.97
	10min	5.66	100

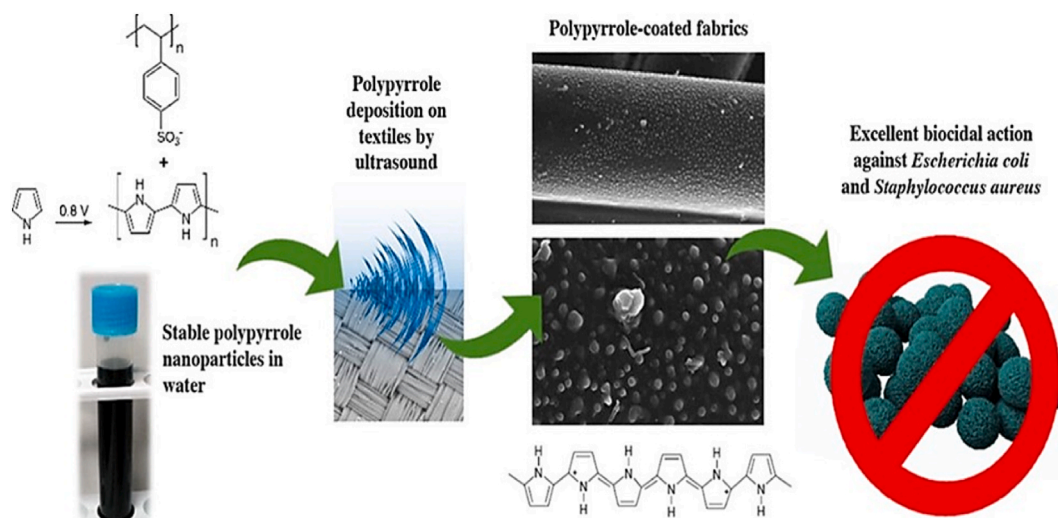


Fig. 11. The synthesis process of PPy-treated fabrics is by ultrasound deposition to eradicate the bacteria [226].

nanoclay exhibited an impressive maximum specific capacitance of 425 F/g and an energy density of 37.81 Wh/kg at a scan rate of 10 mV/s in a 1 M aqueous KCl solution. These findings were further supported by galvanostatic charging–discharging at 5 A/g, showcasing an excellent rate capability and cyclic stability. Remarkably, even after 2000 cycles, the specific capacitance retention remained at 94 % [234].

Mudila et al. studied electrocapacitive performance and high density of PPy/GO nanocomposites prepared at reduced temperature for supercapacitor applications to render improved specific conductivity (526.33 F/g) and power density (731.19 W/kg), indicating excellent cyclic stability [235]. Table 6 represents the electrochemical performance of previously reported composites of PPy.

Mittal et al.'s composite material consists of carbon quantum dots (CQDs) and polypyrrole (PPy), with the aim of applying it as an electrode material for supercapacitors [245]. The electrochemical performance of the composite was thoroughly investigated through cyclic voltammetry and galvanostatic charge-discharge studies. A notable finding was a 33 % increase in the specific capacitance of the CQD-PPy composite compared to pure PPy. This enhancement is attributed to potential interfacial charge transfer between the two components. However, the specific capacitance values achieved were relatively low due to inadequate dispersion of the composite during electrode fabrication, resulting in a diminished surface area available for interaction with the solvent during operation. The study acknowledges that an improved selection of solvent and optimization of dispersion methods hold the potential to enhance the specific capacitance and overall performance of the CQD-PPy composite. Despite these limitations, the research represents a valuable initial step in the development of CQD-PPy composite materials for supercapacitor applications. Vandana et al. synthesized ternary composites comprising tin oxide quantum dots, graphene oxide, and polypyrrole (SGP) exhibit distinctive characteristics, such as a substantial specific surface area and cyclic stability, essential for the advancement of supercapacitor electrodes in high-energy storage applications [246]. The fabrication of a supercapacitor device involved employing the SGP composite electrode with a PVA/KOH gel electrolyte as a separator, and the supercapacitor's performance was systematically examined.

Consequently, the SGP ternary composite achieved a maximum specific capacitance of 928.56 F/g at 40 mV/s. Notably, the assembled SGP3 supercapacitor device maintained an energy density of 25.6 Wh kg^{-1} , coupled with a high-power density of 4098 W kg^{-1} , even after undergoing 11,000 successive galvanostatic charging-discharging (GCD) cycles at a current density of 1 A g^{-1} . These findings underscore the tremendous promise of the ternary composite material for applications in portable electronic storage devices.

Table 6

Electrochemical performance of previously reported composites of PPy.

Electrode materials	Electrolyte	Electrode system	C_{sp}	Capacitance retention	SE/ED	SP/PD	Ref.
PPy/G	1 M KCl	Three	237 F/g at 0.01 V/s	–	33 Wh/Kg	1184 W kg^{-1}	[236]
GO/PPy	1 M KCl	Three	728 F/g at 0.5 A/g	93 % after 1000 cycles	–	–	[237]
rGO/PPy	1 M H_2SO_4	Three	424 F/g at 1 A/g	–	–	–	[238]
MnO_2 /PPy	1 M Na_2SO_4	Three	380 F/g at 1 mV/s	90 % after 1000 cycles	–	–	[239]
PPy/ MoS_2	1 M KCl	Three	553.7 F/g at 1 A/g	90 % after 500 cycles	49.2 Wh/Kg	400 W/Kg	[240]
CuS/PPy	1 M KCl	Three	427 F/g at 1 A/g	88 % after 1000 cycles	–	–	[241]
PPy/SWCNT	1 M KCl	Three	144 F/g at 200 mV/s	–	–	–	[242]
PPy/MWCNT	7.5 M KOH	Three	265 F/g	–	–	–	[243]
CNT/PPy	0.5 M H_2SO_4	Three	4.9 F/ cm^3	95 % after 10,000 cycles	–	–	[244]

6.5. Sensors

It is a device that responds to physical parameters like temperature light and can be used to provide information [247,248]. The organic polymers are observed to be fairly fit for sensing purposes due to moderate resistances, a wide spectrum of structural variety, and their changes in the atmosphere [249]. According to Navale et al., there was a need for a gas sensor to detect harmful gases like NO_2 below its threshold value of 25 ppm. Therefore, they synthesized a PPy film-based sensor for the detection of NO_2 . The gas sensor was more selective towards NO_2 gas and exhibited a higher response (36 %), as shown in Fig. 12 [250].

According to Cui et al., conducting polymers are suitable for gas sensors due to their high sensitivity and reliability [251]. Therefore, they formed a gas sensor based on PPy/ TiO_2 . The sensor showed good sensitivity to various gases even at low concentrations (10 ppm) and was selective towards NH_3 [252]. Jahyono et al. used the vapor phase polymerization method to synthesize a strain sensor with PPy and natural rubber. Natural rubber was used as it is somewhat elastic and rigid. The sensor was made to monitor the bending of a finger joint in robots [253]. Ramesan et al. synthesized a novel PPy/Ag–NiO nanocomposite using the in situ polymerization method to be used as a sensor for the identification of ammonia gas, and the best results were obtained with 10 wt% of Ag–NiO [254]. Agarwal et al. synthesized hierarchical ZnO microstructures modified with Ag nanoparticles to improve the performance of hydrogen gas sensors. Synthesis was done through a low-cost chemical co-precipitation method to obtain Ag/ZnO microstructures and morphologically characterized using SEM, which revealed clear hollow tube-like morphology. Gas detection experiments showed that after modification with Ag nanoparticles, the ZnO sensor showed superior sensitivity of 479 % toward 300 ppm hydrogen gas concentration and enhancement was due to the chemical and electronic sensitization effect of Ag nanoparticles [255,256].

Hsieh et al. studied ammonia gas sensor for PPy/titanium oxide (TiO_2)/graphene nanoribbon (GNR) at room temperature, and the results showed that the response value of 3 wt% SnO_2 nanoparticles with exposure of 1 ppm NH_3 is 92.7, which is three times greater than that of pure PPy. This composite sensor sensitively detects NH_3 between 0.6 and 2 ppm concentrations at room temperature. It also reveals high repeatability and selectivity when exposed to 1 and 2 ppm NH_3 at RT, as shown in Fig. 13 [257]. It is also considered a promising gas-sensing material for detecting kidney disease in human health. Sood et al. synthesized PPy/ WS_2 with different weight percentages (1 wt%, 5 wt%, 10 wt%, 20 wt%, and 30 wt%) using the in-situ chemical oxidative polymerization method. The study revealed that the in-situ synthesized PPy/ WS_2 -5 wt% nanocomposite demonstrated significant response values ranging from 3.04 % to 30.10 % across ammonia concentrations of 50–200 ppm. Moreover, it exhibited remarkable selectivity for ammonia gas compared to other analytes such as H_2 , EtOH, CO, and CO_2 . The enhanced sensing properties of PPy/ WS_2 were attributed to a synergistic effect and the formation of a p-n heterojunction at the interface of the two materials, providing a continuous pathway for majority charge carriers. Notably, these materials exhibited excellent characteristics at room temperature, suggesting the potential use of PPy/ WS_2 nanocomposites in the ammonia sensor industry [258]. Table 7 represents the review for PPy with response time, recovery time, selectivity, and operating temperature (see Table 8).

6.6. Li-ion batteries

Today, our society is confronted with formidable challenges such as the energy crisis, pollution, global warming, and climate change. As a result, researchers and scientists are driven to innovate and develop new electrode materials that exhibit exceptional electrochemical performance [279]. Due to their unique properties, such as lightweight, high specific capacity, stable cycling capability, long lifespan, and design flexibility, LIBs are favored over other existing batteries like Ni–Cd, lead-acid, and Ni-metal hydride. LIBs have been widely adopted as the most promising power sources for portable electronic devices such as mobile phones, charging

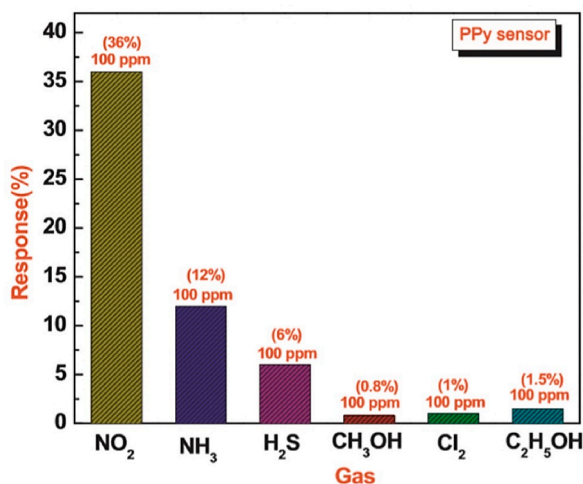


Fig. 12. Selectivity of PPy sensor [250].

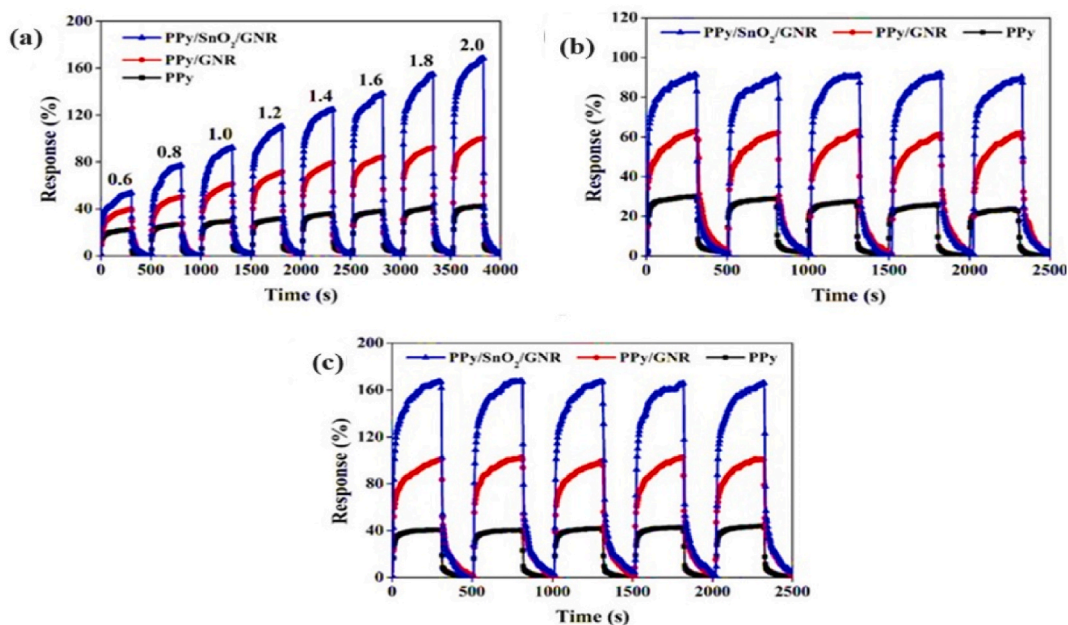


Fig. 13. The response curves of (a) neat PPy polymer matrix, 3 wt% PPy/GNR, and 3 wt% PPy/SnO₂/GNR nanocomposites with exposure of various concentrations of NH₃ at room temperature. The sensing repeatability and reversibility of the 3 wt% PPy/SnO₂/GNR sensor with exposure of (b) 1 ppm and (c) 2 ppm NH₃ at room temperature [257].

Table 7

The review for polypyrrole with response time, recovery time, selectivity and operating temperature.

Composition	Sensor type	Concentration (ppm)	Response	Response time	Recovery time	Selectivity	Operating temp
Py/rGO/PPy	NH ₃	50 ppm	~22 %	–	–	–	RT [259]
Chemically oxidized PPy/rGO	NH ₃	10–500 ppm	1.1%–34.7 %	400s	–	–	RT [92]
Au nanoparticle/PPy	NH ₃	100–300 ppm	1.35,1.45 @100,300 ppm	–	–	More sensitive to NH ₃	RT [260]
Pd nanoparticle/PPy	H ₂	10–10000 ppm	15%–70 %	–	–	More sensitive than CO,NO ₂	RT [261]
Pt nanoparticle/PPy	LPG	400 ppm	~9	–	–	Selective to LPG than other	RT-207 °C [262]
Cu nanowire/PPy	O ₂ and CO ₂	100 ppm	160 %, 300 % [–35 °C]	–	–	–	RT-150 °C [263]
PPy/ZnO	LPG	1000–1800 ppm	21–34.5 %	240s @1400 ppm	2400 s	–	RT [264]
CdS/PPy	NH ₃	100–500 ppm	~160 %	–	–	More selective to NH ₃	RT [265]
PPy/PVA	NH ₃	5ppm–13 ppm	61 %–73 %	25 min	–	–	RT [266]
CeO ₂ /PPy	LPG	Up to 20,000 ppm	<30 %–85 %	–	–	Selective to LPG than NH ₃	RT [267]
SnO ₂ –ZnO/PPy	NH ₃	30–80 ppm	~0.7,~0.82@30 ppm, 70 ppm	67.2s @70 ppm	106 s	–	RT [268]
SnO ₂ –ZnO/PPy	NH ₃	10–85 ppm	47–48 % @ 50 ppm	–	–	More selective to NH ₃	RT [269]
WO ₃ /PPy	H ₂ S	100–1000 ppb	~9 %–~81 %	~360 s	–	More selective to H ₂ S than others	RT [270]
PPy	NH ₃	10–200 ppm	~1.07 @ 80 ppm	–	–	–	RT [271]
PPy/rGO	NH ₃	33.2 ppm	7 %	–	–	–	RT [272]
Graphene/PPy	NH ₃	1–5 ppm	~2.5 %–~9 %	120 s	300 s	More selective	RT [273]
SWCNT/PPy	NO ₂	30 %	~67 %	~36s	~37s	–	RT [274]
rGO/PPy	NH ₃	1–10 ppm	50 % @10 ppm	–	–	More selective	RT [275]
MWCNT/PPy	NH ₃	33.2 ppm	65 %	<10 min	–	–	RT [276]
TiO ₂ /PPy thin film	NH ₃	24–141 ppm	~2.7–7.95 %	~17 s @ 23 ppm	~60 s	Highly sensitive towards humidity	RT [277]
1D ZnO nanorod based PPy composite	NH ₃	300–1000 ppm	~36.1 %@1000 ppm	3–5 ppm	600s	More selective to NH ₃	RT [152]
Ag ₂ S/PPy (1 %)	NH ₃	100–150 ppm	~7.7 %	20 s	>600 s	–	RT [265]

Table 8

An overview of polypyrrole based composites properties and potential applications published in last ten years.

S no.	Material	Method	Morphology	Properties	Application	Year	Ref.
1	Flexible PPy/ TiO ₂ /MXene	Electrochemical polymerization	–	Specific capacitance = 191.4 mF cm ⁻²	Supercapacitor	2024	[121]
2	PPy/TaS ₂	chemical polymerization	Globular	Electrical Conductivity = 4.6 × 10 ⁻³ S/cm	Design of low and mild frequency devices	2023	[122]
3	PPy/carbon fabric	Electrochemical polymerization	–	Specific capacitance = 698.8 F/g	Supercapacitor	2022	[136]
4	PPy/WS ₂	In-situ chemical polymerization	Granular/2D layered structure	AC conductivity	Humidity sensor	2021	[123]
5	PPy/graphene	In-situ polymerization	Granular/sheet-like structure	Electrical Conductivity = Matrix = 10 ⁻¹² to 10 ⁻⁸ S/ m Filler = 10 S/m	Electrochemical devices	2020	[159]
6	PPy/zinc cobalt oxide (ZCO)	Hydrothermal method	ZCO = octahedron shaped with clear edges PPy = granular shaped particles	AC conductivity	–	2019	[124]
7	PPy/Ag–NiO	in-situ polymerization	Spherically shaped	AC conductivity and DC conductivity	Ammonia gas sensing	2018	[254]
8	PPy/TiO ₂	Chemical polymerization	–	–	Photocatalysis	2017	[177]
9	Fe ₃ O ₄ /PPy/CNT	Hydrothermal and co- precipitation	Spherical morphology	Magnetic and microwave absorption properties	EMI Shielding	2016	[196]
10	PPy/ZnO/ Chitosan	Electrochemical polymerization	small globular morphology	Electrical Conductivity = 62.36 S/cm	Antioxidant and antibacterial activities	2015	[278]
11	PPy/ferrofluid (PFF)	in-situ polymerization	Coral-like morphology	Electrical Conductivity = 10 ⁻² S/cm	EMI Shielding	2014	[160]
12	PPy/GO	Electrochemical polymerization	fiber-like morphology	Electronic Conductivity	Fuel cell	2013	[137]

lamps, hybrid electric vehicles, and renewable power stations [280].

Cui et al. reported that SnO₂/PPy nanocomposites (NCs) exhibit a higher Li⁺ diffusion coefficient ($D_{Li} \sim 6.7 \times 10^{-8} \text{ cm}^2 \text{ s}^{-1}$), improved charging/discharging cyclability, and lower activation energy ($E_a \sim 47.3 \text{ kJ mol}^{-1}$ at 0.5 V) compared to pure SnO₂. This enhancement is attributed to the 1D nanostructures of the resulting NCs, where the highly conductive and porous PPy serves as efficient channels for Li⁺ ions and prevents the aggregation of Sn particles, thus mitigating the stress caused by significant volume changes during lithium insertion and extraction [281]. Liu et al. reported the synthesis of core-shell hollow SnO₂/PPy nanocomposites (NCs) by preparing SnO₂ cores using a hydrothermal method (autoclaved at 180 °C for 24 h) and coating them with a PPy shell via in situ chemical polymerization. The resulting NCs demonstrated an excellent capacity of 448.4 mAhg⁻¹ after 100 cycles with a coulombic efficiency greater than 97 % and a larger diffusion length ($7.4 \times 10^{-9} \text{ cm}^2 \text{ s}^{-1}$) compared to hollow SnO₂ spheres. The ample vacant space within the hollow SnO₂ accommodates significant volume changes during the charging/discharging cycles. Additionally, the flexible and conductive PPy coating not only prevents the aggregation of Sn/SnO₂ nanoparticles but also protects the hollow SnO₂ spheres from pulverization [282].

In another study, the authors improved the rate capabilities ($>117.6 \text{ mAh g}^{-1}$ at 3900 mA g⁻¹) and cycling performance (647.8 mAh g⁻¹ after 100 cycles) of SnO₂/rGO/PPy ternary anodes. Graphene, known for its exceptional conductivity, large surface area (2630 m² g⁻¹), and flexibility, was used along with PPy as a shell to coat the SnO₂ hollow core in the SnO₂/rGO/PPy nanocomposite (NC). The synergistic effect of PPy and the robust rGO framework enhanced electron transfer, increased the Li⁺ diffusion coefficient ($1.8 \times 10^{-8} \text{ cm}^2 \text{ s}^{-1}$), and reduced accumulated strain in the lithium-ion batteries [283]. Zhao et al. developed a SWNTs/SnO₂/PPy coaxial nanocable by dispersing SnO₂ nanoparticles (NPs) on the surface of single-walled carbon nanotubes (SWNTs) via a noncovalent method and coating them with polypyrrole (PPy) using in situ chemical oxidative polymerization. This unique architecture demonstrated exceptional electrochemical performance, with a notable rate performance of 480 mAh g⁻¹ at 3000 mA g⁻¹, a high coulombic efficiency of 98 %, and excellent cycling retention capability of 823 mAh g⁻¹ after 100 cycles, making it a promising anode material for lithium-ion batteries (LIBs). The outstanding performance is attributed to the coaxial nanocable structure, where the presence of SWNTs and PPy enhances electrical and ionic conductivity, accommodates the volume variation of SnO₂, and prevents Sn aggregation. Additionally, the PPy coating limits direct contact between the electrolyte and SnO₂, forming a stable solid electrolyte interface (SEI) layer. The authors also reported that the SnO₂ in this SWNTs/SnO₂/PPy nanostructure exhibited a high initial capacity of 1487 mAh g⁻¹, close to the theoretical capacity of 1493 mAh g⁻¹, and showed better capacity retention of 95 % over 100 cycles [284].

6.7. Electrocatalysis

Polypyrrole (PPy) shows promise as an electrocatalyst due to several interesting properties. Conductivity: PPy is a conducting polymer, meaning it can conduct electricity. This is crucial for electrocatalysis, where the catalyst needs to efficiently transfer electrons between the electrode and the reacting molecules. Environmental Stability: PPy is relatively stable in various environments, making it

a durable option for electrocatalytic applications. Enhanced Activity: PPy can improve the efficiency of some reactions by providing a larger surface area for reactants to interact with the catalyst.

Brijesh et al. chemically prepared PPy/ZnWO₄ nanocomposite electrodes for electrocatalytic water splitting. The electrodes made of ZnWO₄, PPy, and PPy/ZnWO₄ have been evaluated as bifunctional electrocatalysts for the hydrogen evolution reaction (HER) and oxygen evolution reaction (OER) using constant current chronopotentiometry (CP) and linear sweep voltammetry (LSV). The electrochemical surface area and electrocatalytic activity of the PPy/ZnWO₄ nanocomposite for HER and OER are superior to those of pure ZnWO₄ and PPy. The Tafel slopes of the PPy/ZnWO₄ nanocomposite are 76 mV dec⁻¹ in 0.5 M H₂SO₄ and 84 mV dec⁻¹ in 1 M KOH at room temperature for HER and OER, respectively. These results indicate that the PPy/ZnWO₄ nanocomposite is an excellent candidate for a bifunctional electrocatalyst for water splitting [285]. Co₃O₄/Polypyrrole/Carbon (Co₃O₄/PPy/C) nanocomposite was prepared through a simple dry chemical method and used to catalyze the oxygen evolution reaction (OER) and hydrogen evolution reaction (HER) by Jayaseelan and his co-workers. The Co₃O₄/PPy/MWCNT composite exhibits enhanced bifunctional electrocatalytic activity for both the oxygen evolution reaction (OER) and hydrogen evolution reaction (HER), with relatively low overpotential (340 mV vs. 490 mV at 10 mA cm⁻²) and a lower Tafel slope (87 vs. 110 mV dec⁻¹). Additionally, the MWCNT-supported Co₃O₄/PPy nanocomposite demonstrates excellent electronic conductivity and electrochemical stability for up to 2000 potential cycles. These results clearly suggest that the Co₃O₄/PPy/MWCNT nanocomposite is a promising bifunctional electrocatalyst for efficient water electrolysis [286].

Loguercio et al. synthesize congo-red doped polypyrrole film embedded with gold nanoparticles (PPy-CR-AuNP). This study discusses for the first time the electrocatalytic properties of PPy-CR and PPy-CR-AuNP as counter-electrode in dye-sensitized solar cell (DSSC). Physicochemical characterizations of the films with and without AuNP have been presented. Both films/electrodes displayed excellent charge transfer abilities, as demonstrated by cyclic voltammetry analysis. Notably, PPy-CR-AuNP exhibited enhanced electron transfer kinetics with a 17 % increase in electroactive surface area and improved efficiency in the I⁻/I³⁻ redox pair activity compared to PPy-CR. Following extended storage under ambient conditions, PPy-CR-AuNP maintained a better mass transport and electron transfer at the electrode-electrolyte interface [287].

7. Conclusions and future prospectives

Polypyrrole (PPy) is a well-known conducting polymer. In this review article, we have given a detailed description of the polymer mentioned above. Different synthesis modes have been described in detail, including chemical oxidative polymerization, electrochemical polymerization, enzymatic polymerization, and several other novel methods. The polymer possesses several properties, with electrical, mechanical, and optical properties being the most crucial. It is known that by adding fillers and forming a composite, the properties of PPy can be enhanced. Therefore, a detailed description of the composite is also given, including various methods of synthesis and various properties.

In the future, the large production of PPy with different fillers will be a significant production concern, and simple laboratory synthesis will be compared with other methods. When the same method is bought on an industrial scale, the cost of chemicals, equipment, and operation increases drastically, given that it requires high pressure and temperature. Techniques such as electrochemical and chemical oxidative synthesis have emerged that use mild conditions for better products on the laboratory scale. The easy oxidation of the conductive polymer will be a significant issue. After extended use, the electrical conductivity will drastically diminish. At high temperatures, this is even worse. Doping some large hydrophobic anions into PPy is one approach to solve these problematic issues because PPy doped with large hydrophobic anions can be preserved in the air for several years without significant change; however, PPy doped with small anions will age slowly in the air. They are leading to loss of electrical conductivity. The second tactic is synthesizing the PPy compounds with metal oxides or carbon compounds. Technology development has high requirements for the performance of absorbing materials, such as multiband and low frequency, high temperature, and corrosion resistance. High-performance multispectral absorbing materials have become important in developing current absorbing materials. Extensive research is imperative to materialize the commercial success of PPy-based adsorbents, providing a new dimension in adsorption technology to mitigate the environmental pollution problem. The majority of PPy-based composites as sensors accomplish exotic gas sensing response, low response time, and ultralow LOD. Still, some critical challenges to using this material in the real field exist, such as high recovery time and long-term environmental stability at various temperatures and wide humidity ranges. Until now, synthesizing a 1D/2D configuration of PPy nanostructure on a mass scale is a serious challenge to researchers due to the lack of unambiguous control and alignment of the nanostructures. Various literature claims excellent selectivity of the PPy composite sensor; however, the exact reason for the selectivity issue is still not resolved. More research should be done in the study, as mentioned earlier arena. With the UN's Sustainable Development Goals in mind, we must prioritize a green and sustainable reaction to potentially dangerous scenarios while synthesizing PPy-based composites. Laboratories need to establish green research regulations and SOPs to support a sustainable future for the environment [251]. For economic growth and people's well-being, it is important to understand the "one world, one climate" idea [252]. This, in turn, makes it important to know the basics of climate rejuvenation strategies for green research. Overall, two primary sources of improvement led to the greening of the PPy research methodology: a) The health risks to operators from being exposed to or working with chemical or biochemical compounds need to be cut a lot. b) Lending the environmental damage caused by unsustainable behaviors is important. As a result, we can certainly predict positive futures for greenified PPy research.

Funding

Not applicable.

Informed consent statement

Not applicable.

Data availability statement

Data will be made available on request.

CRediT authorship contribution statement

Yuvika Sood: Conceptualization. **Kartika Singh:** Data curation. **Harish Mudila:** Formal analysis. **P.E. Lokhande:** Investigation. **Lakhveer Singh:** Methodology. **Deepak Kumar:** Software. **Anil Kumar:** Validation. **Nabisab Mujawar Mubarak:** Validation. **Mohammad Hadi Dehghani:** Writing – review & editing, Writing – original draft.

Declaration of competing interest

The authors declare that they have no known competing financial interests or personal relationships that could have appeared to influence the work reported in this paper.

References

- [1] H. Shirakawa, The discovery of polyacetylene film: the Dawning of an Era of conducting polymers (Nobel Lecture), *Angew. Chemie Int. Ed.* 40 (2001) 2574–2580, [https://doi.org/10.1002/1521-3773\(20010716\)40:14<2574::AID-ANIE2574>3.0.CO;2-N](https://doi.org/10.1002/1521-3773(20010716)40:14<2574::AID-ANIE2574>3.0.CO;2-N).
- [2] A. Kumar, V. Kumar, K. Awasthi, Polyaniline–carbon nanotube composites: preparation methods, properties, and applications, *Polym. Plast. Technol. Eng.* 57 (2018) 70–97, <https://doi.org/10.1080/03602559.2017.1300817>.
- [3] S. Wang, Y. Zhou, Y. Liu, L. Wang, C. Gao, Enhanced thermoelectric properties of polyaniline/polypyrrole/carbon nanotube ternary composites by treatment with a secondary dopant using ferric chloride, *J. Mater. Chem. C* 8 (2020) 528–535, <https://doi.org/10.1039/C9TC06300E>.
- [4] M. Harjo, Z. Zondaka, K. Leemets, M. Järvekülg, T. Tamm, R. Kiefer, Polypyrrole-coated fiber-scaffolds: concurrent linear actuation and sensing, *J. Appl. Polym. Sci.* 137 (2020) 48533, <https://doi.org/10.1002/app.48533>.
- [5] A. Kumar, L.K. Jangir, Y. Kumari, M. Kumar, V. Kumar, K. Awasthi, Electrical behavior of dual-morphology polyaniline, *J. Appl. Polym. Sci.* 133 (2016) 1–9, <https://doi.org/10.1002/app.44091>.
- [6] A. Kumar, V. Kumar, M. Kumar, K. Awasthi, Synthesis and characterization of hybrid PANI/MWCNT nanocomposites for EMI applications, *Polym. Compos.* 39 (2018) 3858–3868, <https://doi.org/10.1002/pc.24418>.
- [7] A. Kumar, A. Mishra, K. Awasthi, V. Kumar, Thermal stability and electrical properties of polyaniline synthesized by oxidative polymerization method, *Macromol. Symp.* 357 (2015) 168–172, <https://doi.org/10.1002/masy.201400218>.
- [8] A. Tiwari, A.P. Mishra, S.R. Dhakate, R. Khan, S.K. Shukla, Synthesis of electrically active biopolymer-SiO₂ nanocomposite aerogel, *Mater. Lett.* 61 (2007) 4587–4590, <https://doi.org/10.1016/j.matlet.2007.02.076>.
- [9] A. Håkansson, S. Han, S. Wang, J. Lu, S. Braun, M. Fahlman, M. Berggren, X. Crispin, S. Fabiano, Effect of (3- Glycidyloxypropyl) Trimethoxysilane (GOPS) on the Electrical Properties of PEDOT : PSS Films, vol.55 (n.d.) 814–820.
- [10] J. Dong, G. Portale, Role of the processing solvent on the electrical conductivity of PEDOT:PSS, *Adv. Mater. Interfaces.* 7 (2020), <https://doi.org/10.1002/admi.202000641>.
- [11] T. V Vernitskaya, O.N. Efimov, Polypyrrole: a conducting polymer; its synthesis, properties and applications, *Russ. Chem. Rev.* 66 (1997) 443–457, <https://doi.org/10.1070/rc1997v066n05abeh000261>.
- [12] M. Barakzahi, M. Montazer, F. Sharif, T. Norby, Electrochimica Acta A textile-based wearable supercapacitor using reduced graphene oxide/polypyrrole composite, *Electrochim. Acta* 305 (2019) 187–196, <https://doi.org/10.1016/j.electacta.2019.03.058>.
- [13] V.B. Mamlayya, V.J. Fulari, Polypyrrole/copper nanoparticles composite thin films for high-sensing performance, *Polym. Bull.* 75 (2018) 4753–4767, <https://doi.org/10.1007/s00289-018-2293-2>.
- [14] M. Belén, Y. Vieira, E.A. Wolski, E.L. Foletto, S. Silvestri, Journal of Water Process Engineering Biological degradation coupled to photocatalysis by ZnO/polypyrrole composite for the treatment of real textile wastewater, *J. Water Process Eng.* 35 (2020) 101230, <https://doi.org/10.1016/j.jwpe.2020.101230>.
- [15] Y. Tian, J. Zhang, S. Tang, L. Zhou, W. Yang, Polypyrrole composite nanoparticles with morphology- dependent Photothermal effect and Immunological responses, 721–726, <https://doi.org/10.1002/sml.201503319>, 2016.
- [16] J. Cao, Y. Wang, J. Chen, X. Li, F.C. Walsh, J. Ouyang, D. Jia, Y. Zhou, Three-dimensional graphene oxide/polypyrrole composite electrodes fabricated by one-step electrodeposition for high performance supercapacitors, *J. Mater. Chem. A Mater. Energy Sustain.* 3 (2015) 14445–14457, <https://doi.org/10.1039/C5TA02920A>.
- [17] K. Keiji Kanazawa, A.F. Diaz, W.D. Gill, P.M. Grant, G.B. Street, G. Piero Gardini, J.F. Kwak, Polypyrrole: an electrochemically synthesized conducting organic polymer, *Synth. Met.* 1 (1980) 329–336, [https://doi.org/10.1016/0379-6779\(80\)90022-3](https://doi.org/10.1016/0379-6779(80)90022-3).
- [18] J. Iqbal, A. Numan, M.O. Ansari, P.R. Jagadish, R. Jafer, S. Bashir, S. Mohamad, K. Ramesh, S. Ramesh, Facile synthesis of ternary nanocomposite of polypyrrole incorporated with cobalt oxide and silver nanoparticles for high performance supercapattery, *Electrochim. Acta* 348 (2020) 136313, <https://doi.org/10.1016/j.electacta.2020.136313>.
- [19] A.L. Pang, A. Arsal, M. Ahmadipour, Synthesis and factor affecting on the conductivity of polypyrrole: a short review, *Polym. Adv. Technol.* 32 (2021) 1428–1454, <https://doi.org/10.1002/pat.5201>.
- [20] O. Folorunso, Y. Hamam, R. Sadiku, S.S. Ray, G.J. Adekoya, Synthesis methods of borophene, graphene-loaded polypyrrole nanocomposites and their benefits for energy storage applications: a brief overview, *FlatChem* 26 (2021) 100211, <https://doi.org/10.1016/j.flatc.2020.100211>.
- [21] M. Maruthapandi, A.P. Nagvenkar, I. Perelshtein, A. Gedanken, Carbon-Dot initiated synthesis of polypyrrole and polypyrrole@CuO micro/nanoparticles with enhanced antibacterial activity, *ACS Appl. Polym. Mater.* 1 (2019) 1181–1186, <https://doi.org/10.1021/acsspm.9b00194>.
- [22] C. Wang, M. Yang, L. Liu, Y. Xu, X. Zhang, X. Cheng, S. Gao, Y. Gao, L. Huo, One-step synthesis of polypyrrole/Fe₂O₃ nanocomposite and the enhanced response of NO₂ at low temperature, *J. Colloid Interface Sci.* 560 (2020) 312–320, <https://doi.org/10.1016/j.jcis.2019.10.076>.
- [23] S.T. Maleki, M. Babamoradi, M. Rouhi, A. Maleki, Z. Hajizadeh, Facile hydrothermal synthesis and microwave absorption of halloysite/polypyrrole/Fe₃O₄, *Synth. Met.* 290 (2022) 117142, <https://doi.org/10.1016/j.synthmet.2022.117142>.
- [24] A. Afzal, F.A. Abuilawi, A. Habib, M. Awais, S.B. Waje, M.A. Atieh, Polypyrrole/carbon nanotube supercapacitors Technological advances and challenges, *J. Power Sources* 352 (2017) 174–186, <https://doi.org/10.1016/j.jpowsour.2017.03.128>.
- [25] Y. Sood, V.S. Pawar, H. Mudila, A. Kumar, A review on synthetic strategies and gas sensing approach for polypyrrole-based hybrid nanocomposites, *Polym. Eng. & Sci.* 61 (2021) 2949–2973, <https://doi.org/10.1002/pen.25822>.

- [26] X.T. Tran, S.S. Park, S. Song, M.S. Haider, S.M. Imran, M. Hussain, H.T. Kim, Electroconductive performance of polypyrrole/reduced graphene oxide/carbon nanotube composites synthesized via in situ oxidative polymerization, *J. Mater. Sci.* 54 (2019) 3156–3173, <https://doi.org/10.1007/s10853-018-3043-4>.
- [27] N. Gill, V. Gupta, M. Tomar, A.L. Sharma, O.P. Pandey, D.P. Singh, Improved electromagnetic shielding behaviour of graphene encapsulated polypyrrole-graphene nanocomposite in X-band, *Compos. Sci. Technol.* 192 (2020) 108113, <https://doi.org/10.1016/j.compscitech.2020.108113>.
- [28] J. Stejskal, Interaction of conducting polymers, polyaniline and polypyrrole, with organic dyes: polymer morphology control. *Dye Adsorption and Photocatalytic Decomposition*, Springer International Publishing, 2020, <https://doi.org/10.1007/s11696-019-00982-9>.
- [29] C.J. Reese, S.G. Boyes, Progress in Polymer Science New methods in polymer brush synthesis : non-vinyl-based semiflexible and rigid-rod polymer brushes, *Prog. Polym. Sci.* 114 (2021) 101361, <https://doi.org/10.1016/j.progpolymsci.2021.101361>.
- [30] H. Mudila, P. Prasher, A. Kumar, M.G.H. Zaidi, A. Verma, Effect of temperature on the polymerization and optical conductivity of thin flexible polypyrrole/Starch composites, *J. Phys. Conf. Ser.* 1531 (2020), <https://doi.org/10.1088/1742-6596/1531/1/012105>.
- [31] Y. Kumari, L. Kumar, A. Kumar, M. Kumar, K. Awasthi, Investigation of thermal stability of TiO₂ nanoparticles using 1-thioglycerol as capping agent, *Solid State Commun* 263 (2017) 1–5, <https://doi.org/10.1016/j.ssc.2017.07.001>.
- [32] A. Yussuf, M. Al-Saleh, S. Al-Enezi, G. Abraham, Synthesis and characterization of conductive polypyrrole: the influence of the oxidants and monomer on the electrical, thermal, and morphological properties, *Int. J. Polym. Sci.* 2018 (2018), <https://doi.org/10.1155/2018/4191747>.
- [33] J. Wen, Y. Tian, Z. Mei, W. Wu, Y. Tian, Synthesis of polypyrrole nanoparticles and their applications in electrically conductive adhesives for improving conductivity, *RSC Adv* 7 (2017) 53219–53225, <https://doi.org/10.1039/c7ra09725e>.
- [34] Y. Du, H. Niu, J. Li, Y. Dou, S.Z. Shen, R. Jia, J. Xu, Morphologies tuning of polypyrrole and thermoelectric properties of polypyrrole nanowire/graphene composites, *Polymers (Basel)* 10 (2018) 6–13, <https://doi.org/10.3390/polym10101143>.
- [35] Y. Sood, H. Mudila, A. Katoch, P.E. Lokhande, D. Kumar, A. Sharma, A. Kumar, Eminence of oxidants on structural–electrical property of Polypyrrole, *J. Mater. Sci. Mater. Electron.* 34 (2023), <https://doi.org/10.1007/s10854-023-10834-8>.
- [36] S. Sadki, P. Schottland, N. Brodie, G. Sabouraud, The mechanisms of pyrrole electropolymerization, *Chem. Soc. Rev.* 29 (2000) 283–293, <https://doi.org/10.1039/A807124A>.
- [37] B. Liu, Z. Zhang, J. Wan, S. Liu, Enhanced corrosion protection of polypyrrole coatings on carbon steel via electrodeposition, *Int. J. Electrochem. Sci.* 12 (2017) 994–1003, <https://doi.org/10.20964/2017.02.20>.
- [38] E.M. Genies, G. Bidan, A.F. Diaz, Spectroelectrochemical study of polypyrrole films, *J. Electroanal. Chem.* 149 (1983) 101–113, [https://doi.org/10.1016/S0022-0728\(83\)80561-0](https://doi.org/10.1016/S0022-0728(83)80561-0).
- [39] D.D. Ateh, H.A. Navsaria, P. Vadgama, Polypyrrole-based conducting polymers and interactions with biological tissues, *J. R. Soc. Interface.* 3 (2006) 741–752, <https://doi.org/10.1098/rsif.2006.0141>.
- [40] Y. Kumari, L.K. Jangir, A. Kumar, M. Kumar, K. Awasthi, Jo ur na l P re of, *Phys. B Phys. Condens. Matter.* (2020) 412465, <https://doi.org/10.1016/j.physb.2020.412465>.
- [41] L.K. Jangir, Y. Kumari, A. Kumar, M. Kumar, Structural and morphological study of PS-ZnO nanocomposite membrane, 218–222, <https://doi.org/10.1002/masy.201500020>, 2015.
- [42] N. Goujon, N. Casado, N. Patil, R. Marcilla, D. Mecerreyes, Progress in Polymer Science Organic batteries based on just redox polymers, *Prog. Polym. Sci.* 122 (2021) 101449, <https://doi.org/10.1016/j.progpolymsci.2021.101449>.
- [43] M. Lo, N. Ktari, D. Gningue-Sall, A. Madani, S.E. Aaron, J.-J. Aaron, Z. Mekhalif, J. Delhalle, M.M. Chehimi, Polipirrol: Polímero Conductor Reactivo y Funcional Para La Detección Electroquímica Selectiva de Metales Pesados En Agua, *Emergent Mater.* 3 (2020) 815–839.
- [44] M. Kazazi, High-performance electrode based on electrochemical polymerization of polypyrrole film on electrophoretically deposited CNTs conductive framework for supercapacitors, *Solid State Ionics* 336 (2019) 80–86, <https://doi.org/10.1016/j.ssi.2019.03.021>.
- [45] U. Samukaite-Bubniene, A. Valiūnienė, V. Bucinskas, P. Genys, V. Ratautaite, A. Ramanaviciene, E. Aksun, A. Tereshchenko, B. Zeybek, A. Ramanavicius, Towards supercapacitors: cyclic voltammetry and fast Fourier transform electrochemical impedance spectroscopy based evaluation of polypyrrole electrochemically deposited on the pencil graphite electrode, *Colloids Surfaces A Physicochem. Eng. Asp.* 610 (2021), <https://doi.org/10.1016/j.colsurfa.2020.125750>.
- [46] R.B. Choudhary, S. Ansari, B. Purty, Robust electrochemical performance of polypyrrole (PPy) and polyindole (PIIn) based hybrid electrode materials for supercapacitor application : a review, *J. Energy Storage.* 29 (2020) 101302, <https://doi.org/10.1016/j.est.2020.101302>.
- [47] O.I. Istakova, D.V. Konev, A.T. Glazkov, T.O. Medvedeva, E.V. Zolotukhina, M.A. Vorotyntsev, Electrochemical synthesis of polypyrrole in powder form, *J. Solid State Electrochem.* 23 (2019) 251–258, <https://doi.org/10.1007/s10008-018-4129-2>.
- [48] A. Nautiyal, M. Qiao, J.E. Cook, X. Zhang, T.S. Huang, High performance polypyrrole coating for corrosion protection and biocidal applications, *Appl. Surf. Sci.* 427 (2018) 922–930, <https://doi.org/10.1016/j.apsusc.2017.08.093>.
- [49] G. El-enany, S.A.A. El-makoud, R. Hamouda, F. El-seify, Electrochemical polymerization and characterizations of polypyrrole in aqueous micellar medium, *Der Pharma Chem* 8 (2016) 156–162.
- [50] S. Maiti, D. Das, K. Sen, Electrochemical polymerization of pyrrole: Key process control parameters, *J. Electrochem. Soc.* 159 (2012) 154–158, <https://doi.org/10.1149/2.050209jes>.
- [51] S. Kim, L.K. Jang, H.S. Park, J.Y. Lee, Electrochemical deposition of conductive and adhesive polypyrrole-dopamine films, *Sci. Rep.* 6 (2016) 1–8, <https://doi.org/10.1038/srep30475>.
- [52] A.M.R. Ramírez, M.A. Gacitúa, E. Ortega, F.R. Díaz, M.A. del Valle, Electrochemical in situ synthesis of polypyrrole nanowires, *Electrochem. Commun.* 102 (2019) 94–98, <https://doi.org/10.1016/j.elecom.2019.04.007>.
- [53] H. Song, T. Li, Y. Han, Y. Wang, C. Zhang, Q. Wang, Optimizing the polymerization conditions of conductive polypyrrole, *J. Photopolym. Sci. Technol.* 29 (2016) 803–808, <https://doi.org/10.2494/photopolymer.29.803>.
- [54] A. Saad, E. Cabet, A. Lilienbaum, S. Hamadi, M. Abderrabba, M.M. Chehimi, Polypyrrole/Ag/mesoporous silica nanocomposite particles: design by photopolymerization in aqueous medium and antibacterial activity, *J. Taiwan Inst. Chem. Eng.* 80 (2017) 1022–1030, <https://doi.org/10.1016/j.jtice.2017.09.024>.
- [55] S. Kasisomayajula, N. Jadhav, V.J. Gelling, Conductive polypyrrole and acrylate nanocomposite coatings: Mechanistic study on simultaneous photopolymerization, *Prog. Org. Coatings.* 101 (2016) 440–454, <https://doi.org/10.1016/j.porgcoat.2016.07.023>.
- [56] V.E. Podaşca, T. Buruiana, E.C. Buruiana, Photocatalytic degradation of Rhodamine B dye by polymeric films containing ZnO, Ag nanoparticles and polypyrrole, *J. Photochem. Photobiol. A Chem.* 371 (2019) 188–195, <https://doi.org/10.1016/j.jphotochem.2018.11.016>.
- [57] S. Asmusen, G. Arenas, C. Vallo, Photopolymerization of pyrrole/methacrylate mixtures using α -cleavage type photoinitiators in combination with idonium salt, *Synth. Met.* 209 (2015) 304–312, <https://doi.org/10.1016/j.synthmet.2015.08.004>.
- [58] B. Horváth, J. Kawakita, T. Chikyow, Adhesion of silver/polypyrrole nanocomposite coating to a fluoropolymer substrate, *Appl. Surf. Sci.* 384 (2016) 492–496, <https://doi.org/10.1016/j.apsusc.2016.05.079>.
- [59] S.C. Buenviaje, K.A.S. Usman, L.M. Payawan, Synthesis and characterization of titanium dioxide-polypyrrole nanocomposites for the photodegradation of bromophenol blue, *AIP Conf. Proc.* 1958 (2018), <https://doi.org/10.1063/1.5034546>.
- [60] K. Jlassi, M.H. Sliem, F.M. Benslimane, N.O. Eltai, A.M. Abdullah, Design of hybrid clay/polypyrrole decorated with silver and zinc oxide nanoparticles for anticorrosive and antibacterial applications, *Prog. Org. Coatings.* 149 (2020) 105918, <https://doi.org/10.1016/j.porgcoat.2020.105918>.
- [61] H.R. Heydarnezhad, B. Pourabbas, M. Tayefi, Conducting electroactive polymers via photopolymerization: a review on synthesis and applications, *Polym. - Plast. Technol. Eng.* 57 (2018) 1093–1109, <https://doi.org/10.1080/03602559.2017.1370111>.
- [62] A.W. Rinaldi, M.H. Kunita, M.J.L. Santos, E. Radovanovic, A.F. Rubira, E.M. Giroto, Solid phase photopolymerization of pyrrole in poly(vinylchloride) matrix, *Eur. Polym. J.* 41 (2005) 2711–2717, <https://doi.org/10.1016/j.eurpolymj.2005.05.029>.
- [63] W. Prissanaroon-Ouajai, A. Sirivat, P.J. Pigram, Polypyrrole/polyethylenimine hybrid film with improved potentiometric response for urea sensing application, *Mater. Today Proc.* 17 (2019) 1843–1851, <https://doi.org/10.1016/j.matpr.2019.06.222>.

- [64] I.D. Antonio-Carmona, S.Y. Martínez-Amador, V.M. Ovando-Medina, G. Neira-Vázquez, H. Martínez-Gutiérrez, Plasma polymerization of pyrrole and aniline on polyurethane foams for microorganism immobilization and wastewater treatment, *Desalin. Water Treat.* 155 (2019) 15–23, <https://doi.org/10.5004/dwt.2019.24001>.
- [65] S. Cogal, A.K. Ali, S. Erten-Ela, G. Celik Cogal, J. Kulicek, M. Micusik, M. Omastova, A.U. Oksuz, Plasma-based preparation of polyaniline/graphene and polypyrrole/graphene composites for dye-sensitized solar cells as counter electrodes, *J. Macromol. Sci. Part A Pure Appl. Chem.* 55 (2018) 317–323, <https://doi.org/10.1080/10601325.2018.1426386>.
- [66] F.G. Ince, S. Şen, Z. Özbek, H. Göktaş, M.E. Öze, R. Çapan, Fabrication of plasma polymerized polythiophene and polypyrrole thin films as chloroform vapor sensors, *J. Optoelectron. Adv. Mater.* 11 (2009) 1182–1185.
- [67] J.L. Yagüe, N. Agulló, S. Borrós, Plasma polymerization of polypyrrole-like films on nanostructured surfaces, *Plasma Process. Polym.* 5 (2008) 433–443, <https://doi.org/10.1002/ppap.200700139>.
- [68] D.H. Kim, C.S. Park, W.H. Kim, J.G. Hong, B.J. Shin, T.S. Park, H.S. Tae, Investigation of plasma polymerized pyrrole under various gas flow rates and input power using atmospheric pressure plasma jets, *Mol. Cryst. Liq. Cryst.* 651 (2017) 26–34, <https://doi.org/10.1080/15421406.2017.1338489>.
- [69] C.S. Park, D.H. Kim, B.J. Shin, D.Y. Kim, H.K. Lee, H.S. Tae, Conductive polymer synthesis with single-crystallinity via a novel plasma polymerization technique for gas sensor applications, *Materials (Basel)* 9 (2016) 1–11, <https://doi.org/10.3390/ma9100812>.
- [70] Z. Zhang, J. Dou, F. Yan, X. Zheng, X. Li, S. Fang, Plasma polymerized pyrrole films for biological applications: correlation between protein adsorption properties and characteristics, *Plasma Process. Polym.* 8 (2011) 923–931, <https://doi.org/10.1002/ppap.201000156>.
- [71] E.N. Zare, T. Agarwal, A. Zarepour, F. Pinelli, A. Zarrabi, F. Rossi, M. Ashrafzadeh, A. Maleki, M.A. Shahbazi, T.K. Maiti, R.S. Varma, F.R. Tay, M.R. Hamblin, V. Mattoli, P. Makvandi, Electroconductive multi-functional polypyrrole composites for biomedical applications, *Appl. Mater. Today.* 24 (2021) 101117, <https://doi.org/10.1016/j.apmt.2021.101117>.
- [72] N. German, A. Popov, A. Ramanaviciene, A. Ramanavicius, Enzymatic formation of polyaniline, polypyrrole, and polythiophene nanoparticles with embedded glucose oxidase, *Nanomaterials* 9 (2019) 5–8, <https://doi.org/10.3390/nano9050806>.
- [73] N. German, A. Ramanaviciene, A. Ramanavicius, Formation of polyaniline and polypyrrole nanocomposites with embedded glucose oxidase and gold nanoparticles, *Polymers (Basel)* 11 (2019) 19–24, <https://doi.org/10.3390/POLYM11020377>.
- [74] A. Kausaite-minkstimiene, V. Mazeiko, A. Ramanaviciene, A. Ramanavicius, Sensors and Actuators B : chemical Evaluation of amperometric glucose biosensors based on glucose oxidase encapsulated within enzymatically synthesized polyaniline and polypyrrole, *Sensors Actuators B. Chem.* 158 (2011) 278–285, <https://doi.org/10.1016/j.snb.2011.06.019>.
- [75] R. Bouldin, S. Ravichandran, A. Kokil, R. Garhwal, S. Nagarajan, J. Kumar, F.F. Bruno, L.A. Samuelson, R. Nagarajan, Synthesis of polypyrrole with fewer structural defects using enzyme catalysis, *Synth. Met.* 161 (2011) 1611–1617, <https://doi.org/10.1016/j.synthmet.2011.05.026>.
- [76] K. Junker, G. Zandomeneghi, L.D. Schuler, R. Kissner, P. Walde, Enzymatic polymerization of pyrrole with *Trametes versicolor* laccase and dioxygen in the presence of vesicles formed from AOT (sodium bis-(2-ethylhexyl) sulfosuccinate) as templates, *Synth. Met.* 200 (2015) 123–134, <https://doi.org/10.1016/j.synthmet.2015.01.004>.
- [77] G.A. Grijalva-Bustamante, A.G. Evans-Villegas, T. Del Castillo-Castro, M.M. Castillo-Ortega, R. Cruz-Silva, F. Huerta, E. Morallón, Enzyme mediated synthesis of polypyrrole in the presence of chondroitin sulfate and redox mediators of natural origin, *Mater. Sci. Eng. C.* 63 (2016) 650–656, <https://doi.org/10.1016/j.msec.2016.03.042>.
- [78] L. Pan, H. Qiu, C. Dou, Y. Li, L. Pu, J. Xu, Y. Shi, Conducting polymer nanostructures: template synthesis and applications in energy storage, *Int. J. Mol. Sci.* 11 (2010) 2636–2657, <https://doi.org/10.3390/ijms11072636>.
- [79] K.J. Ahn, Y. Lee, H. Choi, M.S. Kim, K. Im, S. Noh, H. Yoon, Surfactant-templated synthesis of polypyrrole nanocages as redox mediators for efficient energy storage, *Sci. Rep.* 5 (2015), <https://doi.org/10.1038/srep14097>.
- [80] T.T. Bui, Y.S. Kim, H. Chun, D.D. La, S.V. Bhosale, Template synthesis of micro/mesoporous Cl-doped polypyrrole using vapor phase polymerization, *Mater. Lett.* 192 (2017) 80–83, <https://doi.org/10.1016/j.matlet.2016.12.054>.
- [81] J.G. Wang, B. Wei, F. Kang, Facile synthesis of hierarchical conducting polypyrrole nanostructures via a reactive template of MnO₂ and their application in supercapacitors, *RSC Adv* 4 (2014) 199–202, <https://doi.org/10.1039/c3ra45824e>.
- [82] T. Uemura, Y. Kadowaki, N. Yanai, S. Kitagawa, Template synthesis of porous polypyrrole in 3D coordination nanochannels, *Chem. Mater.* 21 (2009) 4096–4098, <https://doi.org/10.1021/cm901361m>.
- [83] M.J.T. Raaijmakers, N.E. Benes, Current trends in interfacial polymerization chemistry, *Prog. Polym. Sci.* 63 (2016) 86–142, <https://doi.org/10.1016/j.progpolymsci.2016.06.004>.
- [84] V. Georgakilas, P. Dallas, D. Niarchos, N. Boukos, C. Trapalis, Polypyrrole/MWNT nanocomposites synthesized through interfacial polymerization, *Synth. Met.* 159 (2009) 632–636, <https://doi.org/10.1016/j.synthmet.2008.12.007>.
- [85] R. Jain, N. Jadon, A. Pawaiya, Polypyrrole based next generation electrochemical sensors and biosensors: a review, *TrAC Trends Anal. Chem.* 97 (2017) 363–373, <https://doi.org/10.1016/j.trac.2017.10.009>.
- [86] K. Klucińska, E. Jaworska, P. Gryczan, K. Maksymiuk, A. Michalska, Synthesis of conducting polymer nanospheres of high electrochemical activity, *Chem. Commun.* 51 (2015) 12645–12648, <https://doi.org/10.1039/c5cc03705k>.
- [87] Q.H. Yang, Z.Y. Tu, N.Y. Zhao, Research on interfacial polymerization of pyrrole assist with Span80 system, *IOP Conf. Ser. Mater. Sci. Eng.* 137 (2016), <https://doi.org/10.1088/1757-899X/137/1/012070>.
- [88] J. Hazarika, A. Kumar, Scalable and low cost synthesis of highly conducting polypyrrole nanofibers using oil-water interfacial polymerization under constant stirring scalable and low cost synthesis of highly conducting polypyrrole nanofibers using oil-water interfacial polymeri. <https://doi.org/10.1021/acs.jpcc.7b03179>, 2017.
- [89] M. Shen, Y. Han, X. Lin, B. Ding, L. Zhang, X. Zhang, Preparation and electrochemical performances of porous polypyrrole film by interfacial polymerization, *J. of Appl. Sci.* (2012) 1–7, <https://doi.org/10.1002/app.37958>.
- [90] O. Gu, Structural , optical and electrical properties of polypyrrole in ionic liquid, *Poly. Bulletin* (2016) 2625–2639, <https://doi.org/10.1007/s00289-016-1856-3>.
- [91] M. Kang, K. Kim, I. Sub, Y. Son, Electrical properties of polypyrrole wires measured by scanning probe microscope, 259–263, <https://doi.org/10.1016/j.jcis.2006.03.075>, 2006.
- [92] D.C. Tiwari, P. Atri, R. Sharma, Sensitive detection of ammonia by reduced graphene oxide/polypyrrole nanocomposites, *Synth. Met.* 203 (2015) 228–234, <https://doi.org/10.1016/j.synthmet.2015.02.026>.
- [93] A. Kausaite-Minkstimiene, V. Mazeiko, A. Ramanaviciene, A. Ramanavicius, Evaluation of chemical synthesis of polypyrrole particles, *Colloids Surfaces A Physicochem. Eng. Asp.* 483 (2015) 224–231, <https://doi.org/10.1016/j.colsurfa.2015.05.008>.
- [94] J. Tabaciarová, M. Mícuščík, P. Fedorko, M. Omastová, Study of polypyrrole aging by XPS, FTIR and conductivity measurements, *Polym. Degrad. Stab.* 120 (2015) 392–401, <https://doi.org/10.1016/j.polydegradstab.2015.07.021>.
- [95] L. Liang, G. Chen, C.Y. Guo, Polypyrrole nanostructures and their thermoelectric performance, *Mater. Chem. Front.* 1 (2017) 380–386, <https://doi.org/10.1039/c6qm00061d>.
- [96] H. Khan, K. Malook, M. Shah, Synthesis, characterization, and electrical properties of polypyrrole–bimetallic oxide composites, *J. Appl. Polym. Sci.* 47680 (2019) 2–10, <https://doi.org/10.1002/app.47680>.
- [97] S. Majumdar, K. Sarmah, D. Mahanta, A simple route to prepare polypyrrole-coated filter papers via vapor phase polymerization and their gas sensing application, *ACS Appl. Polym. Mater.* 2 (2020) 1933–1942, <https://doi.org/10.1021/acscpm.0c00147>.
- [98] B. Bideau, J. Bras, S. Saini, C. Daneault, E. Loranger, Mechanical and antibacterial properties of a nanocellulose-polypyrrole multilayer composite, *Mater. Sci. Eng. C.* 69 (2016) 977–984, <https://doi.org/10.1016/j.msec.2016.08.005>.
- [99] Y.S. Ko, J.H. Yim, Synergistic enhancement of electrical and mechanical properties of polypyrrole thin films by hybridization of SiO₂ with vapor phase polymerization, *Polymer (Guildf)*. 93 (2016) 167–173, <https://doi.org/10.1016/j.polymer.2016.04.030>.

- [100] E. Andriukonis, A. Stirke, A. Garbaras, L. Mikoliunaite, A. Ramanaviciene, V. Remeikis, B. Thornton, A. Ramanavicius, Yeast-assisted synthesis of polypyrrole: quantification and influence on the mechanical properties of the cell wall, *Colloids Surfaces B Biointerfaces* 164 (2018) 224–231, <https://doi.org/10.1016/j.colsurfb.2018.01.034>.
- [101] Z. Chen, W. Yang, B. Xu, Y. Guo, Y. Chen, X. Yin, Y. Liu, Corrosion behaviors and physical properties of polypyrrole-molybdate coating electropolymerized on carbon steel, *Prog. Org. Coatings* 122 (2018) 159–169, <https://doi.org/10.1016/j.porgcoat.2018.05.022>.
- [102] Y. Chen, L. Du, P. Yang, P. Sun, X. Yu, W. Mai, Significantly enhanced robustness and electrochemical performance of flexible carbon nanotube-based supercapacitors by electrodepositing polypyrrole, *J. Power Sources* 287 (2015) 68–74, <https://doi.org/10.1016/j.jpowsour.2015.04.026>.
- [103] N.S. El-Sayed, M.A. Moussa, S. Kamel, G. Turky, Development of electrical conducting nanocomposite based on carboxymethyl cellulose hydrogel/silver nanoparticles/polypyrrole, *Synth. Met.* 250 (2019) 104–114, <https://doi.org/10.1016/j.synthmet.2019.03.010>.
- [104] Y. Liu, M. Liu, Conductive carboxylated styrene butadiene rubber composites by incorporation of polypyrrole-aromatic wrapped halloysite nanotubes, *Compos. Sci. Technol.* 143 (2017) 56–66, <https://doi.org/10.1016/j.compscitech.2017.03.001>.
- [105] P. Huasheng, D. Jianning, C. Guanggui, L. Zhiyong, Synthesis and Investigation on the Mechanical Properties of the Polypyrrole Film Doped with P-Toluene Sulfonate, vol.464, 2011, pp. 221–224, <https://doi.org/10.4028/www.scientific.net/KEM.464.221>.
- [106] X.S. Wang, H.P. Tang, X.D. Li, X. Hua, Investigations on the mechanical properties of conducting polymer coating-substrate structures and their influencing factors, *Int. J. Mol. Sci.* 10 (2009) 5257–5284, <https://doi.org/10.3390/ijms10125257>.
- [107] D. Zhang, S. Qiu, W. Huang, D. Yang, H. Wang, Z. Fang, Mechanically strong and electrically stable polypyrrole paper using high molecular weight sulfonated alkaline lignin as a dispersant and dopant, *J. Colloid Interface Sci.* 556 (2019) 47–53, <https://doi.org/10.1016/j.jcis.2019.08.029>.
- [108] A. Part, *Springer Handbook of Electronic and Photonic Materials*, 2017, <https://doi.org/10.1007/978-3-319-48933-9>.
- [109] W. Zhao, Y. Wang, A. Wang, Nonlinear optical properties of novel polypyrrole derivatives bearing different aromatic segments, *Mater. Sci. Appl.* 8 (2017) 774–783, <https://doi.org/10.4236/msa.2017.811056>.
- [110] J. V Thombare, S.K. Shinde, G.M. Lohar, U.M. Chougale, S.S. Dhasade, Optical properties of electrochemically synthesized polypyrrole thin films, *J. of Semiconductor* 35 (2014) 1–4, <https://doi.org/10.1088/1674-4926/35/6/063001>.
- [111] J. V Thombare, V.J. Fulari, *Synthesized Polypyrrole (Ppy) Thin Films*, vol. 1, 2012, pp. 1–4.
- [112] O. Gürbüz, B.F. Şenkal, O. İçelli, Structural, optical and electrical properties of polypyrrole in an ionic liquid, *Polym. Bull.* 74 (2017) 2625–2639, <https://doi.org/10.1007/s00289-016-1856-3>.
- [113] J. Han, M. Wang, Y. Hu, C. Zhou, R. Guo, Conducting polymer-noble metal nanoparticle hybrids: synthesis mechanism application, *Prog. Polym. Sci.* 70 (2017) 52–91, <https://doi.org/10.1016/j.progpolymsci.2017.04.002>.
- [114] Y. Fadil, S.C. Thickett, V. Agarwal, P.B. Zetterlund, Progress in Polymer Science Synthesis of graphene-based polymeric nanocomposites using emulsion techniques, *Prog. Polym. Sci.* 125 (2022) 101476, <https://doi.org/10.1016/j.progpolymsci.2021.101476>.
- [115] R. Oraon, A. De Adhikari, S.K. Tiwari, T.S. Sahu, G.C. Nayak, Fabrication of nanoclay based graphene/polypyrrole nanocomposite: an efficient ternary electrode material for high performance supercapacitor, *Appl. Clay Sci.* 118 (2015) 231–238, <https://doi.org/10.1016/j.clay.2015.09.019>.
- [116] J. Marimuthu, M. Rajasekhar, Synthesis and characterization of polypyrrole/copper (II) oxide nanocomposite electrolyte for fuel cell application, *J. Appl. Chem.* 10 (2017) 51–55, <https://doi.org/10.9790/5736-1007035155>.
- [117] D. Müller, B.N. Wesling, G.M. V Dias, J.C. Bernardes, One-step synthesis of conductive BNC/PPy . CuCl 2 hybrid flexible nanocomposites by in situ polymerization, *Advances in Materials Science and Engineering* 2018 (2018).
- [118] M.M.A. Hamid, M. Alruqi, A.M. Elsayed, M.M. Atta, H.A. Hanafi, M. Rabia, Testing the photo-electrocatalytic hydrogen production of polypyrrole quantum dot by combining with graphene oxide sheets on glass slide, *J. Mater. Sci. Mater. Electron.* 34 (2023), <https://doi.org/10.1007/s10854-023-10229-9>.
- [119] J. Xie, W. Pan, Z. Guo, S.S. Jiao, L. Ping Yang, In situ polymerization of polypyrrole on cotton fabrics as flexible electrothermal materials, *J. Eng. Fiber. Fabr.* 14 (2019), <https://doi.org/10.1177/1558925019827447>.
- [120] S. Maity, A. Chatterjee, Textile/polypyrrole composites for sensory applications, *J. Compos.* 2015 (2015) 1–6, <https://doi.org/10.1155/2015/120516>.
- [121] E. Azizi, J. Arjomandi, H. Shi, M.A. Kiani, Flexible polypyrrole/TiO₂/MXene nanocomposite supercapacitor: a promising energy storage device, *J. Energy Storage* 75 (2024), <https://doi.org/10.1016/j.est.2023.109665>.
- [122] A. Sunilkumar, S. Manjunatha, Y.T. Ravikiran, S. Thomas, T. Machappa, AC electrical properties of transition metal dichalcogenide based polypyrrole composites, *Chem. Pap.* 77 (2023) 4913–4921, <https://doi.org/10.1007/s11696-023-02828-x>.
- [123] A. Sunilkumar, S. Manjunatha, Y.T. Ravikiran, M. Revanasiddappa, M. Prashantkumar, T. Machappa, AC conductivity and dielectric studies in polypyrrole wrapped tungsten disulphide composites, *Polym. Bull.* 79 (2022) 1391–1407, <https://doi.org/10.1007/s00289-021-03552-w>.
- [124] R.A. Sutar, L. Kumari, M.V. Murugendrapa, Room temperature ac conductivity, dielectric properties and impedance analysis of polypyrrole-zinc cobalt oxide (PPy/ZCO) composites, *Phys. B Condens. Matter.* 573 (2019) 36–44, <https://doi.org/10.1016/j.physb.2019.07.011>.
- [125] P. Gahlout, V. Choudhary, EMI shielding response of polypyrrole-MWCNT/polyurethane composites, *Synth. Met.* 266 (2020) 116414, <https://doi.org/10.1016/j.synthmet.2020.116414>.
- [126] C.L. Lin, J.W. Li, Y.F. Chen, J.X. Chen, C.C. Cheng, C.W. Chiu, Graphene nanoplatelet/multiwalled carbon nanotube/polypyrrole hybrid fillers in polyurethane nanohybrids with 3D conductive networks for EMI shielding, *ACS Omega* 7 (2022) 45697–45707, <https://doi.org/10.1021/acsomega.2c06613>.
- [127] Y. Chen, H. Feng, L. Li, S. Shang, M. Chun-Wah Yuen, Synthesis and properties of polypyrrole/chitosan composite hydrogels, *J. Macromol. Sci. Part A Pure Appl. Chem.* 50 (2013) 1225–1229, <https://doi.org/10.1080/10601325.2013.843403>.
- [128] R.N. Madhu, R. Awasthi, Polypyrrole composites: electrochemical synthesis, characterizations and applications, *Electropolymerization* (2011), <https://doi.org/10.5772/29083>.
- [129] M. El Rhazi, S. Majid, M. Elbasri, F.E. Salih, L. Oularbi, K. Lafdi, Recent progress in nanocomposites based on conducting polymer: application as electrochemical sensors, *Int. Nano Lett.* 8 (2018) 79–99, <https://doi.org/10.1007/s40089-018-0238-2>.
- [130] M.T. Jafari, M. Saraji, H. Sherafatmand, Polypyrrole/montmorillonite nanocomposite as a new solid phase microextraction fiber combined with gas chromatography-corona discharge ion mobility spectrometry for the simultaneous determination of diazinon and fenthion organophosphorus pesticides, *Anal. Chim. Acta.* 814 (2014) 69–78, <https://doi.org/10.1016/j.aca.2014.01.037>.
- [131] R.A.O. Castro, R.S. Monte, L.G. Mendes, R.F. Furtado, A.R.A. Silva, A. Biswas, H.N. Cheng, C.R. Alves, Electrosynthesis and characterization of polypyrrole/cashew gum composite grown on gold surface in aqueous medium, *Int. J. Electrochem. Sci.* 12 (2017) 50–61, <https://doi.org/10.20964/2017.01.16>.
- [132] Q. Yan, C. Li, Electrochemical synthesis of polypyrrole-SiO₂ composite coating on 316 stainless steel for corrosion protection, *Anti-Corrosion Methods Mater* 64 (2017) 452–460, <https://doi.org/10.1108/ACMM-02-2016-1650>.
- [133] R. Gupta, K. Jayachandran, J.S. Gamare, B. Rajeshwari, S.K. Gupta, J.V. Kamat, Novel electrochemical synthesis of polypyrrole/Ag nanocomposite and its electrocatalytic performance towards hydrogen peroxide reduction, *J. Nanoparticles.* 2015 (2015) 1–6, <https://doi.org/10.1155/2015/149406>.
- [134] S.K. Panda, D. Bandopadhyaya, Synthesis and development of gold polypyrrole actuator for underwater application, *IOP Conf. Ser. Mater. Sci. Eng.* 310 (2018), <https://doi.org/10.1088/1757-899X/310/1/012113>.
- [135] H. Mudila, M.G.H. Zaidi, S. Rana, V. Joshi, S. Alam, Enhanced electrocapacitive performance of graphene oxide polypyrrole nanocomposites, *Int. J. Chem. Anal. Sci.* 4 (2013) 139–145, <https://doi.org/10.1016/j.ijcas.2013.09.001>.
- [136] S. Yazar, G. Atun, Electrochemical synthesis of tunable polypyrrole-based composites on carbon fabric for wide potential window aqueous supercapacitor, *Int. J. Energy Res.* 46 (2022) 14408–14423, <https://doi.org/10.1002/er.8168>.
- [137] Z. Lv, Y. Chen, H. Wei, F. Li, Y. Hu, C. Wei, C. Feng, One-step electrosynthesis of polypyrrole/graphene oxide composites for microbial fuel cell application, *Electrochim. Acta.* 111 (2013) 366–373, <https://doi.org/10.1016/j.electacta.2013.08.022>.
- [138] Sciencedirect-Topic-Enzymatic-Polymerization.pdf, (n.d.).
- [139] V. Krikstolaityte, J. Kuliesius, A. Ramanaviciene, L. Mikoliunaite, A. Kausaite-Minkstimiene, Y. Oztekin, A. Ramanavicius, Enzymatic polymerization of polythiophene by immobilized glucose oxidase, *Polymer (Guildf).* 55 (2014) 1613–1620, <https://doi.org/10.1016/j.polymer.2014.02.003>.

- [140] N. German, A. Ramanaviciene, A. Ramanavicius, Formation of polyaniline and polypyrrole nanocomposites with embedded glucose oxidase and gold nanoparticles, *Polymers (Basel)* 11 (2019) 377, <https://doi.org/10.3390/polym11020377>.
- [141] J. Park, N. Raseda, E.S. Oh, K. Ryu, Laccase-catalyzed synthesis of polypyrrole-multiwalled carbon nanotube composites as energy storage materials for capacitors, *J. Appl. Polym. Sci.* 133 (2016), <https://doi.org/10.1002/app.43307>.
- [142] J. Jang, J.H. Oh, A facile synthesis of polypyrrole nanotubes using a template-mediated vapor deposition polymerization and the conversion to carbon nanotubes, *Chem. Commun.* 4 (2004) 882–883, <https://doi.org/10.1039/b316083a>.
- [143] H. Cheng, B. Wang, Y. Tan, Y. Yin, C. Wang, Low-cost, highly sensitive, and flexible piezoresistive pressure sensor characterized by low-temperature interfacial polymerization of polypyrrole on latex sponge, *Macromol. Mater. Eng.* 306 (2021) 1–11, <https://doi.org/10.1002/mame.202000772>.
- [144] C. Bora, S.K. Dolui, Fabrication of polypyrrole/graphene oxide nanocomposites by liquid/liquid interfacial polymerization and evaluation of their optical, electrical and electrochemical properties, *Polymer (Guildf)*. 53 (2012) 923–932, <https://doi.org/10.1016/j.polymer.2011.12.054>.
- [145] G. Qi, Z. Wu, H. Wang, Highly conductive and semitransparent free-standing polypyrrole films prepared by chemical interfacial polymerization, *J. Mater. Chem. C*. 1 (2013) 7102–7110, <https://doi.org/10.1039/c3tc31340a>.
- [146] C. Bora, S.K. Dolui, Interfacial synthesis of polypyrrole/graphene composites and investigation of their optical, electrical and electrochemical properties, *Polym. Int.* 63 (2014) 1439–1446, <https://doi.org/10.1002/pi.4635>.
- [147] C. Tian, Y. Du, P. Xu, R. Qiang, Y. Wang, D. Ding, J. Xue, J. Ma, H. Zhao, X. Han, Constructing uniform core-shell PPy@PANI composites with tunable shell thickness toward enhancement in microwave absorption, *ACS Appl. Mater. Interfaces*. 7 (2015) 20090–20099, <https://doi.org/10.1021/acsami.5b05259>.
- [148] H. Khan, K. Malook, M. Shah, Synthesis, characterization, and electrical properties of polypyrrole–bimetallic oxide composites, *J. Appl. Polym. Sci.* 137 (2020) 47680, <https://doi.org/10.1002/app.47680>.
- [149] M. Mahmoodian, B. Pourabbas, S. Mohajerzadeh, Effect of anionic dopants on thickness, morphology and electrical properties of polypyrrole ultra-thin films prepared by in situ chemical polymerization, *Thin Solid Films* 583 (2015) 255–263, <https://doi.org/10.1016/j.tsf.2015.03.043>.
- [150] K. Cysewska, S. Virtanen, P. Jasiński, Electrochemical activity and electrical properties of optimized polypyrrole coatings on iron, *J. Electrochem. Soc.* 162 (2015) E307–E313, <https://doi.org/10.1149/2.0821512jes>.
- [151] F. Wolfart, D.P. Dubal, M. Vidotti, R. Holze, P. Gómez-Romero, Electrochemical supercapacitive properties of polypyrrole thin films: influence of the electropolymerization methods, *J. Solid State Electrochem.* 20 (2016) 901–910, <https://doi.org/10.1007/s10008-015-2960-2>.
- [152] Y. Li, M. Jiao, M. Yang, In-situ grown nanostructured ZnO via a green approach and gas sensing properties of polypyrrole/ZnO nanohybrids, *Sensors Actuators, B Chem.* 238 (2017) 596–604, <https://doi.org/10.1016/j.snb.2016.07.089>.
- [153] L.N. Fan, X.C. Xu, A stable iodine-doped multi-walled carbon nanotube-polypyrrole composite with improved electrical property, *Compos. Sci. Technol.* 118 (2015) 264–268, <https://doi.org/10.1016/j.compscitech.2015.09.014>.
- [154] M. Sun, C. Xu, J. Li, L. Xing, T. Zhou, F. Wu, Y. Shang, A. Xie, Protonic doping brings tuneable dielectric and electromagnetic attenuated properties for polypyrrole nanofibers, *Chem. Eng. J.* 381 (2020) 122615, <https://doi.org/10.1016/j.cej.2019.122615>.
- [155] J. Molina, A. Zille, J. Fernández, A.P. Souto, J. Bonastre, F. Cases, Conducting fabrics of polyester coated with polypyrrole and doped with graphene oxide, *Synth. Met.* 204 (2015) 110–121, <https://doi.org/10.1016/j.synthmet.2015.03.014>.
- [156] Y. Liang, J.C.-H. Goh, Polypyrrole-incorporated conducting constructs for tissue engineering applications: a review, *Bioelectricity* 2 (2020) 101–119, <https://doi.org/10.1089/bioe.2020.0010>.
- [157] X. Jian, J. gang Li, H. min Yang, L. le Cao, E. hui Zhang, Z. hai Liang, Carbon quantum dots reinforced polypyrrole nanowire via electrostatic self-assembly strategy for high-performance supercapacitors, *Carbon* N. Y. 114 (2017) 533–543, <https://doi.org/10.1016/j.carbon.2016.12.033>.
- [158] P. Wilczewska, J. Breczeko, D.M. Bobrowska, M. Wysocka-Żołopa, J. Gołcion, A. Basa, K. Winkler, Enhancement of polypyrrole electrochemical performance with graphene quantum dots in polypyrrole nanoparticle/graphene quantum dot composites, *J. Electroanal. Chem.* 923 (2022), <https://doi.org/10.1016/j.jelechem.2022.116767>.
- [159] O. Folorunso, Y. Hamam, R. Sadiku, S.S. Ray, G.J. Adekoya, Statistical characterization and simulation of graphene-loaded polypyrrole composite electrical conductivity, *J. Mater. Res. Technol.* 9 (2020) 15788–15801, <https://doi.org/10.1016/j.jmrt.2020.11.045>.
- [160] S. Varshney, A. Ohlan, V.K. Jain, V.P. Dutta, S.K. Dhawan, Synthesis of ferrofluid based nanoarchitected polypyrrole composites and its application for electromagnetic shielding, *Mater. Chem. Phys.* 143 (2014) 806–813, <https://doi.org/10.1016/j.matchemphys.2013.10.018>.
- [161] L. Ruiz-Perez, L. Rizzello, J. Wang, N. Li, G. Battaglia, Y. Pei, One-pot Synthesis of Organic Conductive Nanoparticles with High Photothermal Conversion Efficiency, (n.d.).
- [162] M. Habib Ullah, C.S. Ha, In situ prepared polypyrrole–Ag nanocomposites: optical properties and morphology, *J. Mater. Sci.* 51 (2016) 7536–7544, <https://doi.org/10.1007/s10853-016-0033-2>.
- [163] P. Saheeda, S. Jayalekshmi, Liquid/liquid interfacial polymerization as an effective synthesis approach for polypyrrole/MWCNTs nanocomposite with impressive nonlinear optical properties, *Opt. Mater. (Amst)*. 104 (2020) 109940, <https://doi.org/10.1016/j.optmat.2020.109940>.
- [164] W. Zhao, Y. Wang, A. Wang, J. Qian, W. Zhu, S. Dou, Q. Wang, Q. Zhong, A. Chen, Novel Bi2O2CO3/polypyrrole/g-C3N4 nanocomposites with efficient photocatalytic and nonlinear optical properties, *RSC Adv* 7 (2017) 7658–7670, <https://doi.org/10.1039/c6ra28346b>.
- [165] A.A. Jatratar, J.B. Yadav, S.V. Kamat, V.S. Patil, D.B. Mahadik, H.C. Barshilia, V. Puri, R.K. Puri, Consequence of oxidant to monomer ratio on optical and structural properties of Polypyrrole thin film deposited by oxidation polymerization technique, *J. Phys. Chem. Solids*. 80 (2015) 78–83, <https://doi.org/10.1016/j.jpcs.2015.01.004>.
- [166] Y.M. Abbas, A.A. Hasan, Optical properties study of polypyrrole doped with TiO₂, WO₃, Fe₂O₃ and SnO₂ nanoparticles, *IOP Conf. Ser. Mater. Sci. Eng.* 928 (2020), <https://doi.org/10.1088/1757-899X/928/7/072017>.
- [167] W. An, J. Zhang, T. Zhu, N. Gao, Investigation on a spectral splitting photovoltaic/thermal hybrid system based on polypyrrole nanofluid: preliminary test, *Renew. Energy*. 86 (2016) 633–642, <https://doi.org/10.1016/j.renene.2015.08.080>.
- [168] H. Ullah, A.A. Tahir, T.K. Mallick, Polypyrrole/TiO₂ composites for the application of photocatalysis, *Sensors Actuators, B Chem.* 241 (2017) 1161–1169, <https://doi.org/10.1016/j.snb.2016.10.019>.
- [169] A. Bahrami, A.R. Sadrolhosseini, G. Mamdoohi, K. Bahzad, M.M. Abdi, Surface plasmon sensor based on polypyrrole multiwalled carbon nanotube composite layer to detect Al (III) in aqueous solution, *Dig. J. Nanomater. Biostructures*. 10 (2015) 535–541.
- [170] H.K. Inamdar, B.C. Sridhar, M. Sasikal, M.V.N. Ambika Prasad, Structural and optical properties of polypyrrole/NiO doped nanocomposites, *J. Nanosci. Technol.* 4 (2018) 400–401, <https://doi.org/10.30799/jnst.112.18040308>.
- [171] S. Jadoun, L. Biswal, U. Riaz, Tuning the optical properties of poly(O-phenylenediamine-co-pyrrole) via template mediated copolymerization, *Des. Monomers Polym.* 21 (2018) 75–81, <https://doi.org/10.1080/15685551.2018.1459078>.
- [172] R.M.F. Batista, S.P.G. Costa, M. Belsley, M.M.M. Raposo, Synthesis and second-order nonlinear optical properties of new chromophores containing benzimidazole, thiophene, and pyrrole heterocycles, *Tetrahedron* 63 (2007) 9842–9849, <https://doi.org/10.1016/j.tet.2007.06.098>.
- [173] J.M. Merkes, T. Lammers, R. Kancherla, M. Rueping, F. Kiessling, S. Banala, Tuning optical properties of BODIPY dyes by pyrrole conjugation for photoacoustic imaging, *Adv. Opt. Mater.* 8 (2020) 1–9, <https://doi.org/10.1002/adom.201902115>.
- [174] M. Raftani, T. Abram, R. Kacimi, M.N. Bennani, M. Bouachrine, Organic compounds based on pyrrole and terphenyl for organic light-emitting diodes (OLED) applications: design and electro-optical properties, *J. Mater. Environ. Sci.* 11 (2020) 933–946.
- [175] E.Z. Mohd Tarmizi, H. Baqiah, Z.A. Talib, H.M. Kamari, Preparation and physical properties of polypyrrole/zeolite composites, *Results Phys* 11 (2018) 793–800, <https://doi.org/10.1016/j.rinp.2018.09.043>.
- [176] M.M. Abdi, H.N.M. Ekramul Mahmud, L.C. Abdullah, A. Kassim, M.Z.A. Rahman, J.L.Y. Chyi, Optical band gap and conductivity measurements of polypyrrole-chitosan composite thin films, *Chinese J. Polym. Sci. (English Ed.)* 30 (2012) 93–100, <https://doi.org/10.1007/s10118-012-1093-7>.
- [177] H. Ullah, A.A. Tahir, T.K. Mallick, Polypyrrole/TiO₂ composites for the application of photocatalysis, *Sensors Actuators, B Chem.* 241 (2017) 1161–1169, <https://doi.org/10.1016/j.snb.2016.10.019>.

- [178] S.S.T. Gülmen, E.A. Güvel, N. Kızılcan, Preparation and characterization of chitosan/polypyrrole/sepiolite nanocomposites, *Procedia - Soc. Behav. Sci.* 195 (2015) 1623–1632, <https://doi.org/10.1016/j.sbspro.2015.06.219>.
- [179] H.H. Stadelmaier, Magnetic properties of materials, *Mater. Sci. Eng. A* 287 (2000) 138–145, [https://doi.org/10.1016/S0921-5093\(00\)00766-8](https://doi.org/10.1016/S0921-5093(00)00766-8).
- [180] Q. Gu, M. Jafarian, S. Salman Seyyed Afghahi, Y. Atassi, R. Al-Qassar, Tuning the impedance matching characteristics of microwave absorbing paint in X-band using copper particles and polypyrrole coating, *Mater. Res. Bull.* 125 (2020) 110780, <https://doi.org/10.1016/j.materresbull.2020.110780>.
- [181] A. Elahi, N.A. Niaz, M.S. Awan, A. Shakoor, K. Mahmood, Y. Khan, Structural, electrical, and magnetic properties of polypyrrole-ZnO.5NiO.45MnO.05Fe2O4 nanocomposites prepared by in situ chemical polymerization, *Polym. Sci. - Ser. B* 57 (2015) 738–749, <https://doi.org/10.1134/S1566090415060044>.
- [182] J. Li, H. Ji, Y. Xu, J. Zhang, Y. Yan, Three-dimensional graphene supported Fe3O4 coated by polypyrrole toward enhanced stability and microwave absorbing properties, *J. Mater. Res. Technol.* 9 (2020) 762–772, <https://doi.org/10.1016/j.jmrt.2019.11.016>.
- [183] H. Akbulut, B. Guler, S. Timur, Y. Yagci, Synthesis, characterization and targeted cell imaging applications of poly(p-phenylene)s with amino and poly(ethylene glycol) substituents, *RSC Adv* 5 (2015) 60861–60869, <https://doi.org/10.1039/c5ra08893c>.
- [184] E.H. El-Ghazzawy, S.N. Alamri, NiCr_xFe_{2-x}O₄ ferrite nanoparticles and their composites with polypyrrole: synthesis, characterization and magnetic properties, *Bull. Mater. Sci.* 38 (2015) 915–924, <https://doi.org/10.1007/s12034-015-0938-4>.
- [185] Y. Sood, A. Kumar, H. Mudila, Influence of polypyrrole morphology on gas sensing influence of polypyrrole morphology on gas sensing, *J. Phys.: Conf. Ser.* 2267 (2022) 012050, <https://doi.org/10.1088/1742-6596/2267/1/012050>.
- [186] U.O. Aigbe, R. Das, W.H. Ho, V. Srinivasu, A. Maity, A novel method for removal of Cr(VI) using polypyrrole magnetic nanocomposite in the presence of unsteady magnetic fields, *Sep. Purif. Technol.* 194 (2018) 377–387, <https://doi.org/10.1016/j.seppur.2017.11.057>.
- [187] P. Gairola, L.P. Purohit, S.P. Gairola, P. Bhardwaj, S. Kaushik, Enhanced electromagnetic absorption in ferrite and tantalum pentoxide based polypyrrole nanocomposite, *Prog. Nat. Sci. Mater. Int.* 29 (2019) 170–176, <https://doi.org/10.1016/j.pnsc.2019.03.011>.
- [188] M.A. Rizvi, S.K. Moosvi, T. Jan, S. Bashir, P. Kumar, W.D. Roos, H.C. Swart, Dielectric, magnetic and photocatalytic activity of PolyPyrrrole/Prussian red nanocomposite for waste water treatment applications, *Polymer (Guildf)* 163 (2019) 1–12, <https://doi.org/10.1016/j.polymer.2018.12.044>.
- [189] K. Zhang, X. Chen, X. Gao, L. Chen, S. Ma, C. Xie, X. Zhang, W. Lu, Preparation and microwave absorption properties of carbon nanotubes/iron oxide/polypyrrole/carbon composites, *Synth. Met.* 260 (2020) 116282, <https://doi.org/10.1016/j.synthmet.2019.116282>.
- [190] X. Li, H. Lu, Y. Zhang, F. He, Efficient removal of organic pollutants from aqueous media using newly synthesized polypyrrole/CNTs-CoFe₂O₄ magnetic nanocomposites, *Chem. Eng. J.* 316 (2017) 893–902, <https://doi.org/10.1016/j.cej.2017.02.037>.
- [191] S. Varshney, S.K. Dhawan, Improved electromagnetic shielding performance of lightweight compression molded polypyrrole/ferrite composite sheets, *J. Electron. Mater.* 46 (2017) 1811–1820, <https://doi.org/10.1007/s11664-016-5233-7>.
- [192] A.G. Arani, G.S. Jafari, R. Kolahchi, Vibration analysis of nanocomposite microplates integrated with sensor and actuator layers using polypyrrole, *Polymers* (2016) 1–14, <https://doi.org/10.1002/pc>.
- [193] H.M. Xiao, S.Y. Fu, Synthesis and physical properties of electromagnetic polypyrrole composites via addition of magnetic crystals, *CrystEngComm* 16 (2014) 2097–2112, <https://doi.org/10.1039/c3ce40995c>.
- [194] A. Batool, F. Kanwal, S. Asim, S. Riaz, S. Atiq, S. Naseem, M.W. Mushtaq, Z. Ullah, Thermally stable polypyrrole/hematite composites with tunable dielectric and magnetic properties, *Polym. Sci. - Ser. A* 61 (2019) 112–117, <https://doi.org/10.1134/S0965545X19010024>.
- [195] T. Bashir, A. Shakoor, E. Ahmed, N.A. Niaz, S. Iqbal, M.S. Akhtar, M.A. Malik, Magnetic, electrical and thermal studies of polypyrrole-Fe₂O₃ nanocomposites, *Polym. Sci. - Ser. A* 59 (2017) 902–908, <https://doi.org/10.1134/S0965545X17060013>.
- [196] R. Bin Yang, P.M. Reddy, C.J. Chang, P.A. Chen, J.K. Chen, C.C. Chang, Synthesis and characterization of Fe₃O₄/polypyrrole/carbon nanotube composites with tunable microwave absorption properties: role of carbon nanotube and polypyrrole content, *Chem. Eng. J.* 285 (2016) 497–507, <https://doi.org/10.1016/j.cej.2015.10.031>.
- [197] S. Kim, L.K. Jang, M. Jang, S. Lee, J.G. Hardy, J.Y. Lee, Electrically conductive polydopamine-polypyrrole as high performance biomaterials for cell stimulation in vitro and electrical signal recording in vivo, *ACS Appl. Mater. Interfaces* 10 (2018) 33032–33042, <https://doi.org/10.1021/acsami.8b11546>.
- [198] R. Aradhana, S. Mohanty, S.K. Nayak, Synergistic effect of polypyrrole and reduced graphene oxide on mechanical, electrical and thermal properties of epoxy adhesives, *Polymer (Guildf)* 166 (2019) 215–228, <https://doi.org/10.1016/j.polymer.2019.02.006>.
- [199] R. Aradhana, S. Mohanty, S.K. Nayak, A review on epoxy-based electrically conductive adhesives, *Int. J. Adhes. Adhes.* 99 (2020) 102596, <https://doi.org/10.1016/j.ijadhadh.2020.102596>.
- [200] J. Stejskal, U. Acharya, P. Bober, M. Hajná, M. Trchová, M. Mi, M. Omastová, I. Pa, N. Gavrilov, Applied Surface Science Surface modification of tungsten disulfide with polypyrrole for enhancement of the conductivity and its impact on hydrogen evolution reaction, *Appl. Surf. Sci.* 492 (2019) 497–503, <https://doi.org/10.1016/j.apsusc.2019.06.175>.
- [201] N. Babu, A.R. Athira, T.S. Xavier, One-pot hydrothermal synthesis of polypyrrole/Fe₂O₃ nano-seeds for energy storage application, *Mater. Today Proc.* 49 (2021) 1185–1188, <https://doi.org/10.1016/j.matpr.2021.06.252>.
- [202] A. Tiwari, Gum Arabic-graft-polyaniline: an electrically active redox biomaterial for sensor applications, *J. Macromol. Sci. Part A Pure Appl. Chem.* 44 (2007) 735–745, <https://doi.org/10.1080/10601320701353116>.
- [203] I.A. Mir, D. Kumar, Development of polypyrrole/epoxy composites as isotropically conductive adhesives, *J. Adhes.* 86 (2010) 447–462, <https://doi.org/10.1080/00218461003704519>.
- [204] G. Cao, L. Wang, Y. Tian, Highly dispersed polypyrrole nanotubes for improving the conductivity of electrically conductive adhesives, *J. Mater. Sci. Mater. Electron.* 31 (2020) 9675–9684, <https://doi.org/10.1007/s10854-020-03513-5>.
- [205] T. Ohtsuka, Corrosion protection of steels by conducting polymer coating, *Int. J. Corros.* 2012 (2012), <https://doi.org/10.1155/2012/915090>.
- [206] A. El Jaouhari, A. Chennah, S. Ben Jaddi, H. Ait Ahsaine, Z. Anfar, Y. Tahiri Alaoui, Y. Naciri, A. Benlachechi, M. Bazzou, Electrosynthesis of zinc phosphate-polypyrrole coatings for improved corrosion resistance of steel, *Surfaces and Interfaces* 15 (2019) 224–231, <https://doi.org/10.1016/j.surfin.2019.02.011>.
- [207] S. Liu, T.J. Pan, R.F. Wang, Y. Yue, J. Shen, Anti-corrosion and conductivity of the electrodeposited graphene/polypyrrole composite coating for metallic bipolar plates, *Prog. Org. Coatings* 136 (2019), <https://doi.org/10.1016/j.porgcoat.2019.105237>.
- [208] N.V. Krstajić, B.N. Grgur, S.M. Jovanović, M.V. Vojnović, Corrosion protection of mild steel by polypyrrole coatings in acid sulfate solutions, *Electrochim. Acta* 42 (1997) 1685–1691, [https://doi.org/10.1016/S0013-4686\(96\)00313-1](https://doi.org/10.1016/S0013-4686(96)00313-1).
- [209] P. Herrasti, P. Ocón, Polypyrrole layers for steel protection, *Appl. Surf. Sci.* 172 (2001) 276–284, [https://doi.org/10.1016/S0169-4332\(00\)00866-7](https://doi.org/10.1016/S0169-4332(00)00866-7).
- [210] R. Rajagopalan, J.O. Iroh, Corrosion performance of polyaniline-polypyrrole composite coatings applied to low carbon steel, *Surf. Eng.* 18 (2002) 59–63, <https://doi.org/10.1179/026708401225001246>.
- [211] D.M. Lenz, M. Delamar, C.A. Ferreira, Application of polypyrrole/TiO₂ composite films as corrosion protection of mild steel, *J. Electroanal. Chem.* 540 (2003) 35–44, [https://doi.org/10.1016/S0022-0728\(02\)01272-X](https://doi.org/10.1016/S0022-0728(02)01272-X).
- [212] J. Li, Y. Lu, Q. Ye, M. Cinke, J. Han, M. Meyyappan, Carbon nanotube sensors for gas and organic vapor detection, *Nano Lett.* 3 (2003) 929–933, <https://doi.org/10.1021/nl034220x>.
- [213] L. Jiang, J.A. Syed, H. Lu, X. Meng, In-situ electrodeposition of conductive polypyrrole-graphene oxide composite coating for corrosion protection of 304SS bipolar plates, *J. Alloys Compd.* 770 (2019) 35–47, <https://doi.org/10.1016/j.jallcom.2018.07.277>.
- [214] R. Babaei-Sati, J. Basiri Parsa, M. Vakili-Azghandi, Electrodeposition of polypyrrole/metal oxide nanocomposites for corrosion protection of mild steel—a comparative study, *Synth. Met.* 247 (2019) 183–190, <https://doi.org/10.1016/j.synthmet.2018.12.009>.
- [215] A.M. Kumar, R.S. Babu, S. Ramakrishna, A.L.F. de Barros, Electrochemical synthesis and surface protection of polypyrrole-CeO₂ nanocomposite coatings on AA2024 alloy, *Synth. Met.* 234 (2017) 18–28, <https://doi.org/10.1016/j.synthmet.2017.10.003>.
- [216] V.V. Tomaev, K.L. Levine, T.V. Stoyanova, A.G. Sirkov, Formation of nanocomposite film (polypyrrol)/(aluminum) oxide on aluminum surface, *AIP Conf. Proc.* 2064 (2019), <https://doi.org/10.1063/1.5087678>.
- [217] A.D. Forero López, I.L. Lehr, L.I. Brugnoli, S.B. Saidman, Improvement in the corrosion protection and bactericidal properties of AZ91D magnesium alloy coated with a microstructured polypyrrole film, *J. Magnes. Alloy.* 6 (2018) 15–22, <https://doi.org/10.1016/j.jma.2017.12.005>.

- [218] S.H.H. Mortazavi, M. Yeganeh, A. Etamad, M. Saremi, Corrosion behavior of polypyrrole (Ppy) coating modified by polyethylene glycol (PEG) doped ammonium bifluoride on AZ31 magnesium alloy, *Prog. Org. Coatings*. 134 (2019) 22–32, <https://doi.org/10.1016/j.porgcoat.2019.04.054>.
- [219] Z. Liao, X. Fang, J. Li, X. Li, W. Zhang, X. Sun, J. Shen, W. Han, S. Zhao, L. Wang, Incorporating organic nanospheres into the polyamide layer to prepare thin film composite membrane with enhanced biocidal activity and chlorine resistance, *Sep. Purif. Technol.* 207 (2018) 222–230, <https://doi.org/10.1016/j.seppur.2018.06.057>.
- [220] J. Zhang, K.G. Neoh, X. Hu, E.T. Kang, Mechanistic insights into response of *Staphylococcus aureus* to bioelectric effect on polypyrrole/chitosan film, *Biomaterials* 35 (2014) 7690–7698, <https://doi.org/10.1016/j.biomaterials.2014.05.069>.
- [221] M.B. González, D.O. Flamini, L.I. Brugnoli, P. Kalleso Pedersen, S.B. Saidman, Silver release from polypyrrole matrix in well water, *J. Electroanal. Chem.* 765 (2016) 105–110, <https://doi.org/10.1016/j.jelechem.2015.09.008>.
- [222] M. Soleimani, M. Ghorbani, S. Salahi, Antibacterial activity of polypyrrole-chitosan nanocomposite: mechanism of action, *Int. J. Nanosci. Nanotechnol.* 12 (2016) 191–197.
- [223] M.T. Ahmed, M.I.A. Hamid, A. Sarhan, A.A. Ali, Synthesis and structural characterization of polypyrrole (PPy) - chitosan (Cs) nanocomposite : influence of UV irradiation, *Global Journal of Physics* 7 (2018).
- [224] E. Nazarzadeh Zare, M. Mansour Lakouraj, M. Mohseni, Biodegradable polypyrrole/dextrin conductive nanocomposite: synthesis, characterization, antioxidant and antibacterial activity, *Synth. Met.* 187 (2014) 9–16, <https://doi.org/10.1016/j.synthmet.2013.09.045>.
- [225] S. Javadian, Z. Ahmadpour, A. Yousefi, Polypyrrole nanocapsules bearing quaternized alkyl pyridine in a green self-healing coating for corrosion protection of zinc, *Prog. Org. Coatings*. 147 (2020), <https://doi.org/10.1016/j.porgcoat.2020.105678>.
- [226] D.O. Sanchez Ramirez, A. Varesano, R.A. Carletto, C. Vineis, I. Perelshtein, M. Natan, N. Perkas, E. Banin, A. Gedanken, Antibacterial properties of polypyrrole-treated fabrics by ultrasound deposition, *Mater. Sci. Eng. C*. 102 (2019) 164–170, <https://doi.org/10.1016/j.msec.2019.04.016>.
- [227] M. Gong, L. Zhang, P. Wan, Polymer nanocomposite meshes for flexible electronic devices, *Prog. Polym. Sci.* 107 (2020) 101279, <https://doi.org/10.1016/j.progpolymsci.2020.101279>.
- [228] A. Tiwari, A. Materials, Hierarchical Aerographite nano- microtubular tetrapodal networks based electrodes as lightweight supercapacitor, *Nano energy* 34 (2017), <https://doi.org/10.1016/j.nanoen.2017.03.004>.
- [229] P.E. Lokhande, S. Kulkarni, S. Chakrabarti, H.M. Pathan, M. Sindhu, D. Kumar, J. Singh, A. Kumar, Y. Kumar Mishra, D.-C. Toncu, M. Syväjärvi, A. Sharma, A. Tiwari, The progress and roadmap of metal-organic frameworks for high-performance supercapacitors, *Coord. Chem. Rev.* 473 (2022) 214771, <https://doi.org/10.1016/j.ccr.2022.214771>.
- [230] K. Lota, G. Lota, A. Sierczynska, I. Acznik, Carbon/polypyrrole composites for electrochemical capacitors, *Synth. Met.* 203 (2015) 44–48, <https://doi.org/10.1016/j.synthmet.2015.02.014>.
- [231] H.P. De Oliveira, S.A. Sydlík, T.M. Swager, Supercapacitors from free-standing polypyrrole/graphene nanocomposites, *J. Phys. Chem. C*. 117 (2013) 10270–10276, <https://doi.org/10.1021/jp400344u>.
- [232] K. Khatil, I. Joshi, M.G.H. Zaidi, Electro-capacitive performance of haemoglobin/polypyrrole composites for high power density electrode, *J. Anal. Sci. Technol.* 9 (2018), <https://doi.org/10.1186/s40543-018-0156-y>.
- [233] Y. Zhao, H. Wang, R. Ma, T. Chen, Preparation and properties of conducting polymer/microcrystalline cellulose composite, *IOP Conf. Ser. Mater. Sci. Eng.* 452 (2018), <https://doi.org/10.1088/1757-899X/452/2/022110>.
- [234] R. Oraon, A. De Adhikari, S.K. Tiwari, G.C. Nayak, Nanoclay-based hierarchical interconnected mesoporous CNT/PPy electrode with improved specific capacitance for high performance supercapacitors, *Dalt. Trans.* 45 (2016) 9113–9126, <https://doi.org/10.1039/c6dt00600k>.
- [235] H. Mudila, V. Joshi, S. Rana, M.G.H. Zaidi, S. Alam, Enhanced electrocapacitive performance and high power density of polypyrrole/graphene oxide nanocomposites prepared at reduced temperature, *Carbon Lett* 15 (2014) 171–179, <https://doi.org/10.5714/CL.2014.15.3.171>.
- [236] A. Davies, P. Audette, B. Farrow, F. Hassan, Z. Chen, J.Y. Choi, A. Yu, Graphene-based flexible supercapacitors: pulse-electropolymerization of polypyrrole on free-standing graphene films, *J. Phys. Chem. C*. 115 (2011) 17612–17620, <https://doi.org/10.1021/jp205568v>.
- [237] J. Li, H. Xie, Y. Li, Fabrication of graphene oxide/polypyrrole nanowire composite for high performance supercapacitor electrodes, *J. Power Sources*. 241 (2013) 388–395, <https://doi.org/10.1016/j.jpowsour.2013.04.144>.
- [238] H.H. Chang, C.K. Chang, Y.C. Tsai, C.S. Liao, Electrochemically synthesized graphene/polypyrrole composites and their use in supercapacitor, *Carbon N. Y.* 50 (2012) 2331–2336, <https://doi.org/10.1016/j.carbon.2012.01.056>.
- [239] W. Yao, H. Zhou, Y. Lu, Synthesis and property of novel MnO₂@polypyrrole coaxial nanotubes as electrode material for supercapacitors, *J. Power Sources*. 241 (2013) 359–366, <https://doi.org/10.1016/j.jpowsour.2013.04.142>.
- [240] G. Ma, H. Peng, J. Mu, H. Huang, X. Zhou, Z. Lei, In situ intercalative polymerization of pyrrole in graphene analogue of MoS₂ as advanced electrode material in supercapacitor, *J. Power Sources*. 229 (2013) 72–78, <https://doi.org/10.1016/j.jpowsour.2012.11.088>.
- [241] H. Peng, G. Ma, K. Sun, J. Mu, H. Wang, Z. Lei, High-performance supercapacitor based on multi-structural CuS@polypyrrole composites prepared by in situ oxidative polymerization, *J. Mater. Chem. A*. 2 (2014) 3303–3307, <https://doi.org/10.1039/c3ta13859c>.
- [242] J. Wang, Y. Xu, X. Chen, X. Sun, Capacitance properties of single wall carbon nanotube/polypyrrole composite films, *Compos. Sci. Technol.* 67 (2007) 2981–2985, <https://doi.org/10.1016/j.compscitech.2007.05.015>.
- [243] K.H. An, K.K. Jeon, J.K. Heo, S.C. Lim, D.J. Bae, Y.H. Lee, High-capacitance supercapacitor using a nanocomposite electrode of single-walled carbon nanotube and polypyrrole, *J. Electrochem. Soc.* 149 (2002) A1058, <https://doi.org/10.1149/1.1491235>.
- [244] M. Hughes, G.Z. Chen, M.S.P. Shaffer, D.J. Fray, A.H. Windle, Electrochemical capacitance of a nanoporous composite of carbon nanotubes and polypyrrole, *Chem. Mater.* 14 (2002) 1610–1613, <https://doi.org/10.1021/cm010744r>.
- [245] S. Sagar Mittal, G. Ramadas, N. Vasanthmurali, V.S. Madaneshwar, M. Sathish Kumar, N.K. Kothurkar, Carbon quantum dot-polypyrrole nanocomposite for supercapacitor electrodes, *IOP Conf. Ser. Mater. Sci. Eng.* 577 (2019), <https://doi.org/10.1088/1757-899X/577/1/012194>.
- [246] M. Vandana, S. Veeresh, H. Ganesh, Y.S. Nagaraju, H. Vijeth, M. Basappa, H. Devendrappa, Graphene oxide decorated SnO₂ quantum dots/polypyrrole ternary composites towards symmetric supercapacitor application, *J. Energy Storage*. 46 (2022), <https://doi.org/10.1016/j.est.2021.103904>.
- [247] L.N.C. Iii, M. Sheplak, Actuators for Active Flow Control, 2011, pp. 247–274, <https://doi.org/10.1146/annurev-fluid-122109-160634>.
- [248] B. Adhikari, S. Majumdar, Polymers in sensor applications, *Prog. Polym. Sci.* 29 (2004) 699–766, <https://doi.org/10.1016/j.progpolymsci.2004.03.002>.
- [249] S.K. Shukla, A. Bharadvaja, A. Tiwari, G.K. Parashar, G.C. Dubey, Synthesis and characterization of highly crystalline polyaniline film promising for humid sensor, *Adv. Mater. Lett.* 1 (2010) 129–134, <https://doi.org/10.5185/amlett.2010.3105>.
- [250] S.T. Navale, A.T. Mane, M.A. Chougule, R.D. Sakhare, S.R. Nalage, V.B. Patil, Highly selective and sensitive room temperature NO₂ gas sensor based on polypyrrole thin films, *Synth. Met.* 189 (2014) 94–99, <https://doi.org/10.1016/j.synthmet.2014.01.002>.
- [251] Y. Sood, A. Kumar, H. Mudila, Influence of Polypyrrole Morphology on Gas Sensing Influence of Polypyrrole Morphology on Gas Sensing, (n.d.), <https://doi.org/10.1088/1742-6596/2267/1/012050>.
- [252] S. Cui, L. Yang, J. Wang, X. Wang, Fabrication of a sensitive gas sensor based on PPy/TiO₂ nanocomposites films by layer-by-layer self-assembly and its application in food storage, *Sensors Actuators, B Chem.* 233 (2016) 337–346, <https://doi.org/10.1016/j.snb.2016.04.093>.
- [253] A.P. Tjahyono, K.C. Aw, J. Travas-Sejdic, A novel polypyrrole-based sensor for robotics applications, *IFAC Proc* 45 (2012) 590–593, <https://doi.org/10.3182/20120905-3-HR-2030.00006>.
- [254] M.T. Ramesan, V. Santhi, Synthesis, characterization, conductivity and sensor application study of polypyrrole/silver doped nickel oxide nanocomposites, *Compos. Interfaces*. 25 (2018) 725–741, <https://doi.org/10.1080/09276440.2018.1439626>.
- [255] S. Agarwal, S. Kumar, H. Agrawal, M.G. Moineddin, M. Kumar, S.K. Sharma, K. Awasthi, An efficient hydrogen gas sensor based on hierarchical Ag/ZnO hollow microstructures, *Sensors Actuators B Chem.* 346 (2021) 130510, <https://doi.org/10.1016/j.snb.2021.130510>.
- [256] N. Saini, K. Awasthi, Insights into the progress of polymeric nano-composite membranes for hydrogen separation and purification in the direction of sustainable energy resources, *Sep. Purif. Technol.* 282 (2022) 120029, <https://doi.org/10.1016/j.seppur.2021.120029>.

- [257] C.H. Hsieh, L.H. Xu, J.M. Wang, T.M. Wu, Fabrication of polypyrrole/tin oxide/graphene nanoribbon ternary nanocomposite and its high-performance ammonia gas sensing at room temperature, *Mater. Sci. Eng. B Solid-State Mater. Adv. Technol.* 272 (2021) 115317, <https://doi.org/10.1016/j.mseb.2021.115317>.
- [258] Y. Sood, S.D. Lawaniya, H. Mudila, K. Awasthi, A. Kumar, Polypyrrole-Tungsten disulphide 2D nanocomposites for ammonia sensing, *Sensors Actuators B Chem.* 394 (2023), <https://doi.org/10.1016/j.snb.2023.134298>.
- [259] T.N. Ly, S. Park, Highly sensitive ammonia sensor for diagnostic purpose using reduced graphene oxide and conductive polymer, *Sci. Rep.* 8 (2018) 1–12, <https://doi.org/10.1038/s41598-018-36468-z>.
- [260] J. Zhang, X. Liu, S. Wu, H. Xu, B. Cao, One-pot fabrication of uniform polypyrrole/Au nanocomposites and investigation for gas sensing, *Sensors Actuators, B Chem.* 186 (2013) 695–700, <https://doi.org/10.1016/j.snb.2013.06.063>.
- [261] P.G. Su, S.L. Liao, Fabrication of a flexible H₂ sensor based on Pd nanoparticles modified polypyrrole films, *Mater. Chem. Phys.* 170 (2016) 180–185, <https://doi.org/10.1016/j.matchemphys.2015.12.037>.
- [262] N. Gaikwad, S. Bhanot, P.V. More, G.H. Jain, P.K. Khanna, Chemically designed Pt/PPy nano-composite for effective LPG gas sensor, *Nanoscale* 6 (2014) 2746–2751, <https://doi.org/10.1039/c3nr05375j>.
- [263] H. Shokry Hassan, A.B. Kashyout, I. Morsi, A.A.A. Nasser, H. Abuklill, Development of polypyrrole coated copper nanowires for gas sensor application, *Sens. Bio-Sensing Res.* 5 (2015) 50–54, <https://doi.org/10.1016/j.sbsr.2015.07.004>.
- [264] S.S. Barkade, D.V. Pinjari, A.K. Singh, P.R. Gogate, J.B. Naik, S.H. Sonawane, M. Ashokkumar, A.B. Pandit, Ultrasound assisted miniemulsion polymerization for preparation of polypyrrole-zinc oxide (PPy/ZnO) functional latex for liquefied petroleum gas sensing, *Ind. Eng. Chem. Res.* 52 (2013) 7704–7712, <https://doi.org/10.1021/ie301698g>.
- [265] B. Yeole, T. Sen, D.P. Hansora, S. Mishra, Effect of electrical properties on gas sensitivity of polypyrrole/cds nanocomposites, *J. Appl. Polym. Sci.* 132 (2015) 1–9, <https://doi.org/10.1002/app.42379>.
- [266] B. Kabita, D. Mausumi, S. Deepali, Polypyrrole nanonetwork embedded in polyvinyl alcohol as ammonia gas sensor, *Res. J. Chem. Sci. Res. J. Chem. Sci.* 5 (2015) 2231–2606.
- [267] S. Seema, M.V.N.A. Prasad, Studies on DC conductivity and LPG sensing behaviour of nanostructured polypyrrole-CeO₂ composites, *AIP Conf. Proc.* 1989 (2018), <https://doi.org/10.1063/1.5047737>.
- [268] G.T. Lamdhade, K.B. Raulkar, S.S. Yawale, S.P. Yawale, Fabrication of multilayer SnO₂-ZnO-PPy sensor for ammonia gas detection, *Indian J. Phys.* 89 (2015) 1025–1030, <https://doi.org/10.1007/s12648-015-0676-x>.
- [269] H.A. Khorami, A. Eghbali, M. Keyanpour-Rad, M.R. Vaezi, M. Kazemzad, Ammonia sensing properties of (SnO₂-ZnO)/polypyrrole coaxial nanocables, *J. Mater. Sci.* 49 (2014) 685–690, <https://doi.org/10.1007/s10853-013-7749-z>.
- [270] P.G. Su, Y.T. Peng, Fabrication of a room-temperature H₂S gas sensor based on PPy/WO₃ nanocomposite films by in-situ photopolymerization, *Sensors Actuators, B Chem.* 193 (2014) 637–643, <https://doi.org/10.1016/j.snb.2013.12.027>.
- [271] C.F. Rose, P. Ott, *Metabolic Brain Disease Ammonia Toxicity*, 2017, pp. 529–538.
- [272] W.K. Jang, J. Yun, H. Il Kim, Y.S. Lee, Improvement of ammonia sensing properties of polypyrrole by nanocomposite with graphitic materials, *Colloid Polym. Sci.* 291 (2013) 1095–1103, <https://doi.org/10.1007/s00396-012-2832-6>.
- [273] X. Tang, D. Lahem, J.P. Raskin, P. Gérard, X. Geng, N. André, M. Debligny, A fast and room-temperature operation ammonia sensor based on compound of graphene with polypyrrole, *IEEE Sens. J.* 18 (2018) 9088–9096, <https://doi.org/10.1109/JSEN.2018.2869203>.
- [274] G. Ayad, *The Nanocomposite Film of Polypyrrole and Functionalized Single Walled Carbon Nanotubes as Gas Sensor of NO₂ Oxidizing Gas * Address for Correspondence the Nanocomposite Film of Polypyrrole and Functionalized Single Walled Carbon Nanotubes as Gas Sensor O*, 2019.
- [275] J. Sun, X. Shu, Y. Tian, Z. Tong, S. Bai, R. Luo, D. Li, C.C. Liu, Facile preparation of polypyrrole-reduced graphene oxide hybrid for enhancing NH₃ sensing at room temperature, *Sensors Actuators, B Chem.* 241 (2017) 658–664, <https://doi.org/10.1016/j.snb.2016.10.047>.
- [276] W.-K. Jang, J.-M. Yun, H.-I. Kim, Y.-S. Lee, Improvement in ammonia gas sensing behavior by polypyrrole/multi-walled carbon nanotubes composites, *Carbon Lett* 13 (2012) 88–93, <https://doi.org/10.5714/cl.2012.13.2.088>.
- [277] H. of T. nanocomposite ultrathin films and application for an N₂ gas sensor Tai, Y. Jiang, G. Xie, J. Yu, M. Zhao, Self-assembly of TiO₂/polypyrrole nanocomposite ultrathin films and application for an NH₃ gas sensor, *Int. J. Environ. Anal. Chem.* 87 (2007) 539–551, <https://doi.org/10.1080/03067310701272954>.
- [278] S. Ebrahimiasl, A. Zakaria, A. Kassim, S.N. Basri, Novel conductive polypyrrole/zinc oxide/chitosan bionanocomposite: synthesis, characterization, antioxidant, and antibacterial activities, *Int. J. Nanomedicine.* 10 (2015) 217–227, <https://doi.org/10.2147/IJN.S69740>.
- [279] N. Nitta, F. Wu, J.T. Lee, G. Yushin, Li-ion battery materials: present and future, *Mater. Today.* 18 (2015) 252–264, <https://doi.org/10.1016/j.mattod.2014.10.040>.
- [280] N.S. Choi, Z. Chen, S.A. Freunberger, X. Ji, Y.K. Sun, K. Amine, G. Yushin, L.F. Nazar, J. Cho, P.G. Bruce, Challenges facing lithium batteries and electrical double-layer capacitors, *Angew. Chemie - Int. Ed.* 51 (2012) 9994–10024, <https://doi.org/10.1002/anie.201201429>.
- [281] L. Cui, J. Shen, F. Cheng, Z. Tao, J. Chen, SnO₂ nanoparticles@polypyrrole nanowires composite as anode materials for rechargeable lithium-ion batteries, *J. Power Sources.* 196 (2011) 2195–2201, <https://doi.org/10.1016/j.jpowsour.2010.09.075>.
- [282] R. Liu, D. Li, C. Wang, N. Li, Q. Li, X. Lü, J.S. Spindelov, G. Wu, Core-shell structured hollow SnO₂-polypyrrole nanocomposite anodes with enhanced cyclic performance for lithium-ion batteries, *Nano Energy* 6 (2014) 73–81, <https://doi.org/10.1016/j.nanoen.2014.03.010>.
- [283] X. Du, T. Yang, J. Lin, T. Feng, J. Zhu, L. Lu, Y. Xu, J. Wang, Microwave-assisted synthesis of SnO₂@polypyrrole nanotubes and their pyrolyzed composite as anode for lithium-ion batteries, *ACS Appl. Mater. Interfaces.* 8 (2016) 15598–15606, <https://doi.org/10.1021/acsami.6b03332>.
- [284] Y. Zhao, J. Li, N. Wang, C. Wu, G. Dong, L. Guan, Fully reversible conversion between SnO₂ and Sn in SWNTs@SnO₂@PPy coaxial nanocable as high performance anode material for lithium ion batteries, *J. Phys. Chem. C.* 116 (2012) 18612–18617, <https://doi.org/10.1021/jp304095y>.
- [285] K. Brijesh, K. Bindu, D. Shanbhag, H.S. Nagaraja, Chemically prepared Polypyrrole/ZnWO₄ nanocomposite electrodes for electrocatalytic water splitting, *Int. J. Hydrogen Energy.* 44 (2019) 757–767, <https://doi.org/10.1016/j.ijhydene.2018.11.022>.
- [286] S.S. Jayaseelan, N. Bhuvanendran, Q. Xu, H. Su, Co₃O₄ nanoparticles decorated Polypyrrole/carbon nanocomposite as efficient bi-functional electrocatalyst for electrochemical water splitting, *Int. J. Hydrogen Energy.* 45 (2020) 4587–4595, <https://doi.org/10.1016/j.ijhydene.2019.12.085>.
- [287] L.F. Loguericio, J. Fonseca, E.C. Kohlrausch, L.A. Santa-Cruz, S. Khan, G. Machado, In-situ electropolymerization of Congo red-doped polypyrrole and gold nanoparticle nanocomposites and its electrocatalytic application, *Electrochim. Acta.* 468 (2023), <https://doi.org/10.1016/j.electacta.2023.143091>.